UNIVERSIDADE DA BEIRA INTERIOR
Ciências

Disposable sensor for the determination and quantification of analytes with interest in health

Development of a screen-printed electrochemical sensor for Bisphenol A detection

Cláudia Caçador Peralta

Dissertação para obtenção do Grau de Mestre em
Biotecnologia
(2º ciclo de estudos)

Orientador: Profª. Doutora Ana Cristina Dias-Cabral
Co-orientador: Filipa Andreia Velez Pires

Covilhã, junho de 2016

To my family

Acknowledgements

As a consequence of the work involving this master's dissertation, there are several people to whom I would like to express gratitude.

First, I would like to thank professors Dra. Ana Cristina Dias-Cabral and Dra. María Julia Arcos Martinez for all the support, dedication, effort and patience, knowing that their help was key in achieving what was proposed.

Secondly, special thanks to Filipa Pires and Hugo Silva, which helped me in many ways throughout the development of this work, providing guidance in times of need. Also, this special thanks is extended to all of the laboratory coworkers, both in Covilhã and in Burgos, for helping ever so often and for proving a cheerful environment, which made work a lot easier.

This work is also dedicated to all my friends, whose support and friendship will be forever esteemed, and to the 9gag community, proving a source for laughter in much needed times.

Finally, to the most important people in my life, goes a thank-you from deep within.

To Miguel, for being so kind, supportive, loving, patient and understanding, being there even when times were rough, with his constant cheering and belief that all will come to a good end.

To my parents, for putting up with all the efforts necessary to put me through university, with the support, patience and unconditional love that will forever be cherished.

At last, a special thank-you to my big brother, knowing that without him none of this would be possible, and for that reason I thank his belief in the capabilities of his litter sister.

Resumo

Num mundo em que a procura por uma maior comodidade levou a que os plásticos fizessem parte do nosso dia-a-dia, surgiu uma nova classe de poluentes que está a causar um grande impacto na saúde humana.

Dentro desta nova classe de poluentes encontra-se o Bisfenol A (BPA), um disruptor endócrino que era usado inofensivamente como monómero na produção de plásticos, até descoberta a sua capacidade de mimetizar as hormonas naturalmente presentes no corpo, ligando-se aos seus recetores e causando um desequilíbrio hormonal que pode levar a vários problemas de saúde.

Desde que foi classificado como perigoso para a saúde humana, estudos envolvendo BPA aumentaram, especialmente procurando métodos alternativos mais baratos para a sua deteção, tentando manter a sensibilidade associada a métodos mais tradicionais de como a cromatografia, mas acrescentando portabilidade e uma mais simples operabilidade.

Os métodos eletroquímicos respondem adequadamente a esta necessidade, sendo ainda mais promissores quando usados elétrodos serigrafados (SPE), isto é, dispositivos contendo o sistema de três elétrodos serigrafados e miniaturizados na superfície de um substrato. Isto faz com que estes sensores tenham elevada portabilidade, sejam fácies de usar e que a sua produção seja de baixo custo, permitindo o seu descarte após uso único.

Mesmo existindo estudos para a deteção eletroquímica de BPA, poucos são aqueles que usam SPE como o sistema de elétrodos. Assim sendo, depois de uma cuidada otimização de vários parâmetros, foi desenvolvido um sensor para a deteção de BPA usando modificadores de superfície como nanotubos de carbono (CNT) e uma rede metalo-orgânica de cobre (Cu-MOF), sendo o último pouco estudado como modificador na área da eletroquímica.

Combinado 60% de CNT e 40% de Cu-MOF na superfície do elétrodo, foi conseguido um limite de deteção de 1.20×10^{-7} M em tampão, comparável e ainda mais baixo que alguns sensores tradicionais descritos na literatura para este analito. Estudando o sensor em meios mais complexos como a urina sintética e humana, foram conseguidos limites de deteção de 2.52×10^{-7} M e 8.91×10^{-7} M, respetivamente, mostrado a natureza promissora do sensor desenvolvido.

Palavras-chave

Bisfenol-A; Elétrodos Serigrafados; Nanotubos de Carbono; Rede Metalo-Orgânica de Cobre.

Resumo Alargado

Considerando o estilo de vida cada vez mais agitado da sociedade dos dias de hoje, o uso de recipientes de plástico tornou-se uma prática comum no dia-a-dia.

Das muitas substâncias usadas como monómeros na produção de plástico e seus derivados, o Bisfenol-A (BPA) encontra-se entre os mais usados, tanto como componente principal na produção de policarbonato e resinas de epóxi (usadas para revestimento do interior de latas), como parte do processo de produção de materiais como polisulfunato, poliacrilato, resinas insaturadas de poliéster e retardantes de chama, sendo um inibidor na síntese de poli(vinil cloreto) e atuando como antioxidante no fabrico de colas, tintas e plásticos. Com o uso destes materiais em áreas com a alimentação e bebidas, saúde, indústria e comércio, o BPA tornou-se ubíquo na vida dos seres humanos.

Quando se encontra na forma de polímero, o BPA não apresenta qualquer problema, contudo, quando é liberto dos materiais do qual é constituinte, seja por ação de processos de aquecimento, aumento ou diminuição de pH ou ainda por contacto com a pele, no caso de recibos ou notas, o BPA torna-se uma substância perigosa para a saúde humana.

O motivo pelo qual o BPA pode ter efeito danosos na saúde humana deve-se ao facto deste possuir a capacidade de mimetizar as hormonas naturalmente presentes no corpo humano. A este tipo de substâncias, dá-se o nome de disruptores endócrinos, e podem exercer a sua ação de diferentes formas, como agonista, em que se ligam aos recetores hormonais e os ativam, ou antagonista, em que se ligam ao recetor e impedem que a hormona endógena se ligue. Dependendo do tipo de recetor, o BPA exerce a sua ação de ambas as formas.

Como consequência desta alteração endócrina, muitos problemas de saúde estão associados ao consumo de BPA, como patologias do foro neurológico, imunológico, cardiovascular, hepático, entre outras. Contudo, e apesar de ter sido considerado, em janeiro de 2015, seguro para consumo pela Autoridade Europeia para a Segurança Alimentar, mais estudos serão necessários para melhor averiguar as consequências do consumo desta substância na saúde humana e meio ambiente.

Dado a grande importância que se tem dado a este tipo de poluentes nos últimos anos, vários métodos comuns existem para a deteção de BPA como cromatografia líquida e gasosa, ensaios de imuno-afinidade mediados por enzimas (ELISA) e sensores de ressonância plasmónica de superficie (SPR) que, apesar de demostrarem elevada afinidade para BPA permitindo a sua deteção a baixas concentrações, têm como desvantagens o elevado custo de operação e/ou de equipamentos, requerendo pessoal especializado para a sua operação, elevado tempo de

operação e/ou possuírem reduzida portabilidade, impossibilitando assim a medição da amostra no local de recolha.

Como forma de combate às desvantagens associadas às técnicas de deteção e quantificação anteriormente referidos, os métodos de deteção eletroquímica têm sido bastantes estudados nesta área, com particular ênfase para o uso de elétrodos serigrafados, isto é, elétrodos miniaturizados e impressos na superfície de um substrato, recorrendo a tintas especializadas que são passadas por um molde e curadas com a forma de cada um dos componentes do sensor. Este tipo de técnica permite o fabrico de elétrodos de baixo custo, que podem ser descartados após uso, possuindo um elevada reprodutibilidade e eliminado problemas como a morosa limpeza de elétrodos nas convencionais técnicas eletroquímicas.

Visto que o uso de elétrodos simples nem sempre oferece a sensibilidade e especificidade para o analito desejada, recorre-se muitas vezes a modificação da sua superfície para aumentar estes dois parâmetros. Para isso podem ser usados elementos biológicos ou elementos químicos, sendo parte integrante destes últimos os nano materiais, como os nanotubos de carbono (CNT) e as nano partículas de ouro (AuNP) que conferem um aumento da área superficial e condutividade, incrementando assim a sensibilidade para com o analito.

Ainda dentro dos modificadores de superfície está um conjunto de compostos que começam a dar os primeiros passos na área da deteção eletroquímica, denominados de redes metalo-orgânicas, das quais é exemplo a rede metalo-orgânica de cobre (Cu-MOF). Este tipo de redes, como o nome indica, são compostas por um elemento metálico, que neste caso é o cobre, ligados por um ligando orgânico, sendo que o ligando orgânico da rede sintetizada possui elevada afinidade para com o BPA, havendo assim uma possibilidade de aumentar a especificidade do sensor desenvolvido.

Sendo que o objetivo do presente trabalho era o desenvolvimento de um sensor eletroquímico em elétrodos serigrafados para a deteção de BPA, vários passos foram necessários para atingir o sensor ideal. Para isso, diversas condições de ensaio foram estudadas, nomeadamente pH do tampão, tipo de tampão, voltagens e tempos de pré-tratamento, método eletroquímico, bem como o tipo de modificador de superfície, sendo que para alguns dos parâmetros estudados se recorreu ao planeamento de experiências por *design* fatorial.

Com as condições de ensaio ideais adquiridas (pH entre 8 e 11, não usar voltagem no pré-tratamento, devido a stress causado no elétrodo, agitar durante 60s, medindo depois com o método eletroquímico de voltametria de pulsos diferenciados) foram conjugadas várias proporções de CNT e Cu-MOF até atingir a proporção ótima.

O melhor resultado em termos de limite de deteção foi de 1.20×10^{-7} M, em tampão fosfato pH 11, sendo comparável ou ainda melhor que muitos resultados previamente descritos na

literatura para a deteção eletroquímica de BPA. Este resultado foi possível graças a conjugação de 60% de nanotubos de carbono e 40% de Cu-MOF.

Quando se fez a tentativa de passar para análises em meios mais complexos, urina sintética e urina humana diluídas foram usadas como meios. Nestas condições, foi possível detetar BPA com um limite de 2.52×10^{-7} M (com 30% CNT e 70% Cu-MOF) para a urina sintética e um limite de 8.91×10^{-7} M (usando 60% CNT e 40% Cu-MOF) para amostras de urina humana, provando a potencialidade do sensor desenvolvido.

Abstract

In a world where the search for commodity has lead for plastic based materials to be part of our everyday life, a new class of pollutants with great impact on human health is emerging.

Part of that class of pollutants is Bisphenol-A (BPA), an endocrine disruptor that was used harmlessly as a monomer in the production of plastics, until its found action in mimicking natural hormones in the body, binding to their receptor and causing a hormone imbalance that can lead to several health issues.

Since being classified as threatening to human health, studies involving BPA have increased, especially in searching alternative low cost methods for BPA detection, maintaining the sensitivity of the more traditionally employed ones such as chromatography, but adding portability and a simple operability.

Fitting in to this need are electrochemical methods, made even more promising by the use of screen-printed electrodes (SPE), that are miniaturized devices containing a three electrode system printed on a substrate. This makes these sensors extremely portable, easy to use and with very low production cost, allowing their disposal after single use.

Even though studies have already been made for BPA using electrochemical methods, few used SPE as an electrode system. As so, after careful optimization of several parameters, a sensor for BPA detection was developed using surface modifiers such as carbon nanotubes (CNT) and a copper metal-organic frame (Cu-MOF), the latter being a new and little studied modifier in electrochemical sensing.

By combining 60% CNT and 40% Cu-MOF on the surface of the electrode, a limit of detection of 1.20×10^{-7} M in buffer was obtained, comparable or even lower than some traditional electrochemical sensors already described in the literature. When studying the sensor for more complex mediums such as synthetic and human urine, detection limits of 2.52×10^{-7} M and 8.91×10^{-7} M, respectively, were attained, showing the promising nature of the developed sensor.

Keywords

Bisphenol-A; Screen-Printed Electrodes; Carbon Nanotubes; Copper Metal-Organic Frame

Table of Contents

List of Images

List of Tables

Abbreviations

AuNP – Gold Nanoparticles

BPA – Bisphenol A

CE – Counter Electrode

CNT – Carbon Nanotubes

Cu-MOF – Copper Metal-Organic Frame

CV – Cyclic Voltammetry

DMF - N,N-Dimethylformamide

DOE – Design of experiments

DP – Differential Pulse

EDC – Endocrine Disrupting Chemical

EFSA - European Food Safety Authority

ELISA - Enzyme-Linked Immunoabsorbent Assay

GC-MS - Gas Chromatography- Mass Spectrometry

HPLC - High Performance Liquid Chromatography

LMS - Least Median of Squares

LOD – Limit of Detection

LSV – Linear Sweep Voltammetry

MECK - Micellar Electrokinetic Chromatography

MIP - Molecularly Imprinted Polymer

MNP – Magnetic Nanoparticles

MOF – Metal-Organic Frame

MS - Mass Spectrometry

MWCNT – Multi-Walled Carbon Nanotubes

NP – Nanoparticle

QD – Quantum Dots

RE – Reference Electrode

SPES – Screen-Printed Electrochemical Sensors

SPR - Surface-Plasmon-Resonance

SWCNT – Single Walled Carbon Nanotubes

SWV – Square Wave Voltammetry

TED - Triethylenediamine

UBI – University of Beira Interior

UV – Ultraviolet

WHO – World Health Organization

1. Introduction

With the industrialization of modern society, and the need for more convenient and practical solutions to keep up with the busy lifestyle of today's families, plastic took over as a preferred material for food and water containers. Confirming this, is the fact that, in 2014, 311 million metric tons of plastic were produced worldwide, which compared to the 1950's is 207 times the volume of plastic produced (1.5 metric tons for 1950) [1].

As one of the major components in plastic production, being used as a monomer in the production of polycarbonate plastic (PC) and epoxy resins, Bisphenol A (BPA), also known as 4,4'-Isopropylidenediphenol, has become, in the latest years, interest of study of many scientists worldwide (Image 1.1) [2–10].

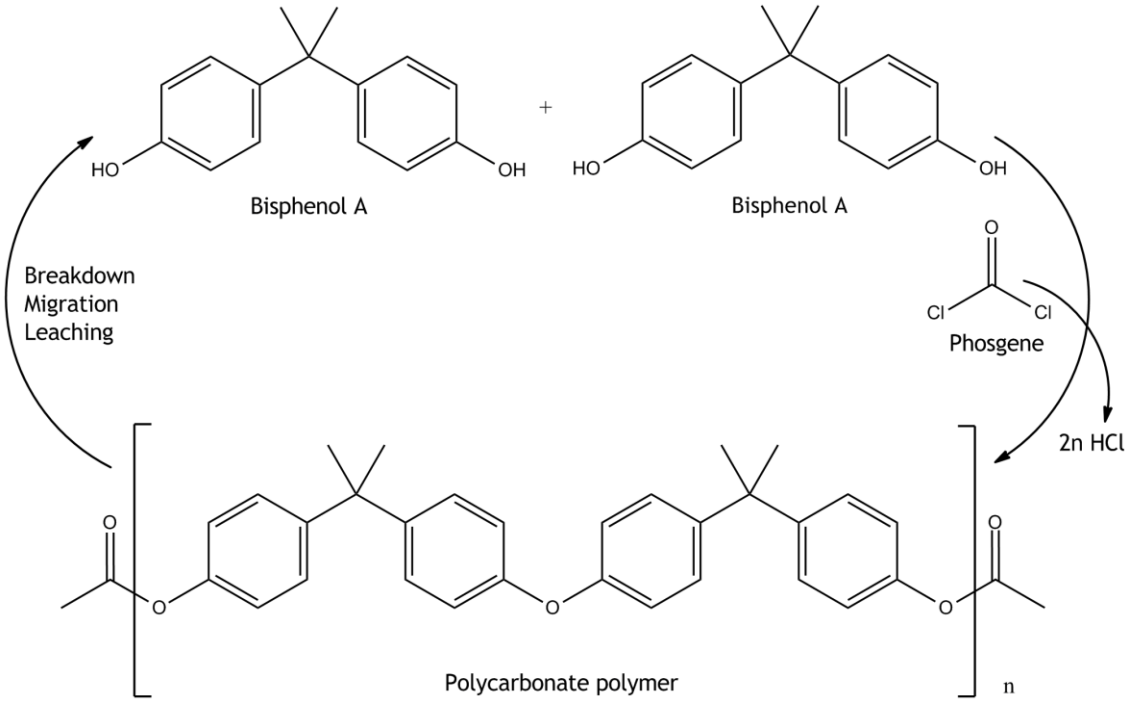

Image 1.1 – Synthesis of polycarbonate polymer using BPA monomer and breakdown of PC to BPA monomers. Adapted from [2]**.**

In 2012, global production of BPA was of 4.6 million tons, Europe being responsible for 25% of said production, with estimated volume of 5.4 million tons in 2015 [11]. These numbers are justified by the broad uses of BPA, not only as a monomer and main constituent, but also as part of the synthesis process in the production of polysulfonate, polyacrylate, unsaturated polyester resins and flame retardants, as well as being a polymerization inhibitor for poly(vinil chloride) and acting as an antioxidant in glues, inks and plastics [2,8,12]. Application for these BPA-including products can be found in household products (baby bottles, kitchenware, water

bottles), medical equipment (for dialysis and blood oxygenation,), dentistry, electronics, automobiles, corrective and protective eyewear, thermal printing paper, currency and for storage of food, beverages and pharmaceuticals in cans or other recipients lined with an epoxy coating [2,6,8,12–14].

1.1 BPA implications on human health

The main concern associated with BPA-based products, besides its discharge into the environment, due to wastewater from the plastic-producing industry, is the leaching of BPA monomer from everyday products [2,14–16]. Whether it is from thermal processes, either from food production or heating processes associated to food consumption, acidic or basic pH of liquids, or even from dermal contact with receipts or currency, BPA is released as result of hydrolysis of the ester bonds that link BPA monomers (Image 1.1) [8,14,16]. The reason why BPA leakage into food, beverages, water and soil is concerning is because BPA is thought to be persistent pollutant with endocrine disrupting activity [2,5–7,12,14–17].

An endocrine disrupting chemical (EDC) is defined by the World Health Organization (WHO) as "an exogenous substance or mixture that alters function(s) of the endocrine system and consequently causes adverse health effects in an intact organism, or its progeny, or (sub)populations" [18]. Besides BPA, many known substances are classified as EDC: man-made chemicals (for example pesticides, polychlorinated bisphenols, dioxins, synthetic hormones for contraceptive effects) and natural chemicals such as human hormones and phytoestrogens [19]. EDC act by disturbing the endocrine system, which can be via receptor mediated mechanisms, hormone synthesis, metabolism and transport; being the receptor mediated mechanism the one with prevalent attention and the mechanism responsible for BPA's endocrine disrupting effect [7,18].

With a structure analogous to natural hormones present in the body (Image 1.2.-A), there is the possibility of BPA to bind to several hormone receptors, causing both agonistic (activation of the receptor, leading to a unwanted response, similar to that would be caused by the natural hormone) and antagonistic (binding to the receptor with no activation, but preventing the binding of endogenous hormones) responses in receptors such as nuclear estrogen receptors and thyroid receptors, in these cases having both agonistic and antagonistic effects, and to androgen receptors, demonstrating only an antagonistic effect (Image 1.2. - B) [2,7,19]. These alterations in hormone recognition are thought to be associated to reproductive issues, as, for example ovary problems, infertility and low sperm count, as well as abnormal thyroid and sex hormone concentrations [2,7,10,14,20].

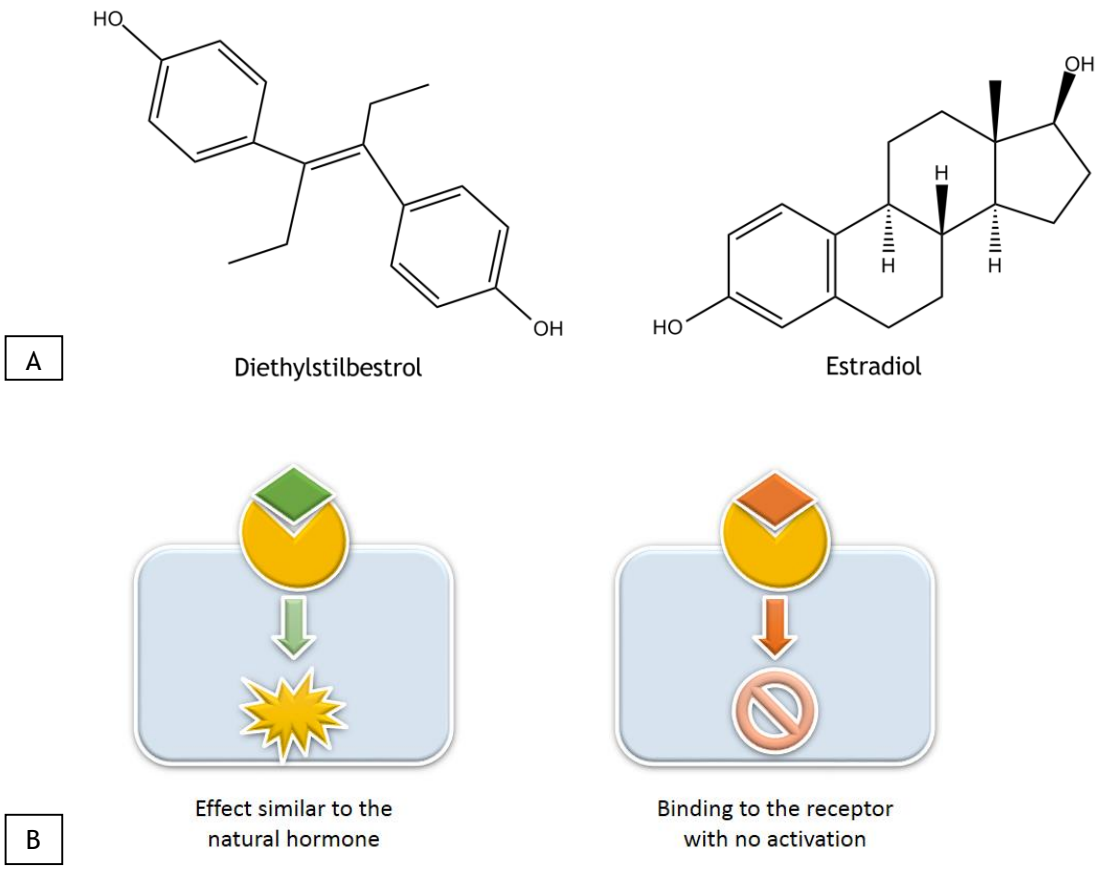

Image 1.2 – A - Natural hormones which BPA mimics [2]**; B – Agonistic (left) and antagonistic (right) effect of BPA on hormone receptors** [7]**.**

Not only has BPA been related to problems directly associated with the endocrine system, but has also been linked to issues that may or may not be in relation with hormone receptors, such as neurological pathologies, immune related diseases, cardiovascular diseases, altered liver functions, oxidative stress and inflammation, type-2 diabetes and altered epigenetic and gene expression, needing some of these possible consequences of BPA absorption further studies [2,7,21].

In a recent press release, from January, 2015, European Food Safety Authority (EFSA) declared that there is no consumer health risk associated to BPA exposure, stating that even after lowering the recommended BPA daily intake to 4µg/kg of bodyweight/day (previously 50 µg/kg of bodyweight/day) that the combination of all possible exposer to this chemical is three to five time lower than the new recommended value, thus not representing any risk for human beings [21]. Notwithstanding, the new attributed safety of BPA products remains uncertain, and BPA's toxic effects have yet to be clarified, mainly due to the unpredictability of this EDC at lower concentrations, owing to its non-monotonic behavior, i.e. the expected response is not proportional to the quantity of BPA, being undetermined which can be the effects at lower

and higher doses [7,21]. For this reason, and for its ubiquitous nature, BPA is still interest of study of many scientists [2,7,22].

1.2 BPA detection

Detection of BPA has been performed recurring to analytical methods, from the more conventional, such as High Performance Liquid Chromatography (HPLC), with various methods of detection (Ultraviolet (UV), Mass Spectrometry (MS), fluorescence and Gas Chromatography-Mass Spectrometry (GC-MS), to the less conventional, such as Micellar Electrokinetic Chromatography (MECK), biosensors (which include microbial biosensors, immunosensors and electrochemical cell-based chip sensors), and chemical electrochemical sensors [2,5,8,10,12,15,20,22].

Chromatography based methods, though very sensitive and with excellent detection limits (Table 1.1.), involve highly trained operators and instruments that are sophisticated, expensive and with low portability. Also, due to the non-polar nature of the analyte and its low concentration in samples, pretreatment steps are often necessary, leading to a time consuming, lack of on-site applicability technique [2,8,20,23].

The more traditional bio-sensing techniques, namely Enzyme-Linked Immunoabsorbent Assay (ELISA) and Surface-Plasmon Resonance (SPR)-based sensors, though reporting good sensitivity and reliability (Table 1.1), especially for less complex matrices, they face similar problems to those associated to chromatographic methods [2,10,20,23].

Table 1.1 - Detection limits for more traditionally used detection techniques. Adapted from [2,8]

Detection Method	Real Sample/Matrix	Limit of Detection	Reference
Gas Chromatography -Mass Spectrometry	Drinking water	1.38×10^{-13} M	Table II number 8 [8]
Gas Chromatography -Mass Spectrometry	Urine	4.38×10^{-10} M	Table II number 13 [8]
HPLC-Flourescence	Plastics	3.50×10^{-10} M	Table III number 8 [8]
HPLC-UV	Urine	4.38×10^{-10} M	Table III number 3 [8]
ELISA - Monoclonal antibodies	Canned vegetables	2.20×10^{-11} M	Table 1 [2]
SPR - Self assembled monolayer polyclonal antibodies	Drinking water	1.75×10^{-11} M	Table 1 [2]

1.2.1 Sensing and biosensing methods

In sensing based methods, the analyte communicates with a specific receptor for its detection, and, by interacting with a transducer, generates a signal which can be, among other, chemical, thermal, difference in mass or optical. This signal is later on communicated to a signal processor which is responsible for converting it to an interpretable reading [24]. Differences in the type of transducer and receptor may be a way to distinguish sensing methods, being this information summarized in Image 1.3.

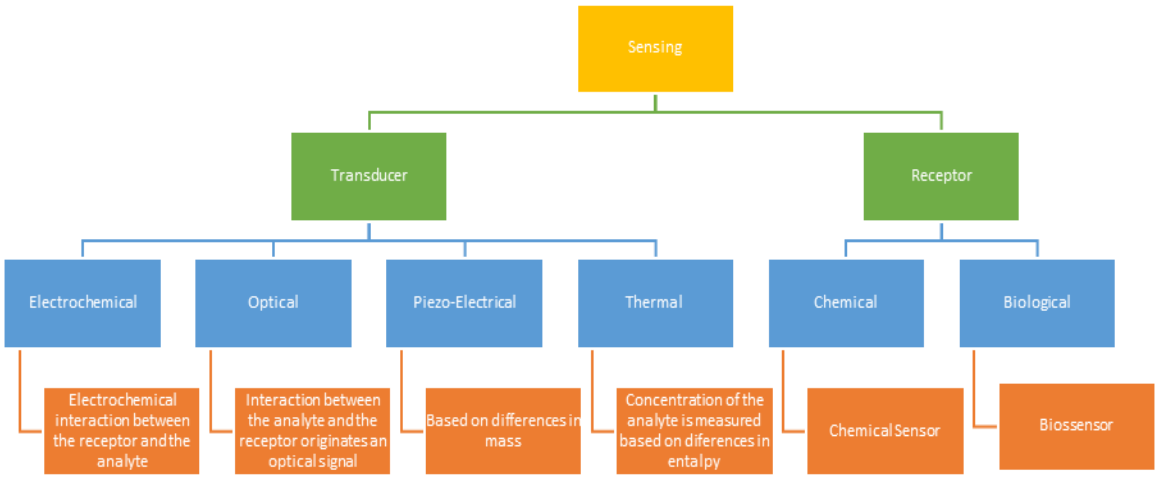

Image 1.3 - Classification of different types of sensing, based on both the transducer and the receptor [24].

1.2.2 Electrochemical sensing and biosensing

Electrochemical sensors have gained, in the past years, great importance in BPA detection. essentially derived from the electrochemical-active nature of this EDC [2]. When detected by electrochemical means, BPA is oxidized on the electrode surface as shown in Image 1.4. [2,25].

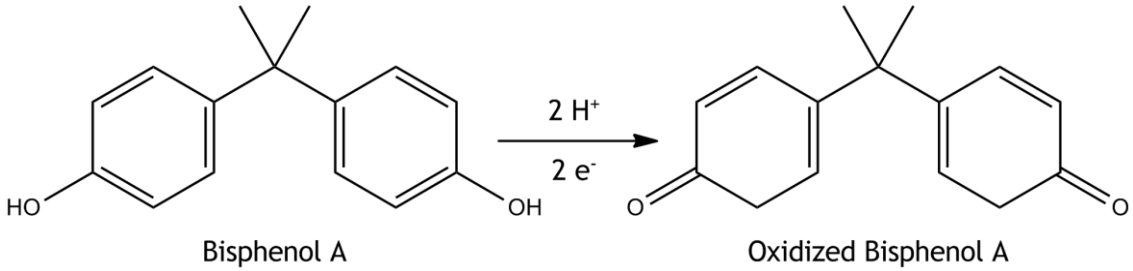

Image 1.4 - Oxidation of BPA on electrode surface [2,25].

The high sensitivity, low cost, low time consumption, reusability, simplified operation as well as simplicity and possibility of modification of electrode surface, makes electrochemical detection a promising candidate to complement or even substitute more traditional methods [2,5,16,20].

Even more promising than the conventional electrochemical sensors are Screen-Printed Electrochemical Sensors (SPE), where the electrochemical system is miniaturized on to the surface of a selected substrate [26]. This is done by passing ink though a stencil with the appropriate design for each component of the electrode system, using thermal curing between layers (Image 1.5) [26,27]. Using different types of stencils allows for a more flexible sensor

design in terms of spatial distribution, form and area of the components in the sensor, thus being possible to make sensors adequate for different needs [27]. This type of manufacturing is denominated by "thick-film" technology [28].

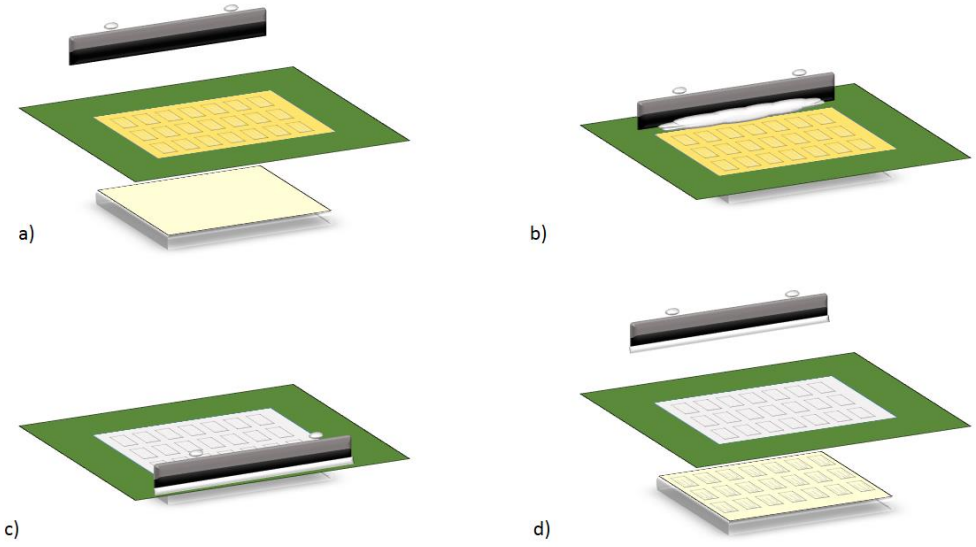

Image 1.5 – Screen-Printing technique overview. a) The substrate is placed and aligned under the stencil which has the desired pattern for the component that is being printed; b) The correct ink is placed near the squeegee in order to start the printing process; c) The squeegee sweeps the ink from one side to the other, forcing it to pass though the apertures in the stencil; d) The ink is deposited on the surface of the substrate with the correct design for the selected component. Following this step, thermal curing takes place and when dry, a new component is printed and the process repeats itself. Adapted from [27].

By using Screen-Printing as a fabrication technique, a more reproducible, stable, low cost and portable system of electrodes is obtained, ideal for *in situ* analysis. Low energy requirements, linear output, high sensitivity, quick response, ability to operate at room temperature with minimum material necessary and disposable nature of the sensors, avoiding tedious electrode cleaning, only add to the factors making SPEs a promising electrochemical system [13,20,26,27].

Electrochemical sensing, both conventional and Screen-Printed, is based on differences in current measured in the reaction cell or drop, being a result of either the oxidation or reduction of the analyte present in solution. Present in the reaction medium, besides electrolyte solution, that allows current passage by the movement of ions, are the electrodes, each responsible for a different action. The counter electrode (CE) is responsible for closing the electric circuit, and usually doesn't directly participate in the electrochemical reaction [29]. The CE is normally made of an inert material, such as platinum, gold, graphite or glassy carbon

(the latest used in conventional electrochemical system) [29]. The reference electrode (RE), usually constituted of materials such as silver, hydrogen, mercury, and copper, (only some of these used on SPE) is an electrode which has a stable and well known potential, and is used as a point of reference for the potential measurement and control [29]. Lastly, the working electrode (WE) is defined by the electrode in which the chemical reaction takes place [29]. This electrode is mostly made of inert materials such as gold, silver, platinum and carbon and can be modified to suit the detection application or to enhance sensitivity or specificity [2,29].

Differences in the material that constitutes each electrode involved in the electrochemical reaction is an important part of electrochemical analysis of BPA, though also important is the electrochemical method applied for that detection. Image 1.6 illustrates the difference between each method.

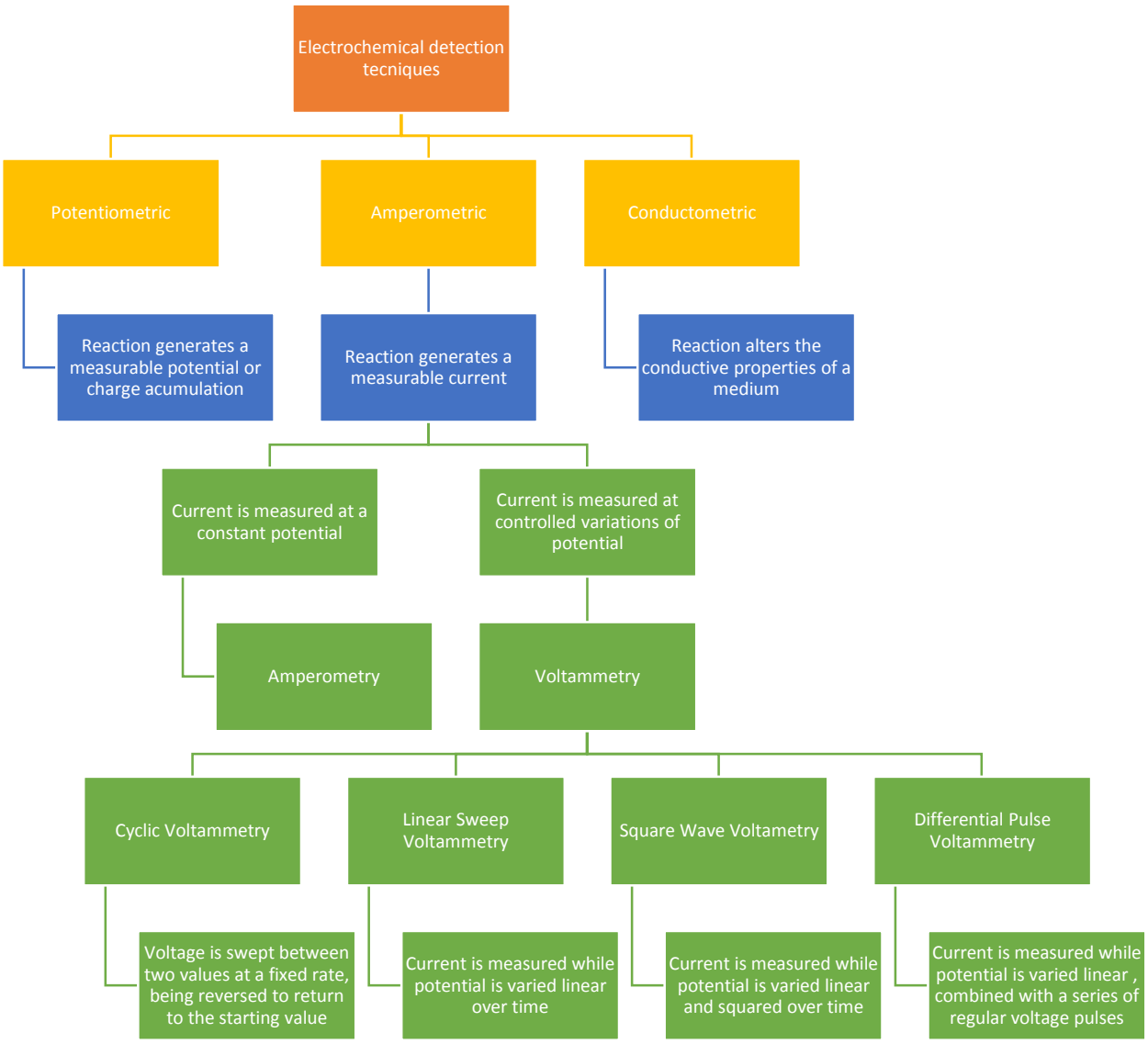

Image 1.6 - Differences between most used electrochemical detection techniques [30,31]

1.2.3 Electrode modifiers

To induce and enhance the electrochemical oxidation of BPA in order to selectively detect this EDC, various modifications can be conducted to the working electrode surface [2]. These modifications are summarized in Image 1.7., divided into chemical or biological.

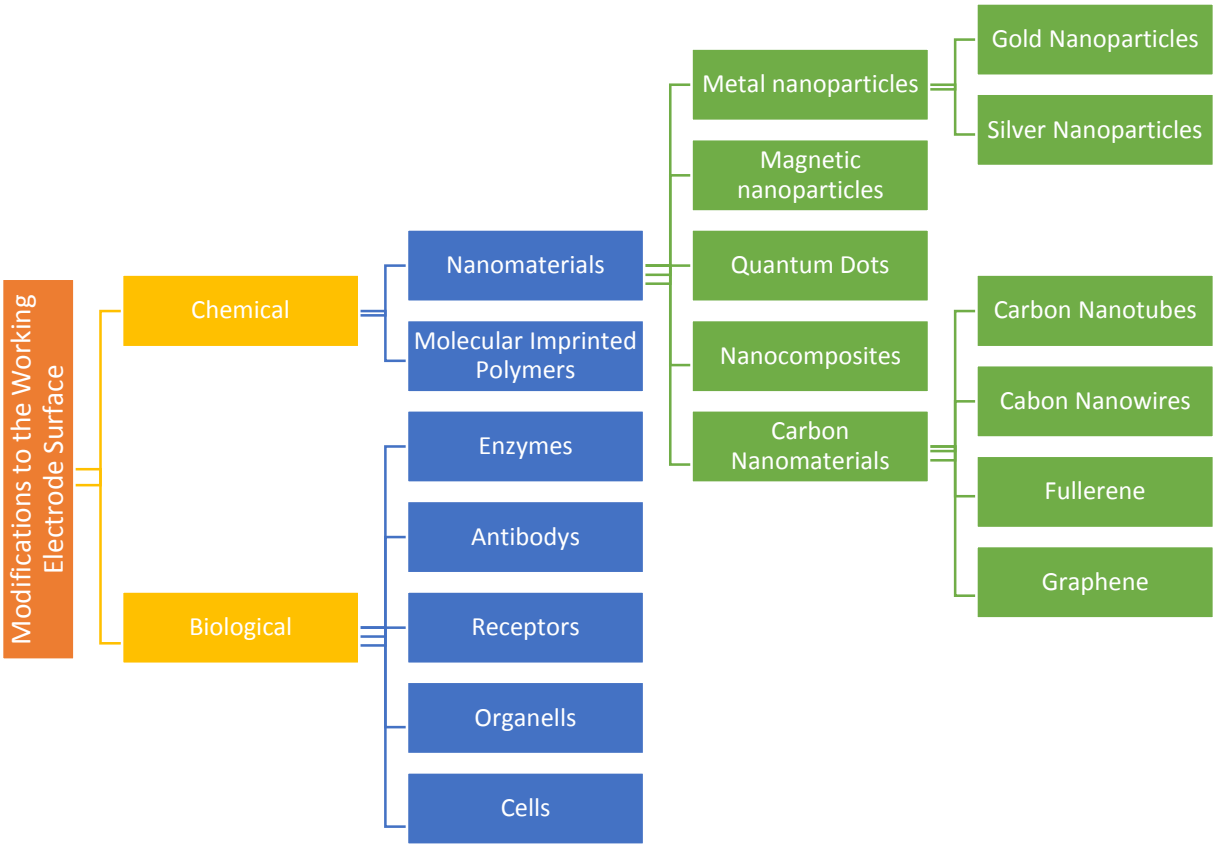

Image 1.7 - Different materials used in working electrode modifications [2].

Biosensors, which possess as a recognition element biological material (namely, enzymes, tissues, organelles, whole cells and immunosystems) are highly sensitive, extremely selective, and provide, not only quantitative information, but also qualitative data, allowing clarification about the pollutants eco-effects in organisms [2,20]. However, the use of biological material as a recognition element can lead lack of stability of the sensor in non-ideal conditions (such as pH, temperature and medium differences), which is considered a major drawback in this type of sensing [2,20].

Chemical modifiers, similarly to the biological modifiers, are used on the electrode surface as a conducting and sensing material. Although sometimes less selective, compensate in general stability in harsh environments, lower cost, simple preparation and storage stability, in comparison to biological modifiers [2,22]. Among the most popular chemical modifiers used for BPA detection are Molecularly Imprinted Polymers (MIPs) and nanomaterials [2,20,22].

MIPs are a somewhat recent class of materials that combine selectiveness similar to biological material with the stability of a chemical modifier [2,20,22]. This is achieved by using a template similar in physical parameters to the analyte, and by removing the template after polymerization of the MIP, leaving a gap that is specific to the target molecule [2,20,22].

In the chemical modifiers class are also included nanomaterials that, due to their reduced size, acquire different properties from those they're derived from. Classified as nanomaterials are, for example, quantum dots (QD), magnetic nanoparticles (MNP), Gold Nanoparticles (AuNP) and carbon based nanomaterials, such as Carbon Nanotubes (CNT), Carbon Nanowires (CNW), graphene and fullerene. Combining these nanomaterials with polymers leads to the creation of nanocomposites that acquire the unique properties of both classes of materials [2]

Quantum Dots are semiconductor structures that possess luminescent properties depending on their size, making them great candidates in dye substitution and in designing nanoprobes. Also, these types of nanoparticles have shown to enhance catalytic activity and adsorption capacity of electrochemical sensors [2,32].

Magnetic nanoparticles (MNP) that, as said in the name, possess magnetic properties that prove to be useful in separation and immobilization, greatly simplifying the electrode modification, and also having as advantages biocompatibility, low toxicity, high adsorption area and easy preparation [2,33].

In the nanomaterial class of chemical modifiers, gold nanoparticles (AuNP) and carbon nanotubes (CNT) are those to which most focus has been paid. Gold Nanoparticles are one of the most used type of metal NP, being considered easy to prepare, enhancing electrochemical signal due to their conducting and catalytic properties and being easily modified [34].

Included in the carbon-based nanomaterials, CNT possess unique properties in comparison to the macro scale material from which they are derived. Higher surface area, chemical and thermal stability, excellent electrical and optical properties, relatively low cost and enhanced electrochemical signals, obtained by electron-transferring and anti-fouling surface which make them a material widely used in electrochemical sensing [2,4,20,34].

Besides these commonly used modifiers, a new class of composites is emerging in the electrochemical sensing area as promising new structures: Metal-Organic Frameworks (MOF) [15,35]. These crystalline molecular materials are formed by coordinating metal centers or clusters with polydentate-bridging organic ligands, forming a well-defined, low density network (Image 1.8.) [15,35]. Possessing great properties such as ultrahigh and permanent porosity, high thermal and chemical stability, tunable pore structure and dimension, and adjustable internal surface properties, they have been applied to numerous areas of study, like catalysis, separation, biomedical imaging, clean energy, drug delivery and gas storage and separation [15,35,36].

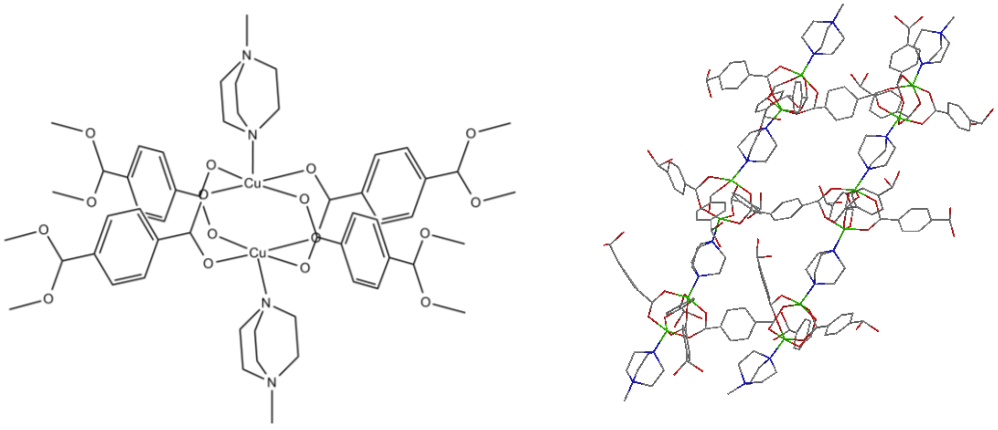

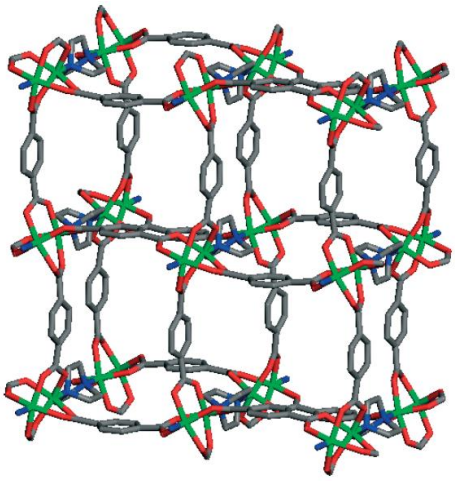

Image 1.8 – Representation of the Cu-MOF network. a) Chemical structure of the paddle wheel building unit of Cu-MOF; b) Representation of six building units of Cu-MOF; c) Representation of network structure of Cu-MOF (from [36]). Color scheme: Red – Oxygen atoms; Gray – Carbon atoms; Green – Copper atoms; Blue – Nitrogen atoms.

The fact that most of MOFs are insulating materials has lead their little exploration in electrochemical sensing [35]. This can be countered by modifying MOFs structure by using, for example, conducting materials such as CNT and MNP, by entrapping them within the framework (Image 1.9.) [35]. Besides this strategy of modification, it is also possible to insert specific organic ligands or dope metal ions in the frame and to apply post-synthesis modifications on MOF, conferring them unique sensing properties, demonstrating the versatility of these composites [35].

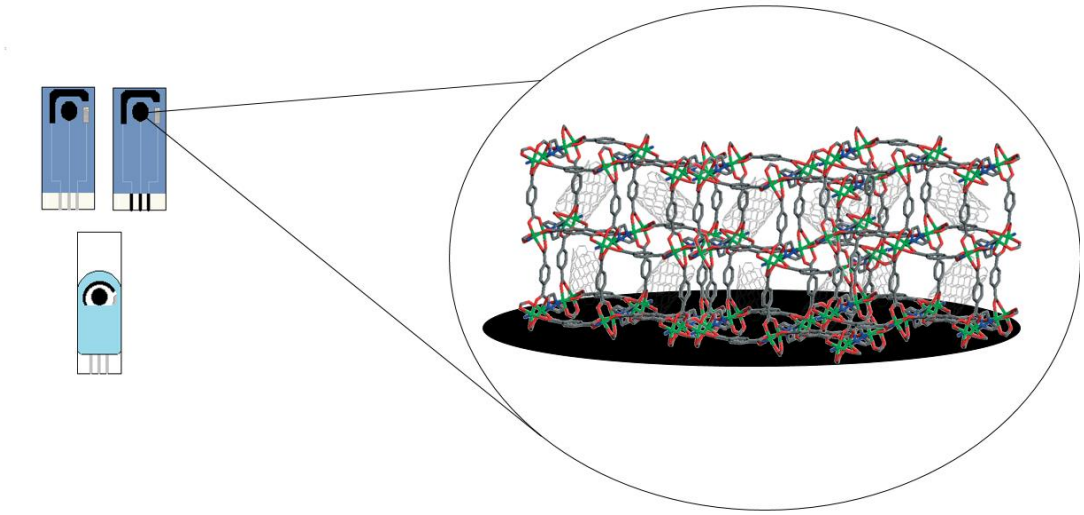

Image 1.9 – Representation of modification of the working electrode with Cu-MOF with entrapped modifiers (CNT). Unscaled image.

More important than all the extraordinary properties already referred to, MOF, in particular the MOF that will be employed in this work (Copper Metal-Organic Frame (Cu-MOF)), is the fact that it has in its constitution the organic ligand bezenedicarboxilate (BDC). This component of the Cu-MOF promotes π-π interactions between the composite and the phenol groups in BPA, allowing a pre-enrichment and an increase in specificity towards this analyte [15].

1.2.4 State of the art on BPA electrochemical sensing and biossensing.

With endocrine disruptors being of great interest to the scientific community, due to their little know impact on human and the environment, it is natural that several methods for BPA detection have already been accessed, especially in the area of electrochemical detection, considering all the advantages associated to them.

As so, a revision of the literature for BPA electrochemical detection is present in the following table, containing limits of detection associated to each sensor.

Table.1.2 Table with some of the known work for sensors and biosensors for BPA detection.

Detection Method	Type of electrodes	Real Sample/Matrix	Limit of Detection	Reference
Molecularly-Imprinted-Polymers (MIPs)-Based Sensor				
TiO_2 nanotubes and polypyrrole-based MIP	Conventional	Five different water samples	LOD: 2.0×10^{-9} M	[37]
MIPs and chitosan	Conventional Acetylene Black paste	Infant nursing bottles, water bottles	LOD: 6.0×10^{-8}M	[38]
2-aminophenol monomer/AuNPs	Conventional Glassy Carbon Electrode (GCE)	Aqueous extract of plastic materials	LOD: 1.38×10^{-7}M	[39]
Magnetic MIPs and surfactant CTAB	Conventional Glassy Carbon Electrode (GCE)	Drinking bottles and lake water	LOD: 1.0×10^{-7}M	[22]
Carbon Based Nanomaterials				
MWCNT-AuNP	Conventional GCE	Plastic Wares	LOD: 7.5×10^{-9}M	[4]
MWCNT-melamine complex	Conventional GCE	Plastic samples	LOD: 5.0×10^{-9}M	[40]
SWCNT/β-cyclodextrin	Conventional GCE	Plastic Samples	LOD: 1×10^{-9}M	[41]
SWCNT/Tyrosinase	Conventional	Polluted surface water	LOD: 2.0×10^{-8} M	[42]
Fullerene (C60)	Conventional GCE	Waste water samples	LOD: 3.7×10^{-9}M	[43]

Graphene	Conventional GCE	Mineral water in plastic wares	LOD: 4.68×10^{-8}M	[44]
Exfoliated Graphene	Conventional Exfoliated Graphene	Water samples	LOD: 7.6×10^{-7}M	[16]
Nitrogen-doped graphene sheets with chitosan	Conventional GCE	Water Samples	LOD: 5.0×10^{-9}M	[45]
Platinum-Graphene-CNT nanocomposite	Conventional GCE	Thermal printing paper	LOD: 4.2×10^{-8}M	[46]
Graphene nanofibers-AuNP composite	Conventional GCE	Baby Bottles	LOD: 3.5×10^{-8}M	[47]
Graphene-Arginine nanocomposite	Conventional GCE	Plastic products	LOD: 1.1×10^{-9}M	[48]
Reduced Graphene-BPA binding peptide	Conventional Thin film reduced graphene	Plastic products	LOD: 5.0×10^{-15}M	[5]
Quantum-dot-based sensors				
CoTe QDs-Poly(amidoamine) (PAMAM) dendrimer	Conventional GCE	Real water samples	LOD: 1.0×10^{-9}M	[32]
Nanocomposites				
Cobalt phthalocyanine	Conventional GCE	Plastic wares	LOD: 1.0×10^{-8}M	[49]
Mg-Al layered double hydroxide	Conventional GCE	Plastic wares	LOD: 5.0×10^{-9}M	[50]
Amorphous hydroxy-iron composites with ß-cyclodextrin	Conventional GCE	Beer samples	LOD: 2×10^{-7}M	[51]

Boron doped diamond	Conventional Boron doped diamond electrode	Bottled drinking water	LOD: 3×10^{-8}M	[52]
Boron doped diamond	Conventional Boron doped diamond electrode	Tap and lake water	LOD: 2.1×10^{-7}M	[53]
PAMAM-Fe_3O_4 magnetic nanoparticles	Conventional GCE	Milk samples	LOD: 5.0×10^{-9}M	[33]
Chitosan- Fe_3O_4	Conventional GCE	Plastic samples	LOD: 8.0×10^{-9}M	[54]
MWCNTs-AuNPs-Imprinted sol-gel polymers	Conventional Gold Electrode	Honey, tap water and grape juice	LOD: 3.6×10^{-9}M	[55]
PAMAM-AuNP-Silk fibroin	Conventional GCE	Water samples	LOD: 5.0×10^{-10}M	[56]
Peptide Modified	Conventional Gold Electrode	Plastic Products	LOD: 7.0×10^{-10}M	[12]
Tyrosinase and MWCNTs-cobalt phthalocyanine-Silk fibroin-composite	Conventional GCE	Plastic Products	LOD: 3.0×10^{-8}M	[57]
Magnetic nanoparticles-exfoliated graphene	Conventional GCE	Plastic Samples	LOD: 1.7×10^{-8}M	[58]
Polyclonal Antibodies-Conducting nanoparticles	Conventional GCE	Human serum	LOD: 1.31×10^{-9}M	[10]
Polyacrilamid hydrogel-cytochrome P450 2C9	Conventional GCE	Buffer	LOD: 5.8×10^{-7}M	[6]
Cu-MOF-Tyrosinase	Conventional GCE	Plastic samples	LOD: 1.3×10^{-8}M	[25]

Tyrosinase-NiNPs	Screen-Printed Carbon Working Electrode	Buffer solution	LOD: 7.1×10^{-9}M	[13]
Tyrosinase-AuNPs	Screen-Printed Carbon Working Electrode	Buffer solution	LOD: 1.0×10^{-8}M	[13]
Tyrosinase-Fe_3O_4NPs	Screen-Printed Carbon Working Electrode	Buffer solution	LOD: 8.3×10^{-9}M	[13]

The already developed methods show promising results, with some of them having comparable sensitivity to the more traditional employed methods (Table 1.1), such as peptide modified electrodes [12] and PAMAM-AuNP-Silk fibroin [56], and with reduced graphene-BPA binding peptide [5] having even better detection limits than GC-MS (position 1 – Table 1.1).

Though numerous studies on electrochemical sensing of BPA have been performed with promising results, only one known work has been done using MOF, differing from the present work by the use of tyrosinase, by not possessing a conductive element and by being performed using conventional electrochemical methods, instead of SPEs [15]. Furthermore, only few of these studies have been completed using SPEs, some of them using only the working electrode screen-printed, while using conventional CE and RE [17].

1.3 Experimental planning

When working with BPA as the analyte in study, it is quite essential to minimize waste generated, due to the pollutant nature of this chemical. Planning the experiments is a good way to address this problem, as it reduces number of experiments needed to obtain reliable results [59].

Design of experiments (DOE) is one of the methods applied to planning and conducting experiments, in order to perform the analysis of multiple inputs in response to values of output, instead of the typical approach of one variable at a time [59,60]. Though several factorial designs are considered, composite central design is highlighted for being able to consider central points, leading to a more accurate estimate of optimal values in case of having low number of variables [59]. Planning the experiment by using DOE allows studying the interaction between variables, conjointly reducing the number of experiments needed, reducing time and chemical waste generated [59,60].

2. Aim of Study

Even though many sensors and biosensors for BPA have already been successfully constructed and applied, with results comparable to the more traditionally employed methods, the aim of the following work is to design an electrochemical BPA sensor using Screen-printed Electrodes. Targeting to enhance selectivity and sensitivity of the sensors without compromising the stability, practicality and on-site use, an array of chemical modifiers with conducting properties will be tested and conjugated with a Copper-Metal-Organic framework that possesses unique properties, such as specificity towards BPA, without unstableness of biological recognition elements.

In order to evaluate the potentiality of the BPA sensor, it is also our objective analyte detection in more complex mediums, such as synthetic urine and real urine samples.

To achieve what is proposed, the sensor development process was divided into six target stages:

- Testing of different types of SPEs (both commercial and home-made);
- Study of ideal conditions using design of experiments;
- Testing SPEs with various surface modifications, such as carbon nanotubes, gold nanoparticles and Cu-MOF
- Examining the combination of several surface modifiers;
- Measuring BPA in synthetic urine samples with the optimized sensor;
- Measuring BPA in real urine samples with the optimized sensor.

3. Experiments

3.1 Reagents

In order to execute the necessary experiments, some chemical products were acquired. From Sigma-Aldrich (Steinhem, Germany) were purchased Bisphenol A ($C_{15}H_{16}O_2$), Potassium Phosphate (K_2PO_4), Creatinine ($C_4H_7N_3O$), Hydrogen tetrachloroaurate(III) hydrate ($HAuCl_4$), Terephthalic acid (1,4 – H_2BDC), Triethylenediamine (TED)($C_6H_{12}N_2$), N,N-Dimethylformamide (DMF)(C_3H_7NO) and Ascorbic Acid ($C_6H_8O_6$).

Sodium Chloride (NaCl), Methanol (CH_3OH), Citric Acid ($C_6H_8O_7$) and Sodium Bicarbonate ($NaHCO_3$) were obtained from Fisher-Scientific (Loughborough, UK).

Merck Chemicals (Darmstadt, Germany) provided Copper Nitrate Trihydrate ($Cu(NO_3)_2.H_2O$), Acetonitrile (C_2H_3N) and Sodium Phosphate Tribasic (Na_3PO_4).

From Panreac-Apllichem (Darmstadt, Germany) was purchased Sodium Phosphate Dibasic (Na_2HPO_4), Sodium Phosphate Monobasic (NaH_2PO_4) and Sulfuric Acid (H_2SO_4).

Urea (CH_4N_2O) was obtained from VWR BDH Prolabo (Leuven, Belgium) and Sodium Hydroxide (NaOH) was obtained from JMGS (Odivelas, Portugal)

From DropSens (Oviedo, Spain) Screen Printed Carbon Electrodes (DRP-110), constituted by conducting silver lanes, reference electrode printed with silver ink, and a working (4mm) and counter electrode printed with carbon ink. Also purchased from DropSens, was the solution of Multi Walled Carbon Nanotubes (MWCNT) (DRP-CNTSOL) and powdered MWCNT (DRP-MWCNT).

To produce Screen-Printed Electrochemical Sensors with silver lanes, several different inks were used, namely C10903P14 (carbon ink) and D2071120D1 (dielectric ink), from Gwent Electronic Materials (Torfaen, UK); and Electrodag 418 (Ag ink) and Electrodag 6037SS (Ag/AgCl ink) from Acheson Colloiden (Scheemda, The Netherlands). The same inks were used when producing Screen-Printed Electrochemical Sensors with Carbon lanes, with exception of Electrodag 418 (Ag ink).

Water used in solution preparation, as well as in washing the electrodes prior to functionalization and use, was obtained from Milli-Q Integral Water Purification System (Millipore Iberica, Madrid, Spain). All used reagents were analytical grade.

3.2 Material and Methods

3.2.1 Methods

In order to access optimal conditions for BPA detection, several conditions varied in the way measurements were performed, such as sensor type, if experiments were performed in a cell or using a single drop and which medium was used. This information is summarized in image 3.10.

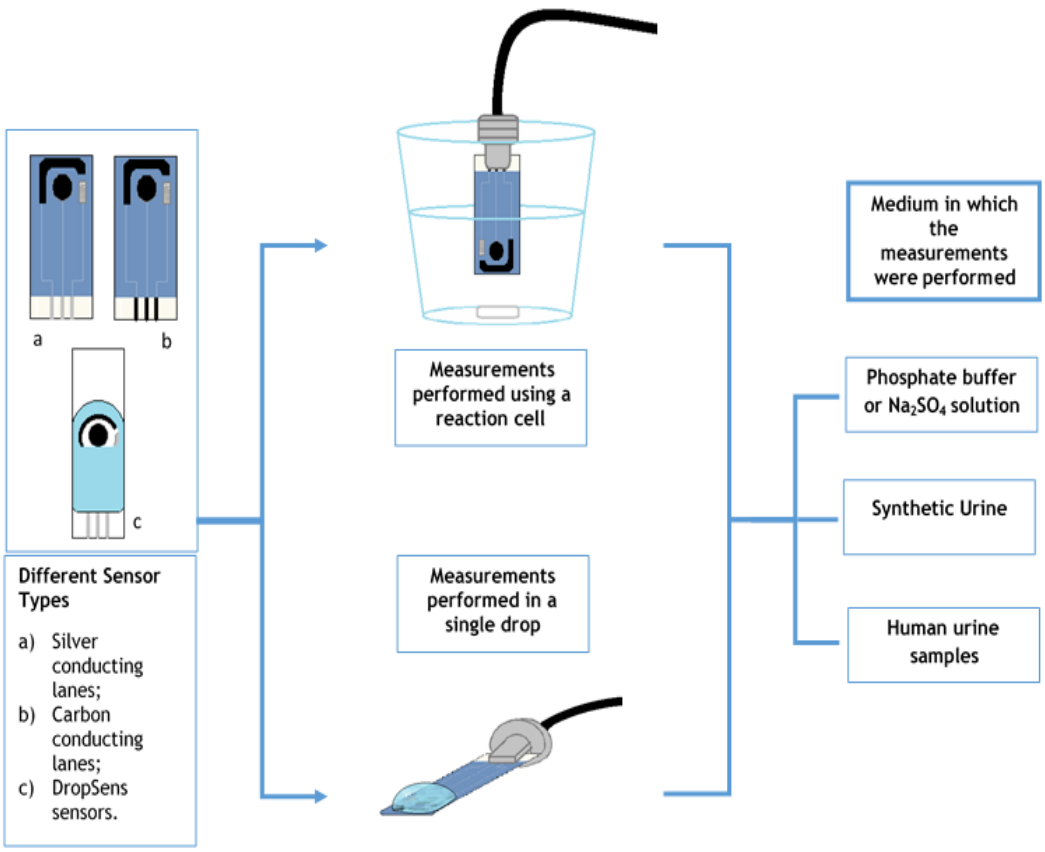

Image 3.10. – Overview of sensors, methods and mediums used in BPA detection.

3.2.1.1 Electrochemical measurements

Several electrochemical techniques were tested in the present work. Since parameters such as scan rate and step potential influence the final result, these values were maintained constant for each technique.

- **Cyclic Voltammetry; Linear Sweep Voltammetry; Square Wave Voltammetry**:
  - Scan rate – 0.05 V/s
  - Step Potential – 0.009 V

- **Differential Pulse Voltammetry**
  - Modular amplitude – 0.05
  - Step Potential – 0.009 V

3.2.1.2 Solutions

3.2.1.2.1 General solutions and buffers

Phosphate buffer with pH below 9 was prepared by adding to a solution of Na_2HPO_4 (0.1M) a solution of NaH_2PO_4 (0.1M), in order to achieve the desired pH for each trail. For phosphate buffer with pH higher than 9, Na_3PO_4 (0.1M) was added, in needed quantity, to a solution of Na_2HPO_4 (0.1M).

Besides Phosphate Buffer, a solution of Na_2S0_4 of pH's 5, 7 and 9 was used as a medium in trials involving Design of Experiments. These pH were attained by adding, to a solution of Na_2SO_4 (0.1M), either NaOH (0.01 M) or H_2SO_4 (0.01M). The volume of the initial solution was then corrected.

3.2.1.2.2 Bisphenol A (BPA)

Knowing that BPA is moderately soluble in water (300 mg/L at room temperature [8]), at first, a solution of this compound was prepared by a method suggested by Ndlovu *et al*. [16]. For this, BPA, was weighed and dissolved in acetonitrile (1:100 proportion), adding phosphate buffer until achieving the right volume. For better dissolution of BPA, the preparation was sonicated for as much time as needed to eliminate BPA precipitates and was kept refrigerated when not in use. This method was latter on discarded, since precipitates tended to reappear.

A better method of BPA dissolution was proposed by Alkasir *et al*. [13], which consisted in dissolving this compound in methanol. As so, the required quantity of BPA to obtain a

concentration of 0.01M was added to a certain volume of methanol, being this stock solution stored at 4ºC. When needed, a working solution was prepared using phosphate buffer or a Na_2SO_4 solution at pH corresponding to that in use.

3.2.1.2.3 Synthetic urine

Synthetic urine was prepared as described in CDC Laboratory Procedure Manual [61]. To prepare this medium, reagents listed below were added in the shown sequence: 500 mL of deionized water; 3.8g of Potassium Chloride (KCl); 8.5g of Sodium Chloride (NaCl); 24.5g of Urea (CH_4N_2O); 1.03g of Citric Acid ($C_6H_8O_7$); 0.34g of Ascorbic Acid ($C_6H_8O_6$); 1.18g of Potassium Phosphate (K_2PO_4); 1.4g of Creatinine ($C_4H_7N_3O$); 0.64g of Sodium Hydroxide (NaOH), added slowly; 0.47g of Sodium Bicarbonate ($NaHCO_3$) and 0.28mL of Sulfuric Acid (H_2SO_4). Finally the volume was corrected to 1 Liter. Synthetic urine was stored at 4ºC until needed.

3.2.1.2.4 Human urine samples

Human urine samples were collected from male donors, analyzed (Appendix images A1 and A2) and stored at -20ºC. When needed, samples encoded GS120390 and JS080590, were defrosted overnight and stored at 4ºC. When in use, urine samples were homogenized and diluted as needed.

3.2.1.3 Disposable Screen-Printed Electrochemical Sensors (SPES)

Screen-Printed Electrochemical Sensors were fabricated by a successive deposition and curing of inks, passing through a stencil which had the shape of the different components in the electrochemical sensor (Image 3.11 and 3.12).

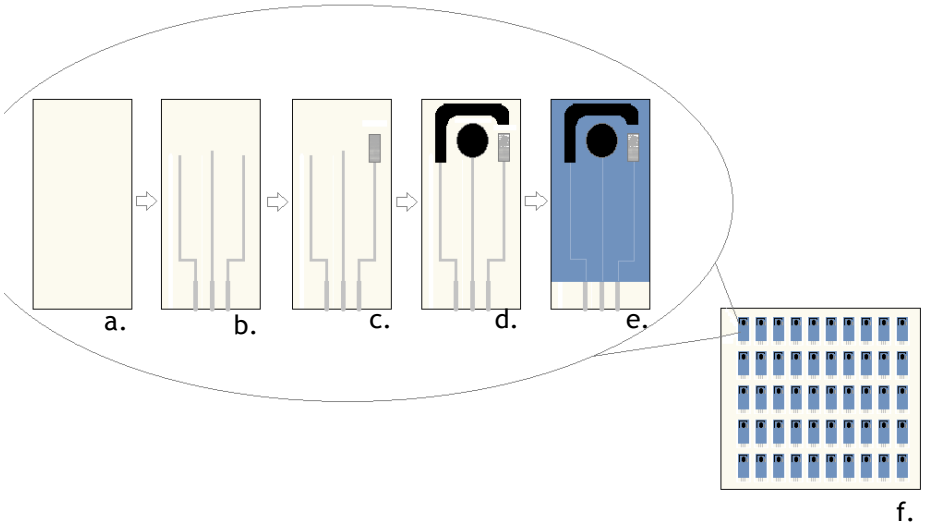

Image 3.11 - Method of Silver Lanes Screen-Printed Electrode fabrication. **a.** PVC substrate; **b.** Deposition of silver ink (**Electrodag 418)** to produce conducting lanes; **c.** Deposition of Ag/AgCl ink (**Electrodag 6037SS**) to form the reference electrode; **d.** Deposition of carbon ink (**C10903P14**) to form both working and counter electrodes; **e.** Deposition of dielectric ink (**D2071120D1**) as the final isolating layer; **f.** Finished sheet of Screen-Printed electrodes.

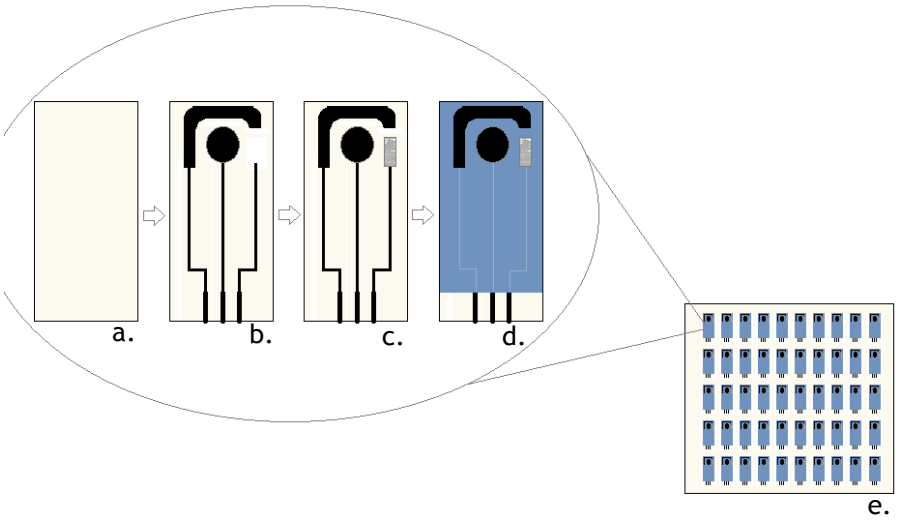

Image 3.12 - Method of fabrication of Carbon Lanes Screen-Printed Electrode. **a.** PVC substrate; **b.** Deposition of carbon ink (**C10903P14)** to produce conducting lanes, working electrode and counter electrode.; **c.** Deposition of Ag/AgCl ink (**Electrodag 6037SS**) to form the reference electrode; **d.** Deposition of dielectric ink (**D2071120D1**) as the final isolating layer; **e.** Finished sheet of Screen-Printed electrodes.

3.2.1.4 Modification of electrochemical sensor surface

3.2.1.4.1 Gold Nanoparticles

Gold Nanoparticles (AuNP) were directly deposited on the three electrode system by electrochemical deposition. In order to do so, 100 µL of a $HAuCl_4$ solution (1mM of HAuCl4 in H_2SO_4 500 mM) was placed on the three electrodes. By Amperometry (Energy applied 0.18V; Duration 20s; Sample time 0.01 s) AuNP were deposited on the electrodes, which was confirmed by a scan performed by Cyclic Voltammetry (from -0.5V to 1V, E_{step} -0.012V and Scan Rate 0.1V/s).

3.2.1.4.2 Carbon Nanotubes

Besides Carbon Nanotubes (CNT) bought in a commercial solution with unknown concentration (Dropsens, Spain), a suspension of CNT, derived from their solid form (Dropsens, Spain), was also used.

To synthetize this dispersion, CNT were weighed and N,N-Dimethylformamide (DMF) was added to achieved a concentration of 3.5g/mL, as suggested by Asturias *et al.*[27]. The solution was sonicated until homogeneity was achieved. While working with this dispersion, it was noticed some difficulties in the drop formation when depositing CNT on the working electrode surface. After searching for DropSens CNT commercial solution product information, it was observed that it has in its constitution deionized water, however, with an unspecified proportion. As so, 1/3 of the content of CNT dispersion was added in water, obtaining a new concentration of 2.33mg/mL of CNT.

To immobilize the CNT on SPE's, working electrode was washed with deionized water and was air dried. After re-suspending CNT by using a vortex, 3 µL of CNT commercial solution or synthetized solution were deposited on the surface of the working electrode and were let air dry until solvent evaporation or overnight. Prior to use, electrode system was washed with deionized water, being the excess removed with a paper towel.

3.2.1.4.3 Copper Metal-Organic Frame

3.2.1.4.3.1 Synthesis

A Metal-Organic Frame (MOF), with the metal element being Copper (Cu-MOF) was synthetized by solvothermal reaction, based on a method suggested by Lee *et al.* [36]. Copper Nitrate Trihydrate ($Cu(NO_3)_2.H_2O$) (0.074g), Terephthalic acid (1,4 – H_2BDC) and TED (Triethylenediamine - 1,4-Diazabicyclo[2.2.2]octane) (0.048g) were dissolved in 15 mL of DMF. After sonication, the blue solution was transferred to a ceramic vessel that was left at 120ºC for 48h in an oven (Image 3.13). After cooling down to room temperature, a blue crystalline powder was scraped from the ceramic vessel, washed with 3×5mL of DMF and was let to dry overnight. Cu-MOF powder was transferred into an eppendorf and weighed, being the total Cu-MOF synthesis yield 20.78%.

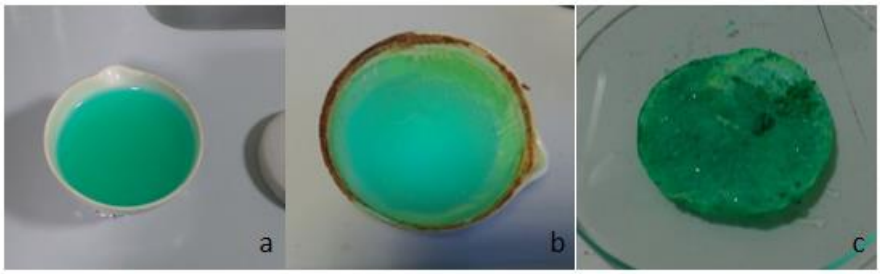

Image 3.13 – Synthesis process of Cu-MOF frame. a) solution of Cu-MOF; b) crystalline powder formed on vessel walls after 48h in an oven ate 120°C; c) powder obtained after washing with DMF and letting dry overnight.

3.2.1.4.3.2 Deposition of Cu-MOF

A suspension of Cu-MOF powder was prepared by weighing the compound and dissolving it in DMF, achieving a final concentration of 1mg/mL. This was done by sonicating the solution for as much time needed to dissolve the powder and to achieve homogeneity. A suspension of 2mg/mL was also tried, although results were not better as the first concentration, therefore the latter suspension was discarded.

To deposit Cu-MOF on the surface of the working electrode, SPE was washed with deionized water and let to dry, being deposited on the working electrode 3µL of the suspension, after its homogenization. SPE was left to dry until solvent evaporation or overnight and was washed with deionized water and dried with a paper towel prior to use.

3.2.1.4.4 Copper Metal-Organic Frame and Carbon Nanotubes

The suspension of Cu-MOF (1mg/mL) was then combined with the CNT (2.33mg/mL) previously synthetized [35].

Cu-MOF and CNT were either combined homogenously, and deposited using the same technique described for Cu-MOF deposition, or were sequentially immobilized. For the last method, three approaches were used, with previous and after care to the electrode similar to those already described:

- Appling 3µL of CNT, allowing solvent complete evaporation, then depositing 3µL of Cu-MOF and leaving it to dry completely;
- Combining, at the same time, on working electrode surface, 3µL of CNT and 3µL of Cu-MOF;
- Combining simultaneously on electrode surface 1.5µL of CNT and 1.5µL (similar to the previous method, but half the volume).

For homogeneous combination of CNT and Cu-MOF, the needed volume of each suspension was measured in order to obtain following relation (Table 3.3).

Table 3.3 - Proportions of CNT (1mg/mL) and Cu-MOF (2.33mg/mL) deposited upon homogeneous combination of both.

5% CNT	95% Cu-MOF
10% CNT	90% Cu-MOF
30% CNT	70% Cu-MOF
60% CNT	40% Cu-MOF
90% CNT	10% Cu-MOF

Upon combination of different proportions of both components, each suspension was sonicated for the amount of time needed to combine both. Deposition of each proportion was carried out by first washing and air drying each electrode, measuring on to working electrode surface 3µL of the suspension, allowing solvent evaporation or letting it dry overnight. Prior to the use of each suspension, vortex homogenization was needed.

3.3 Material and Software

To print SPEs, polyester screens were used on a DEK 248 screen-printing system (DEK, Weymouth, UK). The screens were mounted on a 45º angle to the printer stroke and the printing process was carried out as shown in Images 1.6., 3.11. and 3.12.

To perform electrochemical measurements μAutolab Type III and Autolab PGSTAT128N electrochemical system were used, associated to General Purpose Electrochemical System (GPES) (software version 4.9) from Metrohm-Autolab, Utrecht, the Netherlands.

Design of experiments was planned using Design-Expert software version 7.0 (Stat-Ease, Inc., Minneapolis, USA). Calculation of the detection limits of the sensors were performed by using DETARCHI software, acquired from the University of Burgos, Spain.

4. Results and Discussion

4.1 Bare homemade electrodes

4.1.1 Homemade screen-printed sensors with silver conducting lanes

Since the aim of this work is to develop a sensitive sensor towards Bisphenol-A (BPA), in order to improve the sensors performance, some optimizations were necessary. At first, to determine BPA's electrochemical activity, its detection was carried out on bare working electrodes, with silver conducting lanes and an Ag/AgCl pseudo - reference electrode. Electrochemical measurements were done both in a cell and on a drop, which was deposited on the three electrode system. These two measurement methods allow to better understand if the difference in diffusivity when working at different volumes could play an important role in BPA detection. In each method, measurements of different BPA concentrations were done using the same sensor for each of the analyzed concentrations.

When using the same sensor, it was noticed that current decreased with each measurement performed. This happens due to the BPA polymerization on the electrode surface, which forms a polymeric film and therefore causes electrode fouling [16]. In order to try and minimize this phenomenon, virgin electrodes were used, both for the cell and drop experiments. The best results were obtained for measurements carried out in a cell, leaving us to adopt this procedure in the experiments performed from now on, if nothing said in contrary.

Considering the moderate BPA solubility in aqueous solutions, as previously mentioned and described by Alkasir *et al*. [13] BPA was dissolved in methanol. Because of this, methanol's influence in BPA detection was studied and proven to not interfere with the analyte's detection.

4.1.2 Homemade screen-printed sensors with carbon conducting lanes

To see if the composition of the conducting ink had any influence on the signal detected for BPA, sensors with carbon lanes instead of silver lanes were tested. Since the noise was minimized for this type of sensor, it was used hereinafter for homemade sensors.

For carbon conducting lanes sensors, experiments were carried out on the same electrode and also using one sensor for each BPA concentration, procedure justified, as mentioned before, by the polymerization of BPA on the electrode. When using new sensors for each concentration (Graph 4.1), a linear relation between BPA concentration and current intensity was observed, on the other hand, when using the same sensor (Graph 4.1), no linearity was achieved, essentially due to BPA polymerization and consequent accumulation on the working electrode

surface [46]. When using the same sensor, at a given BPA concentration, current intensity is reduced when compared to intensity presented when a virgin sensor is used.

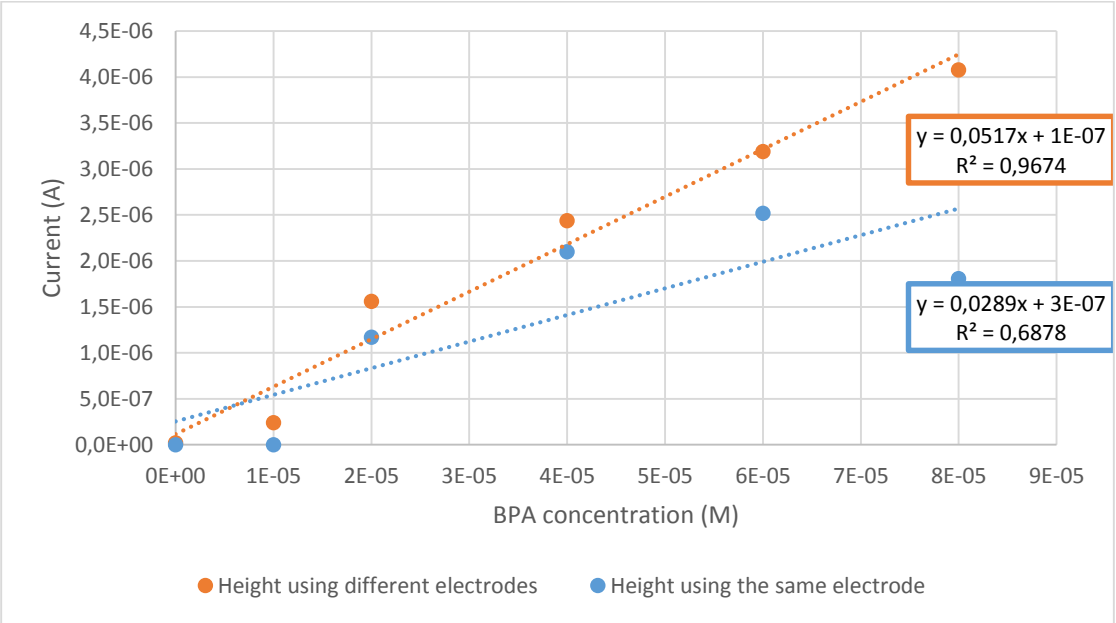

Graph 4.1 - Height of peaks for different BPA concentrations (1×10^{-5}M to 8×10^{-5}M) using the same and new SPE. Cyclic Voltammetry was performed in presence of phosphate buffer pH 8.

4.1.3 Stirring time

In order to evaluate the stirring effect on peak height, and therefore in BPA detection, a range of stirring times were studied using virgin sensors. This variable is important to be studied in electrochemical sensing since it promotes homogeneity of the solution and could influence BPA pre-concentration on the electrode surface, and, therefore the quality of analyte detection. As seen in Graph 4.2., the maximum peak height is achieved for a stirring time of 2 minutes, being unnecessary any further homogenization, as peak heights decrease from there on. Since peak heights were expected to be maintained constant after its maximum, the observed decrease in intensity is believed to be related with the fouling of the working electrode due to excessive accumulation of polymerized BPA.

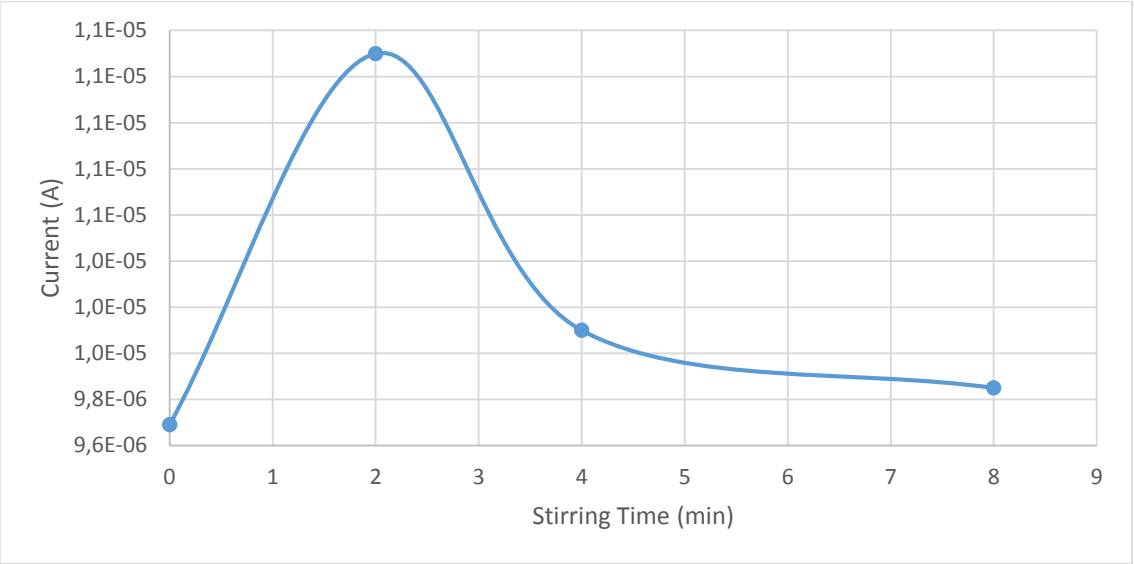

Graph 4.2 - Height of peaks for a constant concentration of BPA of 5×10^{-4}M, using different SPE for each stirring time (0, 2, 4 and 8 minutes). Cyclic Voltammetry was performed in presence of phosphate buffer pH 8.

4.1.4 Pretreatment time and voltage

Tested the influence of stirring time prior to electrochemical measuring of BPA, a series of experiments were conducted to determine if the application of a constant potential before measurements would influence BPA detection by allowing its pre-concentration on the electrode surface. To perform this, virgin electrodes were used, maintaining constant the concentration of BPA (5×10^{-4}M) and the pretreatment time period (30s) (Graph 4.3). A maximum on the oxidation current was attained at a pretreatment voltage of -1V, with no experiments done for potentials bellow that value. When using positive potentials, BPA accumulation and detection was severely reduced.

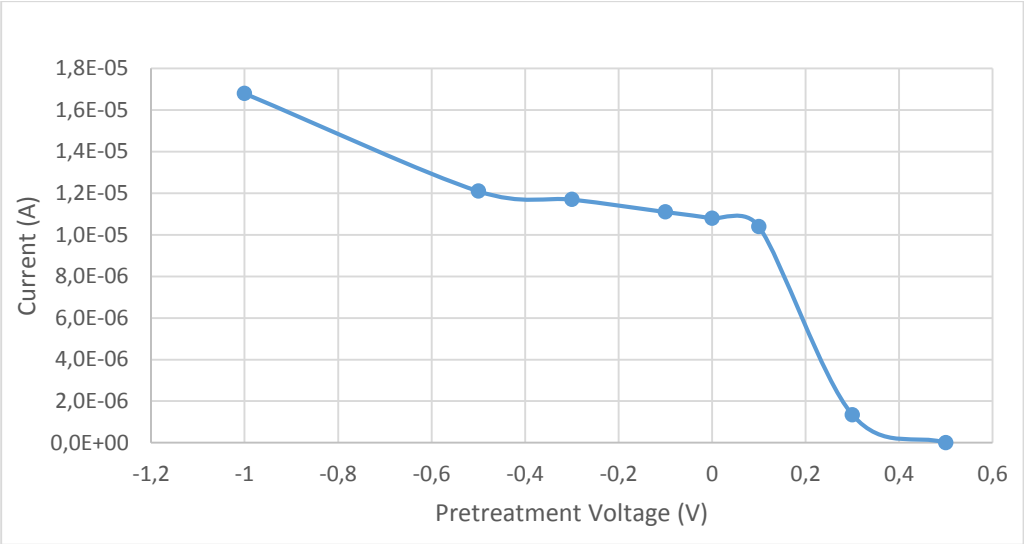

Graph 4.3 - Height of peaks as function of pretreatment voltage (-1, -0.5, -0.3, -0.1, 0, 0.1, 0.3 and 0.5 V). Constant time (30s) and BPA concentration (5×10^{-4}M) were employed. Cyclic voltammetry was performed in presence phosphate buffer pH 8.

Optimum electrode BPA pre-enrichment is also affected by the pretreatment time, thus this parameter was similarly optimized. Using a constant potential of -1V, for which the best results were obtained, different pretreatment times were studied. To better see the difference with and without pretreatment, the concentration of BPA was lowered to 5×10^{-5}M, since the difference between peak heights would be more noticeable for BPA lower concentrations.

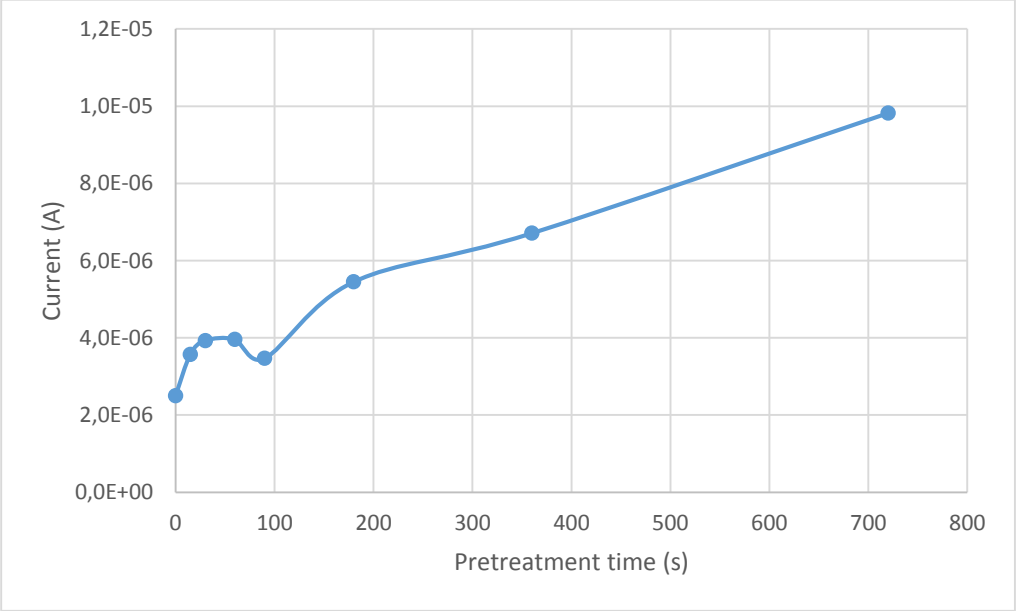

Graph 4.4 - Height of peaks as function of pretreatment time for BPA concentration of 5×10^{-5}M by applying a constant voltage of -1V. Cyclic Voltammetry was used in phosphate buffer pH 8.

As can be seen in Graph 4.4., a plateau is observed for pretreatment times around 60 s. After that, peak height increases with increasing pretreatment time, until 720 s, with no studies being done for higher time periods. Even though peak height is better at 720 s, a deformation of the peak occurred, therefore compromising the preciseness of the method (Appendix – Graph A1). In addition, 720 seconds (12 minutes), makes the process quite time consuming. As so, 60s was the time chosen to apply in BPA pre-concentration.

4.1.5 pH influence

Since previous studies have shown better results for the peak current response at higher pH values, superior to BPA's pK_a (pK_a = 9.73), due to a better adsorption of the dissociated form of BPA compared with its non-dissociated form [46], a different pH, higher than BPA's pK_a, was studied. Therefore, a solution of Na_3PO_4 with a pH of 12 was used as a medium to run cyclic voltammetric experiments. This was done using new sensors for each of the tested concentrations.

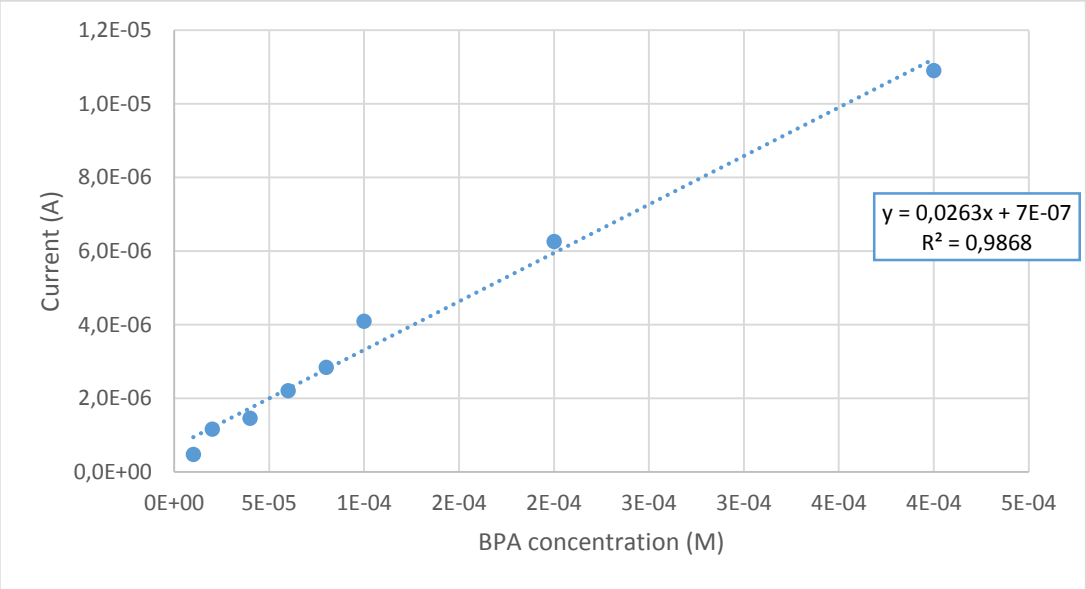

Graph 4.5 - Height of peaks for as function of BPA concentrations (1×10^{-5}M to 4×10^{-4}M) using new sensors for each concentration, in Na_3PO_4 pH12. Cyclic Voltammetry was used.

As noticed from Graph 4.5., and by Graph A2 in the appendix, the height of BPA peaks was relatively proportional to BPA concentration. For this reason, this solution was used as a medium for added studies, being substituted by a basic buffer solution later on.

4.1.6 Working electrode regeneration

The Na_3PO_4 solution with a pH of 12 was also tested when sequential experiments were run on the same sensor. Under these circumstances, an attempt to regenerate the electrode that, as mentioned before, suffers polymerization, was made in order to try to re-use the electrode without compromising the accuracy of detection. This was done by first inducing polymerization of BPA on the electrode surface by performing 5 cyclic voltammetric scans in order to ensure total fouling of the electrode surface, thus maintaining this variable constant. After this, regeneration of the electrode was attempted by doing a defined number of Cyclic Voltammetries in the range of 0V to -1.5V (Graph 4.6). Each of the electrodes was regenerated 3 times to see how much it could withstand this process (Graphs 4.7).

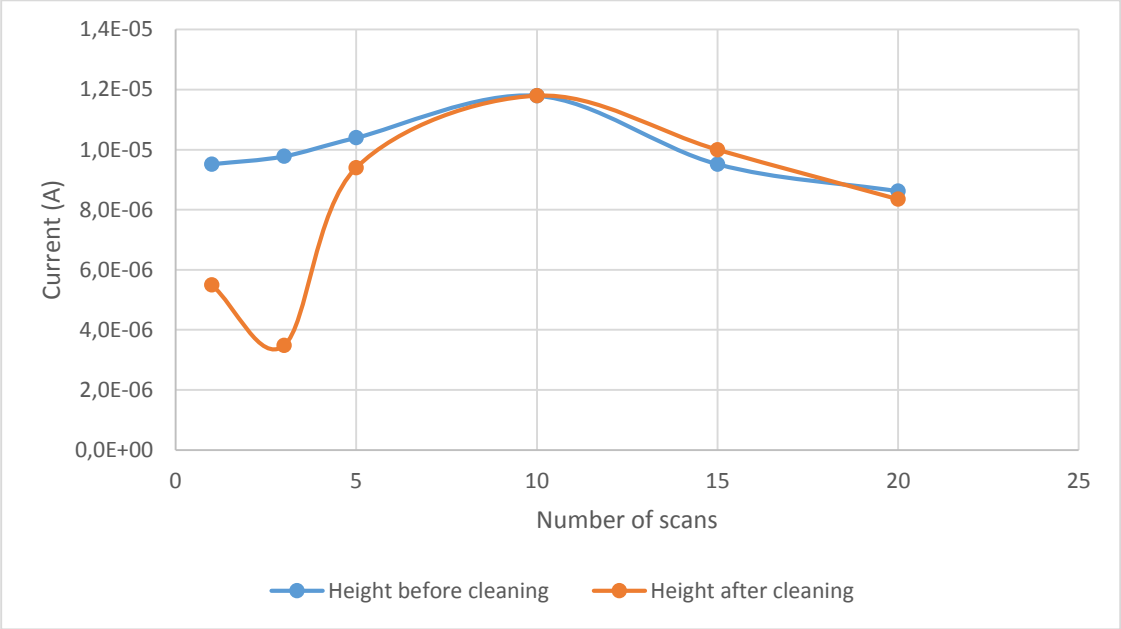

Graph 4.6 - Comparison of the height of the peaks before and after the cleaning process, depending on the number of scans used to clean the electrode (1, 3, 5, 10, 15 or 20 scans). Na_3PO_4 pH12, at a fixed BPA concentration of 5×10^{-4}M. Cyclic Voltammetry was used.

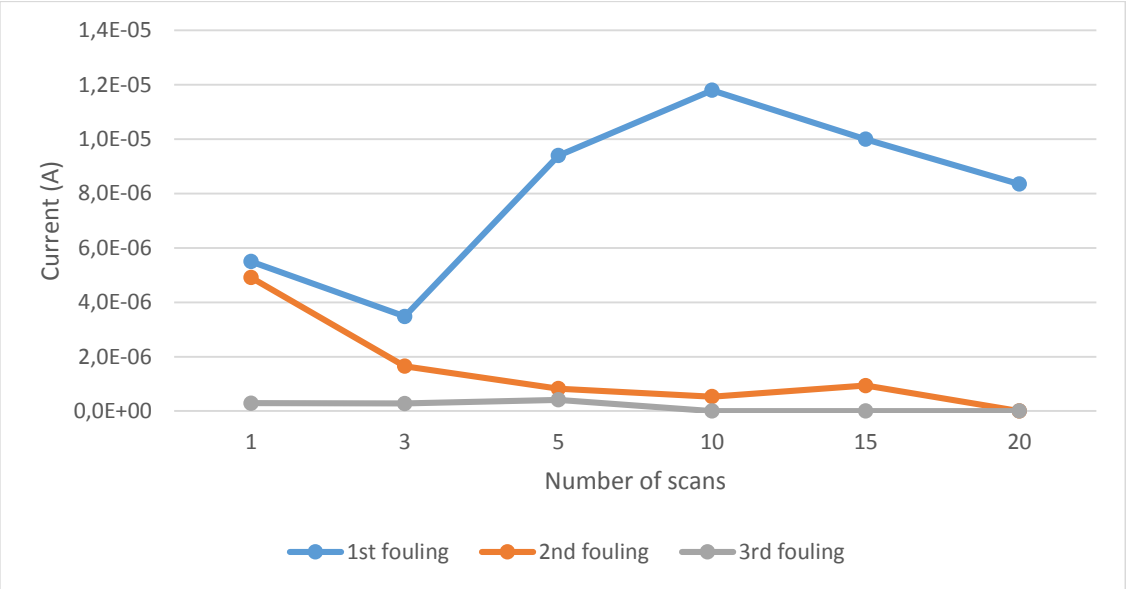

Graph 4.7 - Representation of the height of the peaks for each fouling, depending on the number of scans used to clean the working electrode (1, 3, 5, 10, 15 or 20 scans). Na_3PO_4 pH12, at a fixed BPA concentration of 5×10^{-4}M. Cyclic Voltammetry was used.

When comparing the height of BPA peaks before and after the cleaning procedure (representative curves in Graph A3, Appendix and Graph 4.6), it is noticed that the number of CV scans used to clean the electrode directly influences the success of the working electrode regeneration, with the ideal number of scans being 10 (Graph 4.6). It is also noticed that trying to regenerate the electrode a second and third time leads to a great decrease in its efficacy, due to the electrochemical wearing of the electrode system, being this a trend more pronounced when higher number of scans were used in the cleaning process (Graphs 4.7). For the described reasons, regeneration and re-use of the electrode is not recommended more than once, with an ideal number of scans used to clean the electrode equal to 10, so electrode deterioration can be prevented.

4.2 Design of Experiments

To further access the ideal conditions for the detection of BPA, not evidenced by the previous assays, and to test new conditions, design of experiments (DOE) was used. This type of approach allows the analysis of several variables at the same time, using the minimum number of necessary experiments. It also is ideal to see interactions between variables, which are not easily detected by individual experiments.

In this design, three replicates for each experience where used in a central composite design, different from other types of factorial designs available by including mean points for the variables and therefore allowing a more accurate prediction of optimal values.

The variables studied, in three levels, were: Deposition time; Pretreatment Voltage; Solutions and pH (Table 4.4). These variables were chosen in order to better study interactions between previously optimized parameters and also to study different mediums due to some instability associated with the Na_3PO_4 solution at pH 12.

In order to evaluate the studied variables, the responses chosen were peak height, peak area and position of the peak, or peak potential, the three most important parameters when performing electrochemical studies. Concentration of BPA was maintained constant (5×10^{-5}M) and the method used to measure BPA peaks was Linear Sweep Voltammetry (LSV), chosen for having an improved sensitivity over cyclic voltammetry [62].

Table 4.4 – Studied variables when using DOE and values corresponding to each level.

	Deposition Time (s)	Pretreatment Voltage (V)	pH	Solutions (categorical)
Low	0	-1.5	5	Na_2SO_4
Mean	90	0	7	
High	180	1.5	9	Phosphate Buffer

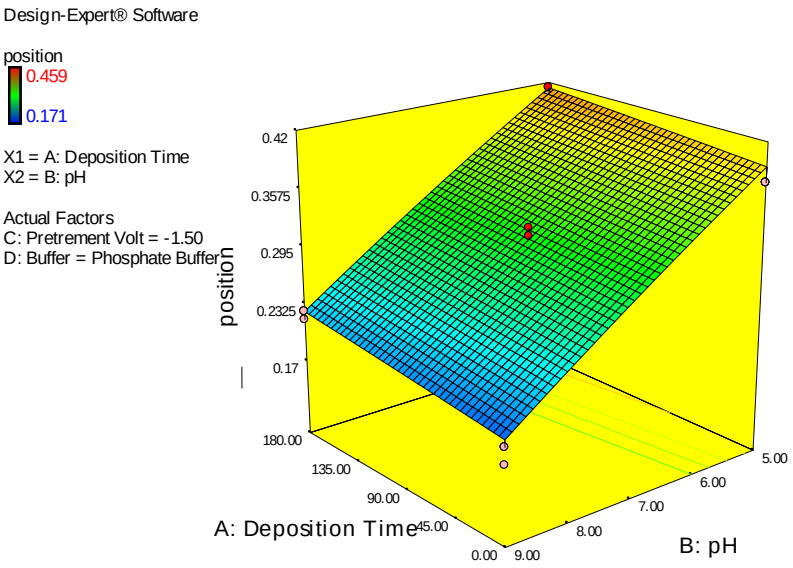

Image 4.14 - Design Expert 3D graph for the response Position (Potential), with pretreatment voltage on the low level (-1.5 V) and using Phosphate buffer.

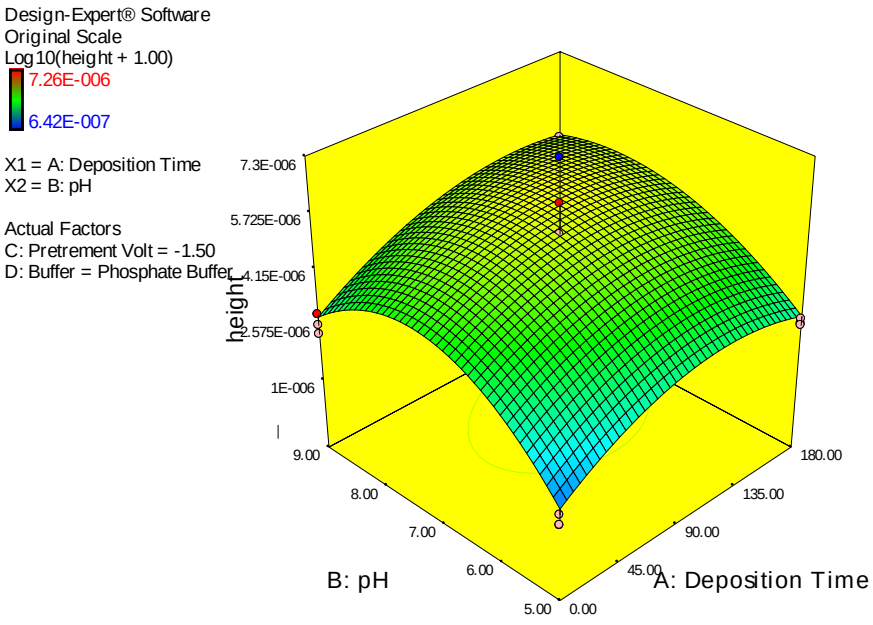

Image 4.15 - Design Expert 3D graph for the response Height of peaks, with pretreatment voltage on the low level (-1.5V) and using Phosphate buffer.

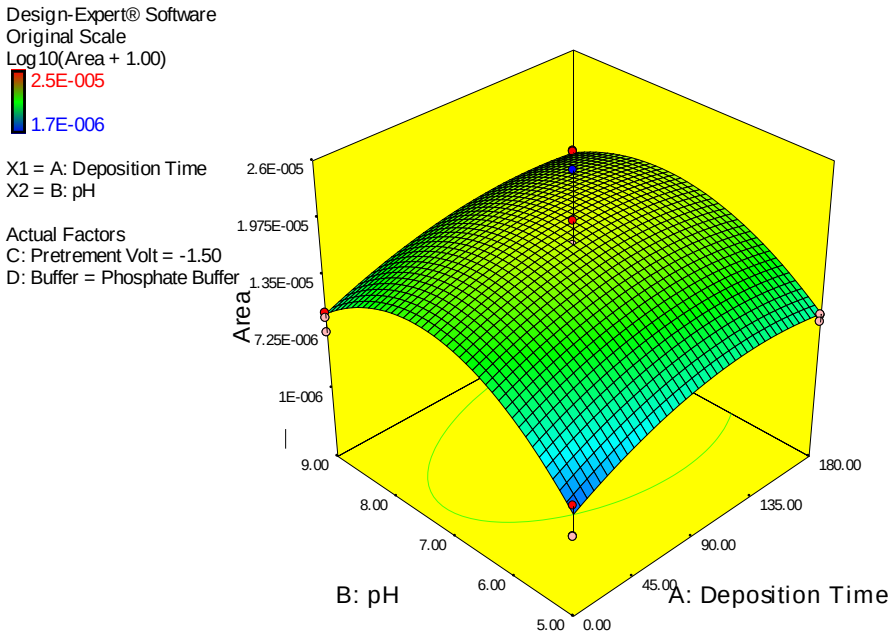

Image 4.16 - Design Expert 3D graph for the response "Area", with pretreatment voltage on the low level (-1.5V) and using Phosphate buffer.

Although being possible to distinguish an ideal frame of work by mere observation of the plotted 3D graphs (Images 4.14 to 4.16), more precise information is suggested by Design Expert software, with various optimal conditions recommended for maximized BPA response: high peak height, allowing a more sensitive detection of BPA, low peak area, which give a more accurate response, and low peak potential, which minimizes interfering agents. These were the conditions chosen to proceed with other experiments.

- **Deposition Time** – 150s
- **Pretreatment Voltage** – (-1.5)V
- **pH** – 8.2
- **Buffer** - Phosphate Buffer

Some of the conditions suggested by the software are in agreement with experiments that were conducted before application of DOE, such as a more negative pretreatment voltage. Pretreatment time has doubled in relation to earlier studies and pH has decreased in comparison to the medium that was being used (Na_3PO_4 – pH 12). The fact that phosphate buffer is a more stable solution played an important role in its better performance, evidenced by the not as good results obtained when using Na_2SO_4 solution (Appendix – Graphs A4 to A6). The

differences that were noticed prove the relevance of this type of design planning in alternative to more traditional one-at-a-time variable studies, allowing for a more accurate prediction of ideal conditions.

4.3 Optimization after design of experiments

In the conditions acquired in the previous study, several experiments testing regeneration techniques and involving deposition time, using new and the same electrode for each concentration, were performed.

Even though the cleaning method showed some potential to regenerate the working electrode, this technique was dropped since it was time consuming and could lead to higher peaks if not well performed, due to some BPA accumulation on the electrode surface. Furthermore, screen printed sensors are known for being disposable, once very low costs are associated with their production.

Different pretreatment deposition times were then applied when was used a new electrode for each analyzed concentration. The range of deposition times chose for pretreatment was based on results obtained in one variable studies (Section 4.1) and the conditions given by DOE. All the experiments were done twice (Graph 4.8).

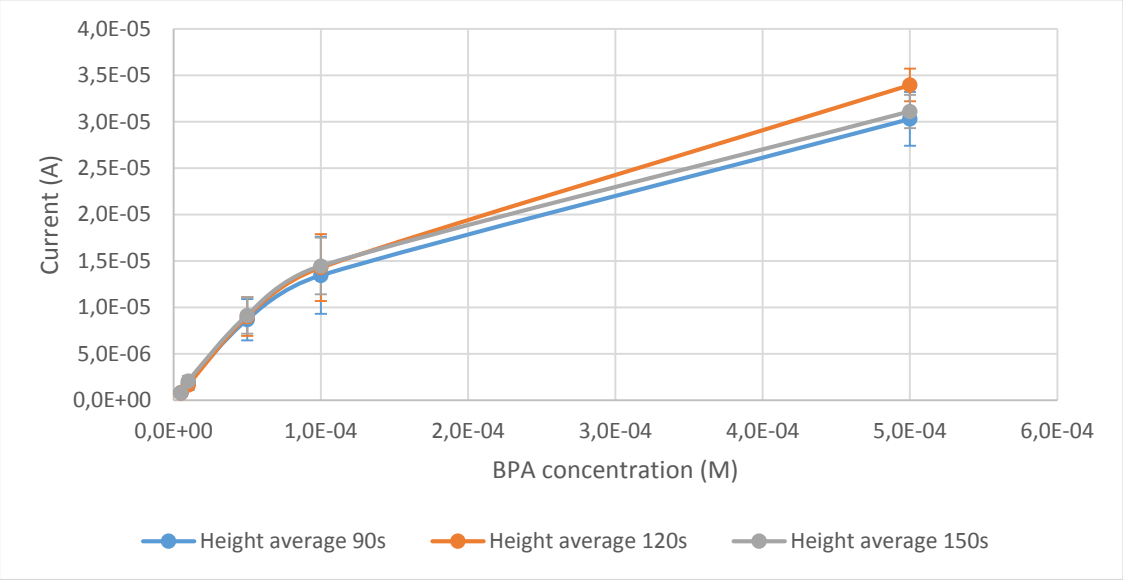

Graph 4.8 - Comparative representation for each deposition time average (90, 120 and 150 s) depending on BPA concentration (ranging from 1×10^{-7} to 5×10^{-4}M), with associated error bars. Performed in phosphate buffer pH8.2, using virgin electrodes and LSV electrochemical detection method.

The conditions obtained in DOE were also tested without using any pretreatment, contrary to what were the optimal results given by Design Expert software, since pretreatment can wear the electrode system. These were tested using the same and virgin electrodes (Graph 4.9) where it is possible to observe once more the saturation of the electrode when using the same SPE for different BPA concentrations (though being linear in lower concentrations) and the

linearity throughout the assay when using virgin SPE. When compared to pretreated electrodes, height of peaks is lower, therefore being well predicted by Design Expert software.

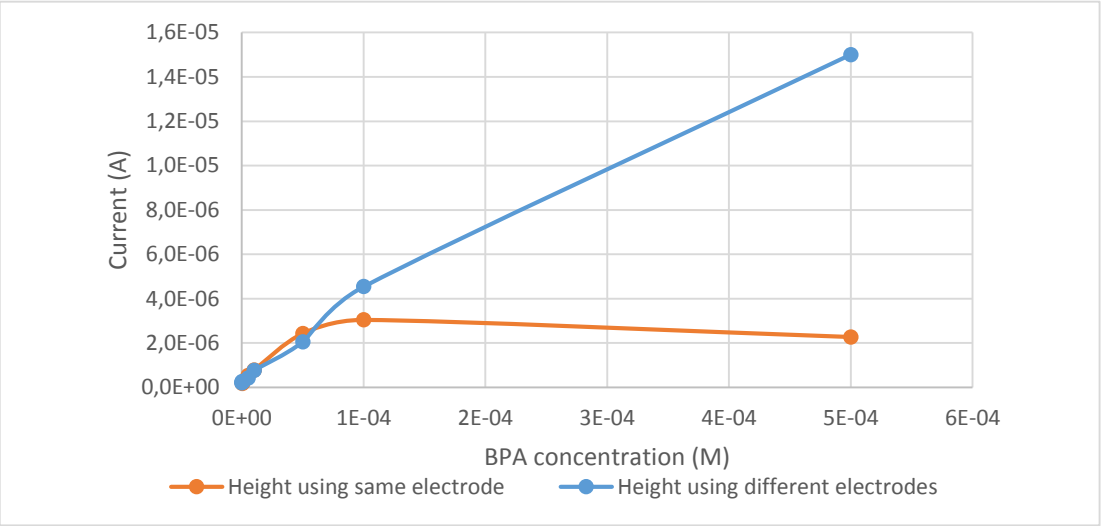

Graph 4.9 - Height of the peaks in phosphate buffer pH8.2, without pretreatment, using virgin and the same sensor for each BPA concentration. LSV with BPA in a range from 1×10^{-7} to 5×10^{-4}M.

Without using any pretreatment different pH were tested as well, to see the difference between them that may have not been clarified in DOE. As expected and shown in graph 4.10 pH 8.2 is the one with the best performance, even though it could be though that the best results were obtained for pH 7, which does not correspond to the truth since peaks for pH 7 were deformed and therefore provided unrealistic good results.

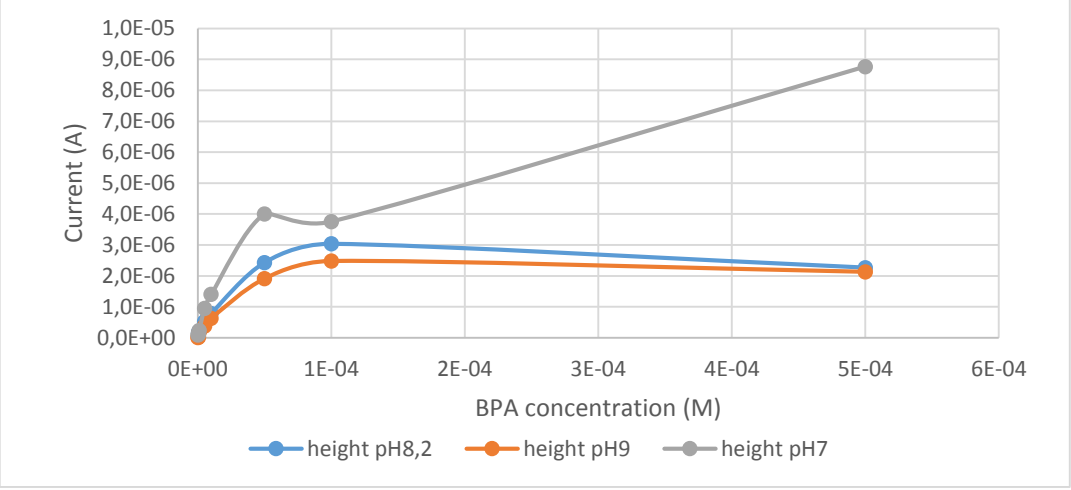

Graph 4.10 - Height of BPA peaks for different pH (7, 8.2, and 9) depending on its concentration. LSV with BPA in a concentration range from 1×10^{-7} to 5×10^{-4}M. Phosphate Buffer pH 8.2 was used.

When measuring BPA peaks, it was noticed that the position in which the peak appeared differed for each concentration, leading to believe that the reference electrode could interact with BPA. To see if peaks displacement was due to this phenomenon, procedures in which the working electrode was isolated and reference electrode was an Ag conventional reference and not an Ag/AgCl pseudo-reference, were carried out. It was verified that displacement of the peaks had nothing to do with the reference electrode, since in this conditions it also happened.

Since Linear Sweep Voltammetry (LSV) is not one of the most sensitive methods of detection, even though being used in DOE and experiments after that, due to good results, an effort was made to change the detection method to a more sensitive one, namely Differential Pulse (DP) or Square Wave Voltammetry (SWV). Both of these methods show diminished background noise since a pulse of potential is applied immediately before and after the measurement and the difference between these two currents is registered. Thus, the capacitive current and the residual faradaic current, that arise from trace impurities, the electrode material, solvent and supporting electrolyte is eliminated from the faradaic current, due to their ability to subtract current values sampled at two different times. In this way, these two pulse techniques are more sensitive methods than LSV, were the potential varies linearly over time, therefore being measured not only analyte signal but also background noise [30,62]. When testing the methods, SWV presented a noise level slightly high, therefore Differential Pulse was chosen.

Once optimized this new method of detection, a problem detected earlier had to be solved. This problem was detected as soon as pretreatment voltage stopped being used. When working with only buffer, a peak appeared, near the same region where BPA was detected. Several assays were conducted to determine the origin of the peak, such as testing normal and diluted buffer.

Peak appearance in the diluted buffer (1:10) continued to be similar to the one obtained without dilution, thus being possible that the problem came from elsewhere (comparative Graph A7 in appendix). Even so, to discard possible buffer contamination with BPA or other substance, fresh phosphate buffer, and also other buffers from the lab, were tested. The peak in the blank solution continued to be present. Therefore, an attempt was made, using the optimal pH, and applying a pretreatment voltage when measuring the buffer signal, to see if the buffer peak disappeared (Graph A8, Appendix). Even with this procedure, the peak continued to appear in the blank test solution. Latter on it was found to be due to contamination of the inks used in the production of home-made SPE, probably with a substance with a similar structure to BPA, owing to the overlapping of the peaks.

Since peak disappearance did not occur, several other pH besides the ideal one (pH 5, 7, 9 and 11) were tested to see if the buffer and BPA peak could be separated, allowing for a better detection of BPA. The best results in separating the analyte and interfering peak were achieved

for higher pHs, such as 8.2, 9 and 11 (Graph A9, in Appendix), with BPA response being proportional to its concentration.

To be sure of the linearity in each of the pH, smaller ranges between BPA concentrations were analyzed. Hence, graphs for concentrations of BPA between 1×10^{-6} to 2×10^{-5} M were rendered, for pH 8.2, 9 and 11, allowing a more detailed analysis of this zone.

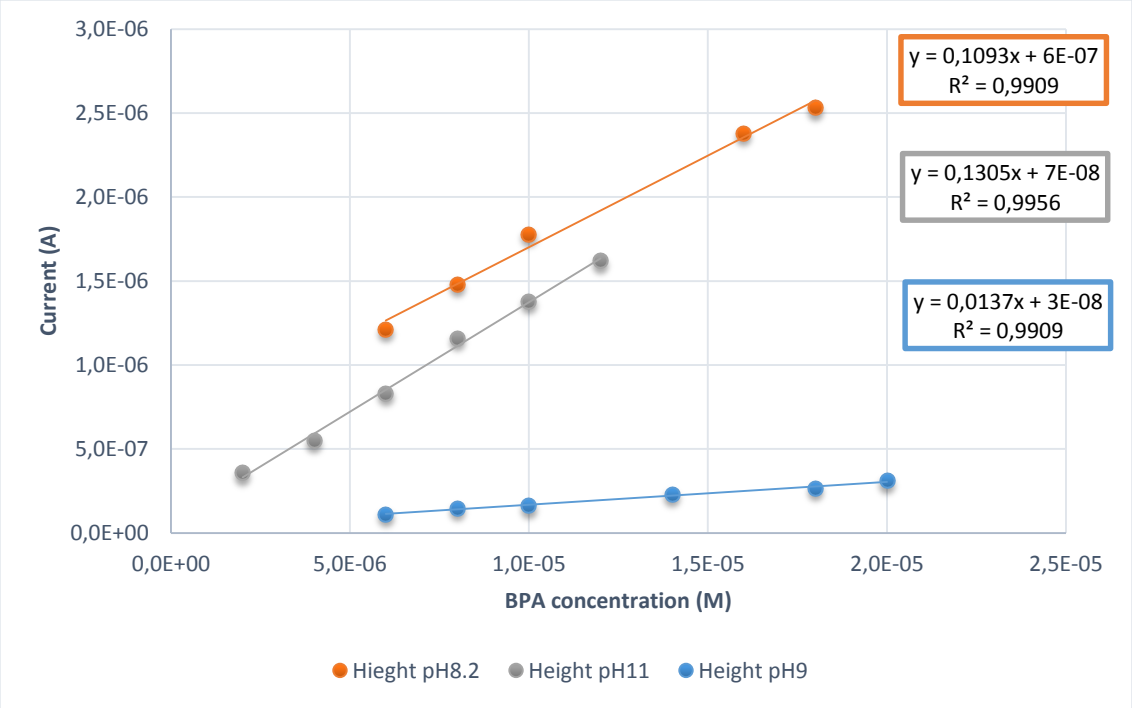

Graph 4.11 - Height for BPA peaks at different pH (8.2, 9 and 11), using virgin sensors. Experiments with BPA concentrations ranging from 1×10^{-6} to 2×10^{-5}M, using DP electrochemical detection technique.

From the analysis of graph 4.11, it can be concluded that there is a linear relationship between BPA concentration and peak height, with better results when using a pH of 11, being preferably used from now on. Even though, the use of pH 8.2 will not be discarded, considering its good results.

4.4 Bare DropSens sensors

Considering the problem observed with homemade screen-printed sensors, another attempt was made to minimize or eliminate the contaminant present in the blank. In this way, commercial sensors from DropSens were tested. DropSens sensors have silver conductive lanes and a silver reference electrode, instead of the Ag/AgCl pseudo – reference electrode of the homemade screen-printed sensors.

DropSens electrodes showed better results when compared to homemade sensors, not only minimizing buffer peak (Appendix Graph A10) (that was thought to be due to contamination from one of the inks used in the homemade sensors production), but also yielding a better slope and correlation coefficient (Graph 4.12). For this reason, DropSens electrodes will be used preferably.

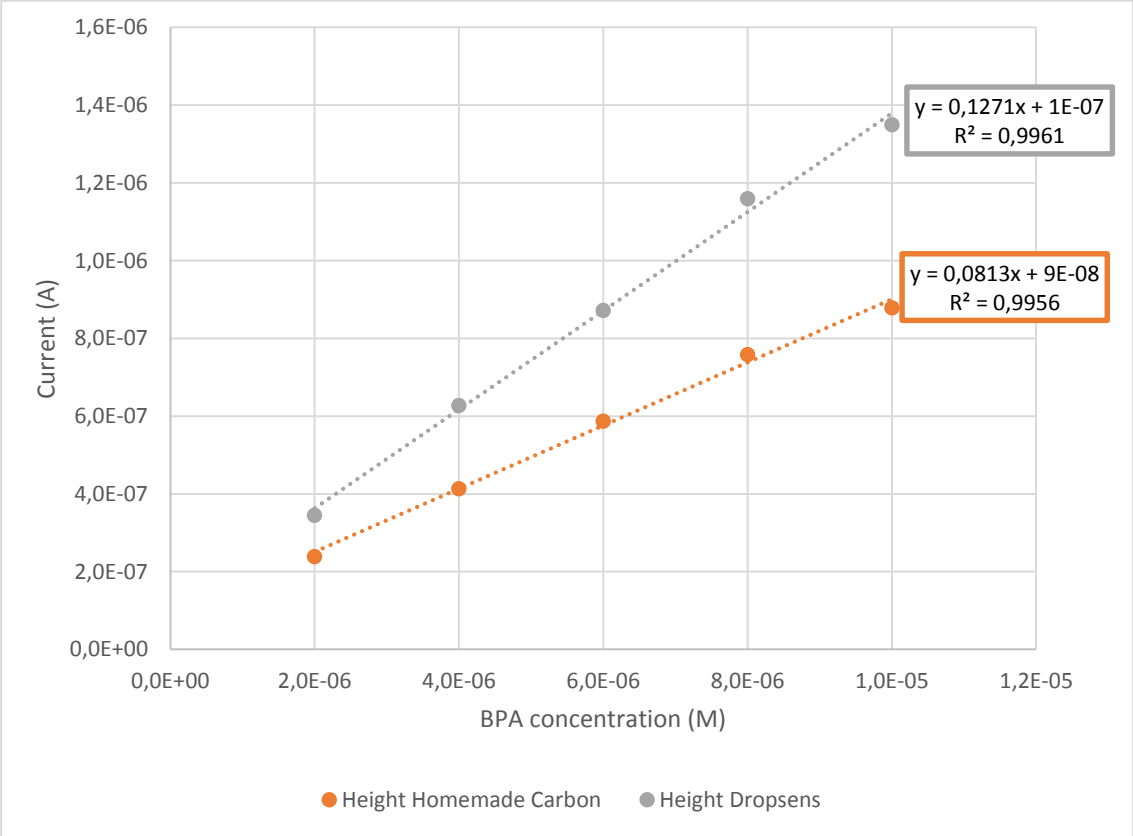

Graph 4.12 - Comparative study of DropSens Sensors with homemade screen-printed sensors with carbon conducting lanes, using phosphate buffer at pH11, using DP electrochemical detection technique and virgin electrodes. BPA concentration ranges from 1×10^{-6} to 8×10^{-5} M.

4.5 Modified electrodes

To enhance the sensitivity of the sensors, several surface modifications of the working electrode were made.

4.5.1 Gold Nanoparticles on homemade screen-printed sensors with carbon conducting lanes

By conferring properties such as greater surface area and enhanced conduction and catalytic properties, gold nanoparticles have become one of the most common surface modifiers used in electrochemical detection [34].

As so, the sensitivity of the electrode towards BPA by using gold nanoparticles on homemade screen-printed sensors was studied on virgin sensors and using the same sensors for each concentration, applying two distinct electrochemical methods: Cyclic Voltametry (CV) and Square Wave Voltametry (SWV). Measurements using electrodes modified with gold nanoparticles were performed early on in this work, while still using homemade sensors, but, due to their relevance, are shown in this section.

Though sensitivity was slightly enhanced with the electrochemical deposition of the nanoparticles (BPA peaks in Graph A11, appendix), it was not justifiable its use, since it didn't confer great advantage over the unmodified sensors (Graph 4.13).

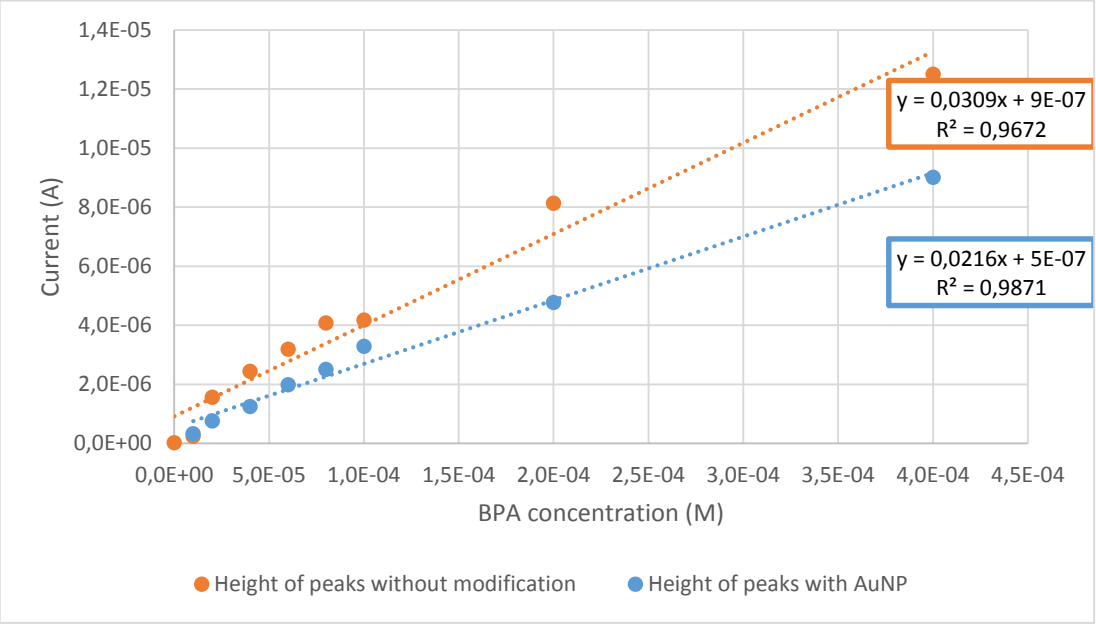

Graph 4.13 - Height of peaks for AuNP modified electrodes and unmodified electrodes, using virgin sensors for each concentration on homemade sensors. BPA concentrations ranged from 1×10^{-6} to 8×10^{-5} M using CV technique and phosphate buffer pH 8 as a medium.

4.5.2 Carbon Nanotubes

As gold nanoparticles, carbon nanotubes (CNT) are one of the most employed modifiers in the electrochemical area. The interest attributed to these type of nanoparticles is due to their high surface area, thermal and chemical stability, providing excellent electrical and optical properties [2,4,34]. For this reason, several studies using CNT will be conducted, on DropSens SPE, in order to access if their use improves BPA detection, in parameters such as sensitivity and fouling reduction, due its large surface area.

4.5.3 CNT on commercial DropSens sensors

DropSens sensors were modified with a commercially available solution from DropSens with unknown concentration (graph 4.14 and Appendix graph A12), as well as 2,33mg/mL solution of carbon nanotubes, to test if there was an increase in sensibility in the detection of BPA.

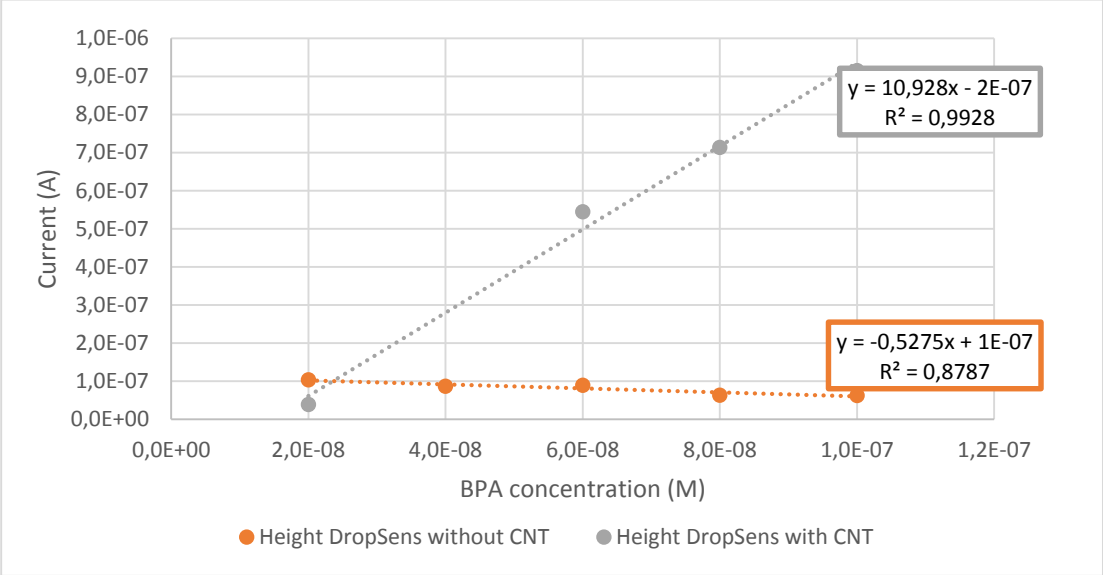

Graph 4.14 - H Height for BPA peaks using DropSens sensors modified and not modified with a commercial solution of nanotubes, performed on the same sensor for each concentration. Experiments using DP electrochemical detection technique, where concentrations of BPA varied from 1×10^{-8} to 8×10^{-7} M. Phosphate buffer pH11.

After seeing that a better slope value was obtained for DropSens electrodes with commercially available carbon nanotubes, more experiences were done in order to access if with the 2.33 mg/mL we could attain similar or even better results. The nanotube solution was initially made by only DMF, with a nanotube content of 3.5 mg/mL, as suggested by Asturias. *et al*, due to good results attained for similar concentrations [27]. A comparison was made between the use of this solution with concentration of 3.5 mg/mL and the one commercially available, differing only on stirring time before measurement (results presented in Appendix, Graph A13).

Since there were some difficulties in depositing nanotubes with the solvent being only DMF, evidenced by the poor results for those CNT (Appendix Graph A13), 1/3 of its content in water was added to the nanotube solution, changing its concentration from 3.5 mg/mL to 2.33 mg/mL. This was done after analyzing DropSens nanotubes solution commercial information. Trials were also made using different stirring times (Graph 4.15).

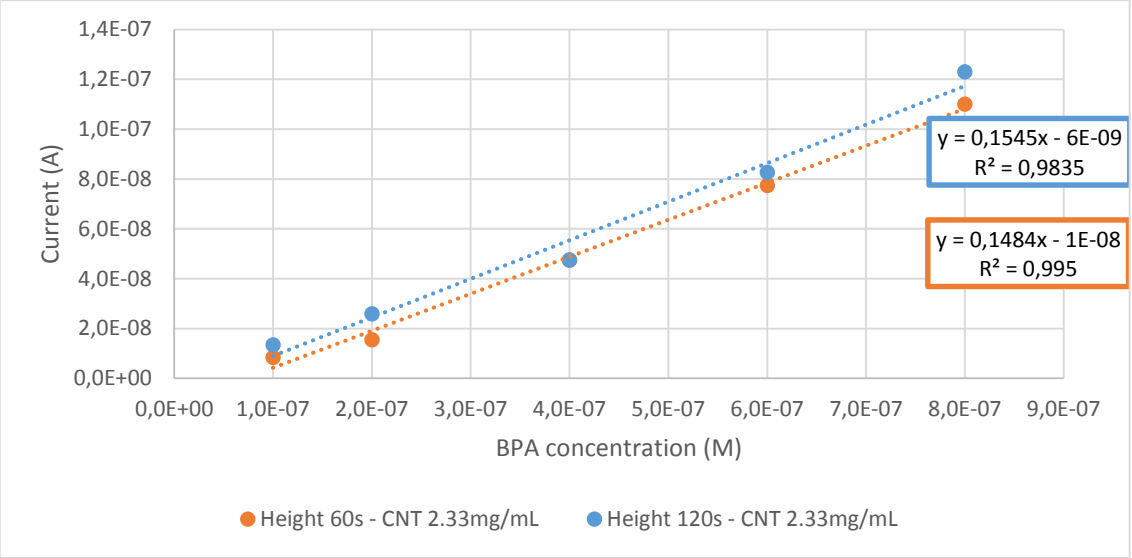

Graph 4.15 - Height for BPA peaks using DropSens sensors modified with a non-commercial solution of nanotubes, containing 1/3 of its content in water (final concentration 2.33mg/mL). Different stirring times (60 and 120s) before measurement were evaluated. Phosphate buffer pH11. Experiments where concentrations varied from 1×10^{-8} to 8×10^{-7}M of BPA using DP technique.

By comparing the results of the DropSens CNT solution (Graph A13) and the prepared dispersion containing 1/3 of its content in water (Graph 4.15), the latter obtained better slopes and intercept, therefore having a better sensitivity. As for stirring time, although 120 seconds of stirring enhanced sensitivity, 60 seconds of stirring provided a more stable curve, and since it was less time consuming, it was chosen to be implemented from now on.

4.5.4 Cu-Metal Organic Frame (MOF) on commercial DropSens sensors

4.5.4.1 Cu-MOF

Metal Organic Frames are recently being studied for their interesting properties, such as ultrahigh and permanent porosity, high thermal and chemical stability, adjustable internal surface properties and tunable pore structure and dimension [15,35]. However, their application in electrochemical sensing is not much explored, and combining this with their enhanced affinity towards BPA, makes Cu-MOF the ideal candidate for a surface modifier.

A Copper Metal Organic Frame (Cu-MOF) was synthetized in an oven, as a method suggested by the authors in Wang *et al.* (Wang, Lu, Wu, & Chen, 2015). After being washed, filtered and air dried overnight, Cu-MOF powder was dissolved in DMF in a concentration of 1mg/mL.

Studies using Cu-MOF were done on DropSens sensors, depositing the solution directly on working electrode surface and letting it air dry (Appendix, Graph A14). Cu-MOF was then combined with CNT.

4.5.4.2 Cu-MOF and CNT

Having the extremely promising characteristics that were already described, and adding to this fact the good results attained with their sole use (as seen in Appendix Graph A14), Cu-MOF has proven to be a promising electrode modifier. However, due to the fact that this substance has isolating properties, electron transport to the surface of the electrode can be difficult, thus compromising BPA detection and sensitivity. As so, a combination of this material with a highly conductive material was thought, thus arising CNT and Cu-MOF arrangements.

4.5.4.2.1 First cell experiments

Several percentages of CNT were combined with Cu-MOF in order to access if their presence had any influence in the limit of detection. Besides combining the two homogenously in an eppendorf and depositing this mixture directly on working electrode surface, other techniques were approached: depositing nanotubes and then depositing Cu-MOF on top after dry (CNTdpsCu-MOF); Depositing 3µL of CNT and 3µL of Cu-MOF at the same time (3CNT+3Cu-MOF) and depositing 1.5µL of CNT and 1.5µL of Cu-MOF ate the same time (1.5CNT+1.5CNT).

By analyzing Graph 4.16, where concentration curves for the different types of CNT and Cu-MOF combinations are present, it is concluded that higher percentage of carbon nanotubes leads to higher slope in the curves, which was expected due to the enhancing nature of this modifier. Therefore, the percentage of CNT with better slope is 60% CNT, closely followed by depositing 3µL of CNT and 3µL of Cu-MOF at the same time, with the slopes being higher than

the ones attained from using only CNT as a surface modifier. Even though higher CNT percentages demonstrate better expected sensitivity, detection of lower concentrations of BPA were improved at lower percentages of CNT, such as 5% CNT (see Appendix Graphs A15 and A16 for 5% CNT curves, and Graphs A17 and A18 for 30% CNT curves).

Another aspect concluded by the analysis of Graph 4.16 is that BPA calibration curves, when using Cu-MOF and CNT, maintain their linearity throughout all concentrations of BPA, even when using the same electrode for all concentrations. This demonstrates the potentiality of the combination of these two compounds in reducing electrode fouling, a problem that is common for BPA detection.

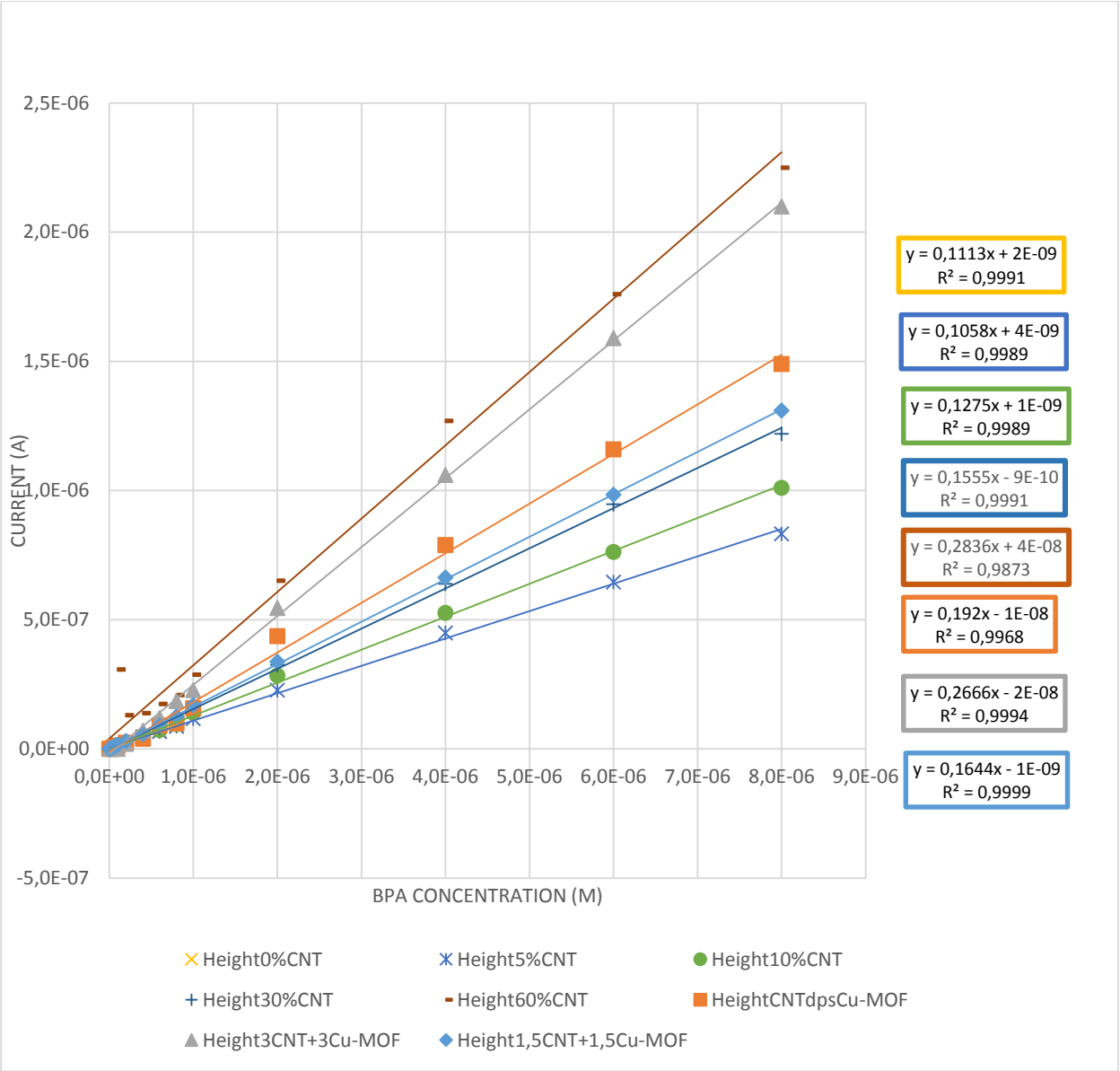

Graph 4.16 - Graph combining several experiments, with different CNT concentrations (0%, 5%, 10%, 30%, 60%, 90%) and methods of applying and combining CNT with Cu-MOF(sequential dropping of 3µL of CNT, followed by 3µL Cu-MOF (heightCNTdpsCu-MOF); simultaneous deposition of 3µL of CNT and Cu-MOF (height3CNT+3Cu-MOF); simultaneous deposition of 1.5 µL of CNT and Cu-MOF (height1.5CNT+1.5Cu-MOF). Phosphate buffer pH11 using DP method, with BPA concentration ranging from 1×10^{-8}M to 8×10^{-6}M. DropSens sensors and CNT solution of 2.33mg/mL.

4.5.4.2.2 Single drop experiments

Single drop experiments were attempted as earlier in this study, in order to see if better results were attained when using the CNT+ Cu-MOF sensor. Since this would be a more practical method for use in non-laboratory measurement situations, it is of great interest a reassessment of this form of measurement. Once measurements at different concentrations of BPA are performed using the same sensor (due to elevated cost of DropSens Sensors), a series of different assays were performed in order to determine which method was best to clean the electrode system between measurements at different concentrations. As so, different cleaning processes were tried:

- Washing 2 times with 1 mL of phosphate buffer;
- Drawing medium of previous measurement with a micropipette;
- Drawing medium of previous measurement with a micropipette and washing 2 times with 1 mL of Phosphate Buffer.

As drawing with the use of a micropipette gave the best results (for more information consult appendix graph A19), as well as being the easiest method to perform without causing great disturbance the system, it was used in all experiments performed in a single drop.

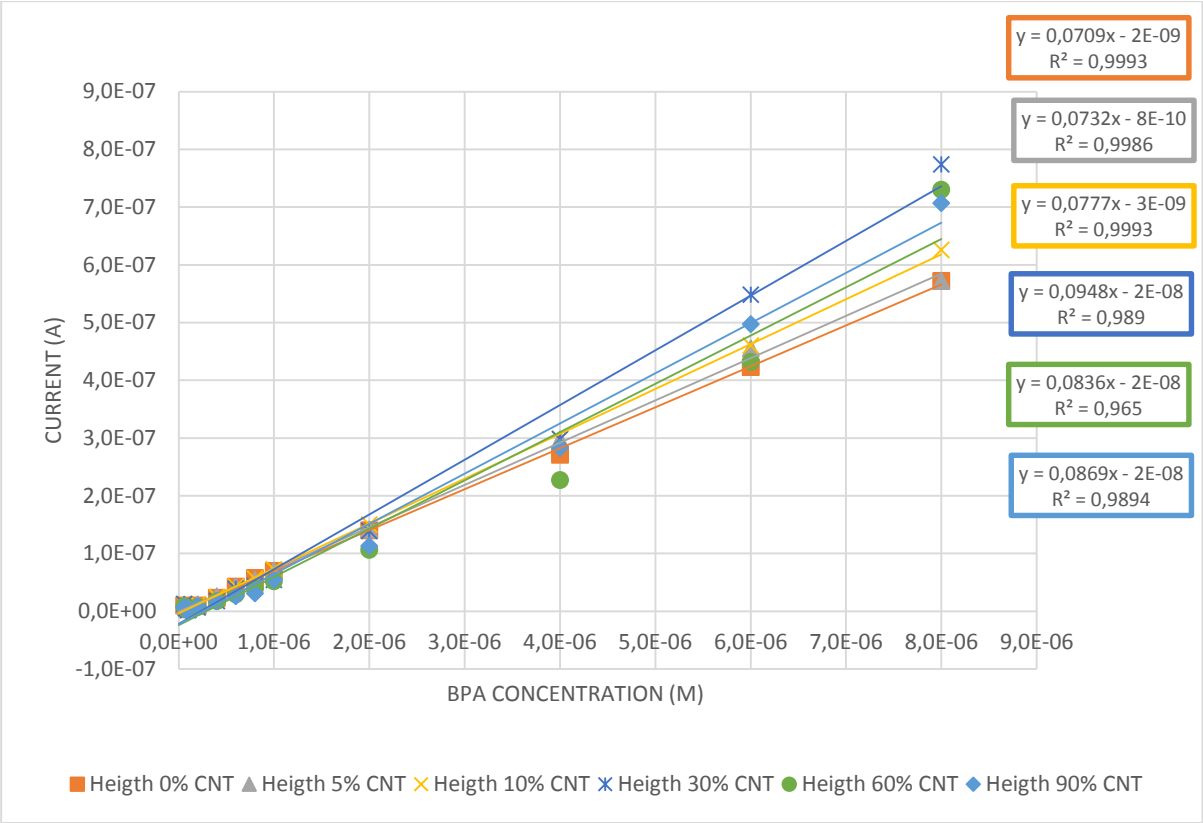

Graph 4.17 - Comparison between different percentages of CNT (0%, 5%, 10%, 30%, 60%, 90%) and Cu-MOF in single drop experiments. Drop Volume - 100 µL. Phosphate Buffer pH11. DropSens Sensors were used with DP method, with BPA concentration ranging from 1×10^{-8}M to 8×10^{-6}M.

By comparing results attained with single drop experiments and cell experiments, it can be seen that sensitivity largely decreases by using single drop technique (comparing Graphs 4.16 and 4.17). Even so, since linearity is also present when using single drop, and results are somewhat similar to both first and second experiments (Graph 4.18. and appendix graphs A20 to A22)), this method could be used for on-site analysis, though having some sensitivity limitations. The reason why first and second experiments in a cell, being done in Burgos (Spain) and Covilhã (Portugal), respectively, have distinct results (as can be seen in graph 4.18 and appendix graphs A20 to A22), derives from the fact that the vessel used in both locations had different formats, which influenced sensor submerging, therefore altering sensor sensitivity.

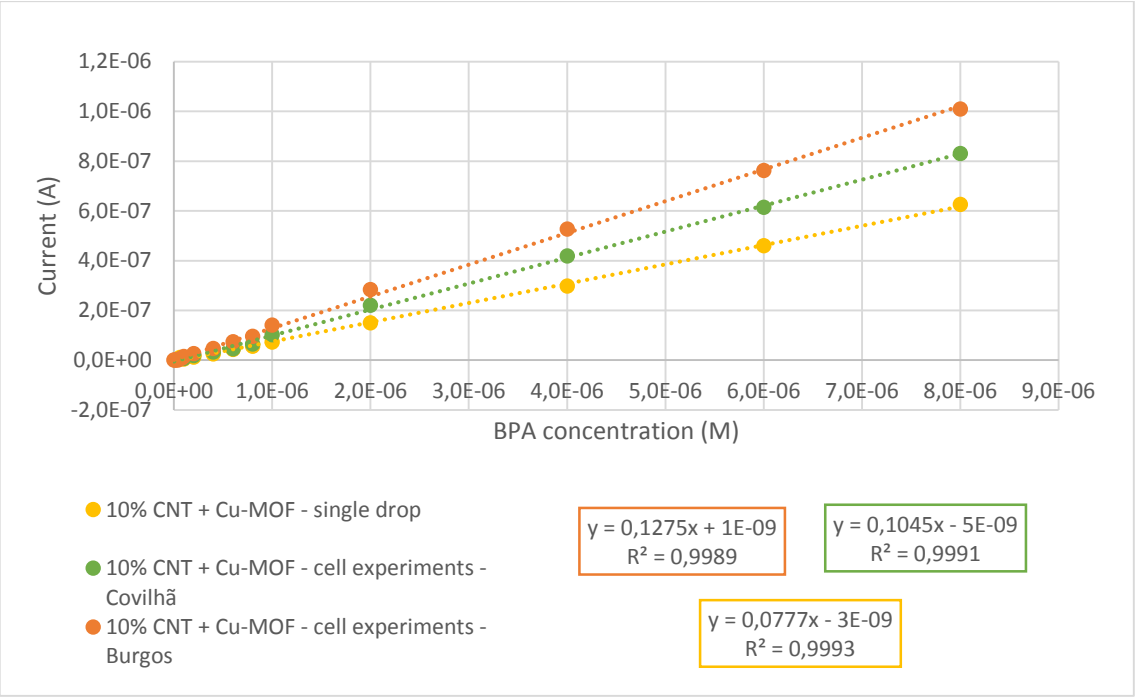

Graph 4.18 - Comparison of height of BPA peaks for 10% CNT + Cu-MOF. Different experiments include Single Drop and Cell experiments (performed both in Burgos, Spain and Covilhã, Portugal). Phosphate Buffer pH 11 and BPA concentration ranging from 1×10^{-8}M to 8×10^{-6}M. Dropsens sensors and DP method.

4.5.4.2.3 Repetitions of cell experiments

To ensure, in cell measurements, a valid number of assays for reproducibility analysis, repetitions were done at all concentrations of CNT + Cu-MOF.

Graphic superposition of calibration curves for different proportions of CNT + Cu-MOF (60% and 90%, other percentages of CNT can be found in graphs A23 to A26 in the appendix), as well as an average calibration curve with its associated error, is presented in Graphs 4.19 and 4.20.

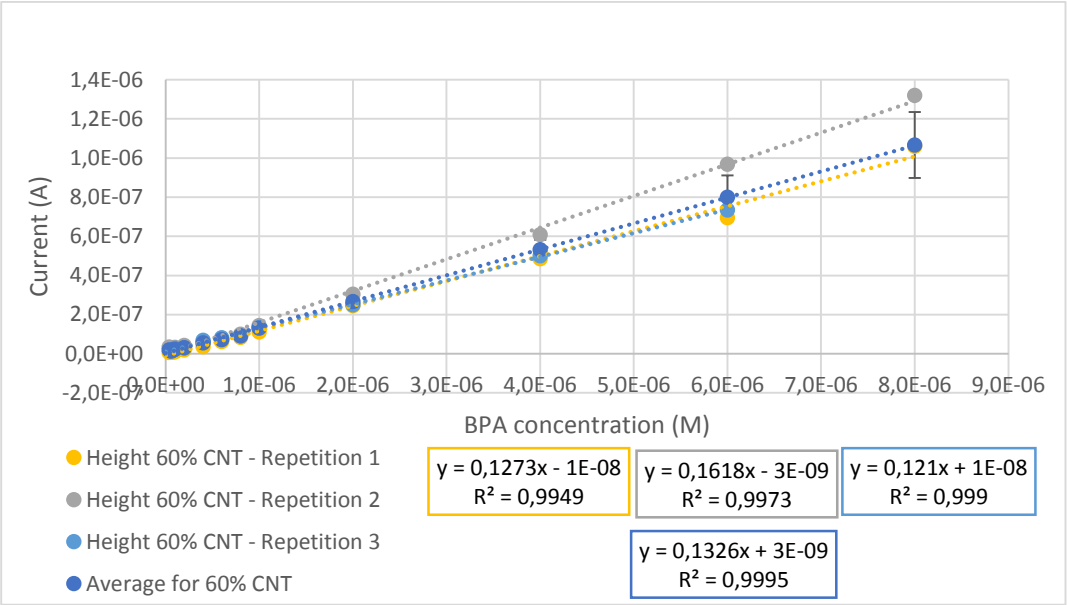

Graph 4.19 - Comparison of 3 repetitions for 60% CNT + Cu-MOF and average curve. Phosphate Buffer pH 11 and BPA concentration ranging from 1×10^{-8}M to 8×10^{-6}M. Dropsens sensors were used.

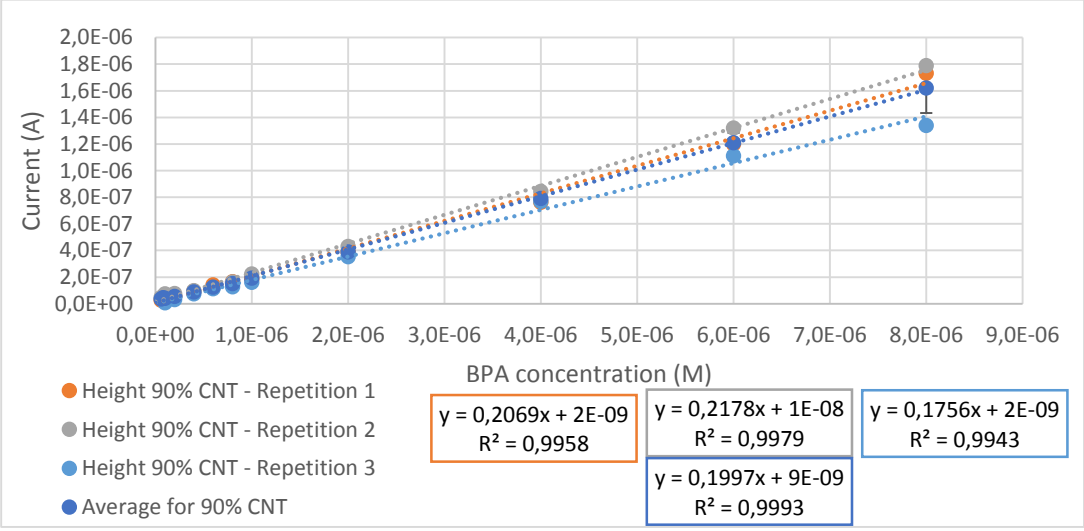

Graph 4.20 - Comparison of 3 repetitions for 90% CNT + Cu-MOF and average curve. Phosphate Buffer pH 11 and BPA concentration ranging from 1×10^{-8}M to 8×10^{-6}M. Dropsens sensors were used.

Based on the average curve for each CNT concentration, the Limit of Detection (LOD), this is, the lowest concentration of analyte that can be detected, was calculated. Least Median of Squares Regression (LMS) was applied in order to eliminate anomalous points that could influence LOD determination, being presented in Table 4.5 the average calibration curve after using this regression. Prior to this, DETARCHI software was used to calculate the LOD, considering the probability of false negatives (β) and false positives (α). This information is summarized in Table 4.5.

Table 4.5 - Comparison of Limits of Detection (LOD), calculated by DETARCHI software (α=β=0.05), for assays performed in buffer, using different CNT percentages.

Percentage of CNT (%)	Average Calibration Curve *(y= ax + b)*	Coefficient of determination (R^2)	Standard Deviation (SD)	Residual Standard Deviation (RSD)	Limit of Detection (LOD)
0%	$0.1083x + 1.57\times 10^{-8}$	0.9979	1.34×10^{-8}	16.57%	2.54×10^{-7} M
5%	$0.1185x + 1.31 \times 10^{-8}$	0.9971	1.69×10^{-8}	19.76%	2.89×10^{-7} M
10%	$0.1089x + 7.60 \times 10^{-9}$	0.9992	8.74×10^{-9}	14.70%	1.65×10^{-7} M
30%	$0.1559x + 5.54 \times 10^{-9}$	0.9992	1.19×10^{-8}	21.11%	1.56×10^{-7} M
60%	$0.1327x + 2.51\times 10^{-9}$	0.9995	7.81×10^{-9}	15.48%	1.20×10^{-7} M
90%	$0.1997x + 8.66 \times 10^{-9}$	0.9993	1.51×10^{-8}	10.85%	1.56×10^{-7} M

As can be seen, the lowest LOD were attained for 30%, 60% and 90% CNT, being in accordance with the slope magnitude for those curves. Coefficient of determination and standard deviation showed good values for all curves, indicating a good linearity and a good fit of the experimental points to the obtained calibration curve. However, residual standard deviation showed high values to what was expected for this kind of sensor, probably due to the differences in vessels for cell experiments.

4.5.4.3 Reuse of sensors used both in cell and single drop experiments

To verify if it is possible to reuse modified electrochemical sensors, even though they have a disposable nature, an analysis of sensors from previous assays was undertaken for both cell and single drop experiments. Prior to second use, sensors were washed with a solution of approx. 50% methanol and, after that, with distilled water.

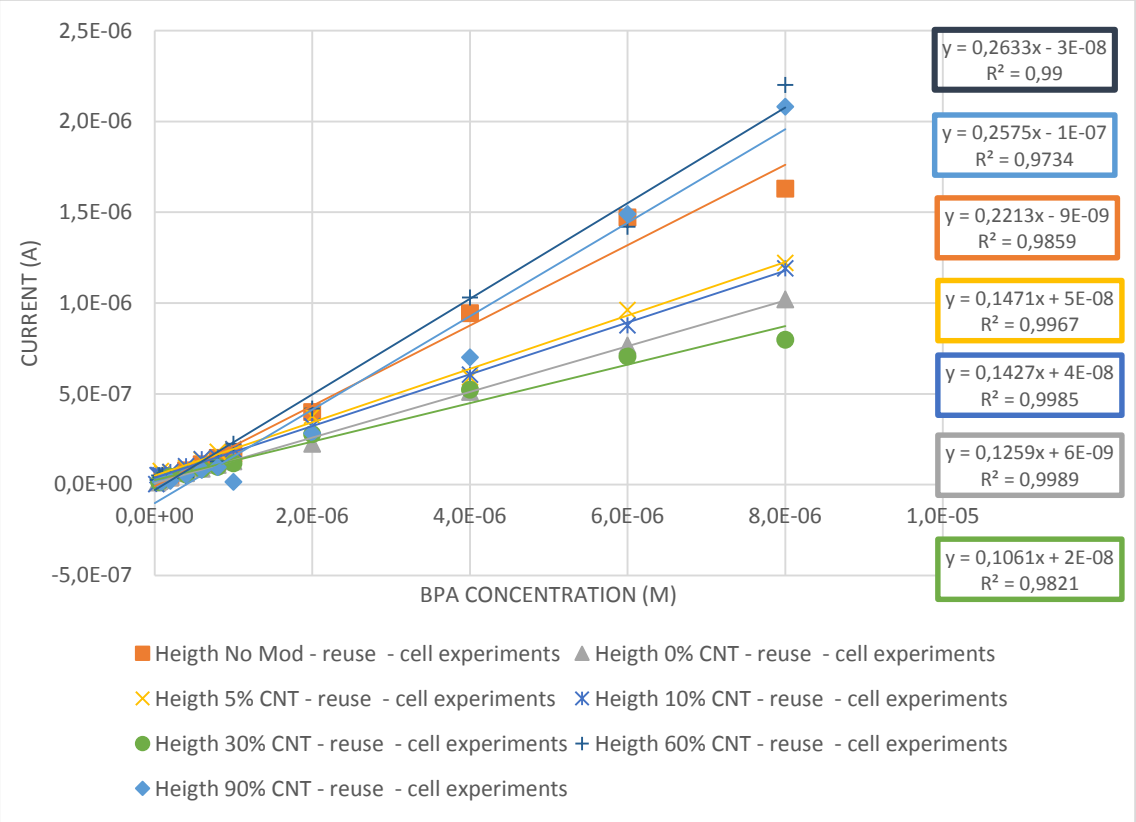

Graph 4.21 - Comparison of curves for different CNT and Cu-MOF percentages (0%, 5%, 10%, 30%, 60% and 90% of CNT), when reusing sensors in cell experiments. Phosphate Buffer pH11 and BPA concentration ranging from 1×10^{-8}M to 8×10^{-6}M. Dropsens sensors were used.

Reuse of sensors was more successful for in-cell experiments (Graph 4.21) than those performed in single drop experiments (Appendix Graph A27). Still, even though not showing presence of BPA in the blank solution, slope for each CNT percentage has increased, therefore being possible that some undetectable accumulation has occurred even with cleaning. For this reason, reuse of SPE will be discarded.

4.6 Synthetic urine

Since one of the aims of this work is to detect BPA in biological samples such as human urine, a good way to start the process of finding ideal conditions is by using a similar medium, with reduced content in contaminants. As so, synthetic urine was used as an intermediate for this change in medium complexity. Since urine pH is closer to 8 than it is to 11, knowing from previous experiments that this value of pH obtained similarly good results to pH 11, buffer was changed to phosphate buffer pH8. The ability to detect BPA in this medium was studied, and the effect of synthetic urine dilution analyzed, as can be seen in Graph 4.22. In Appendix Graphs A28 and A29 are present the DP curves for 30% CNT.

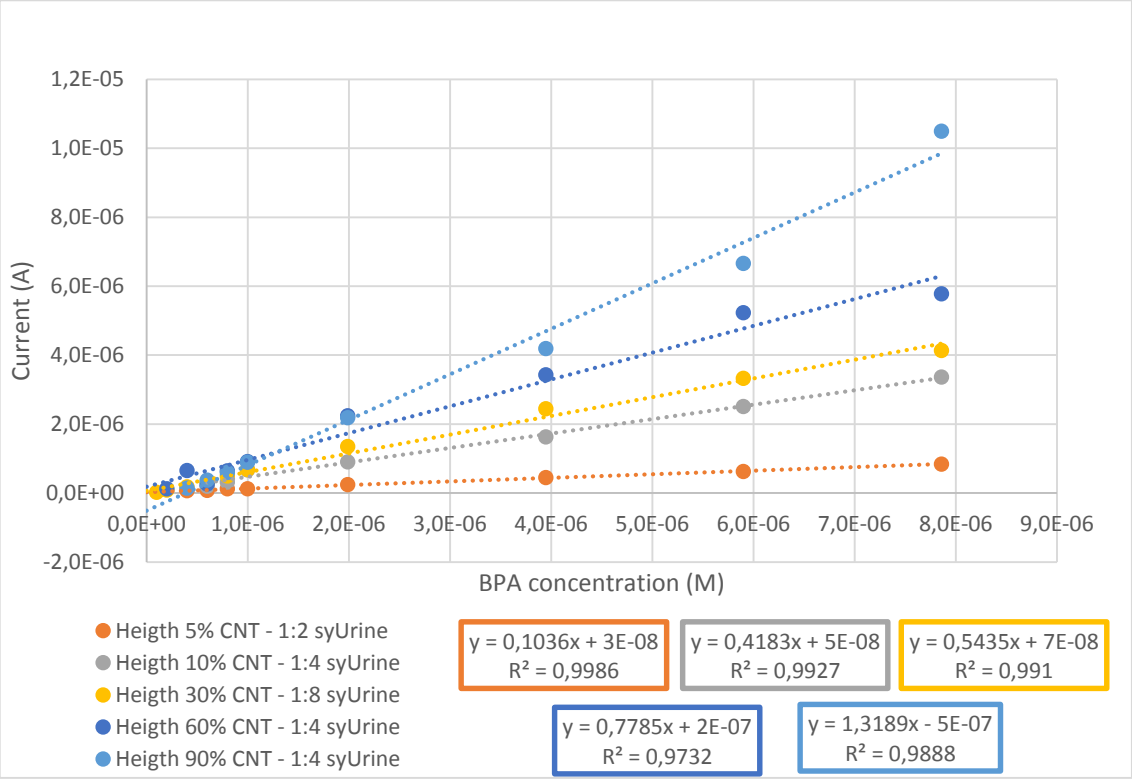

Graph 4.22 - Comparison of curves obtained with different percentages of CNT and Cu-MOF (0%, 5%, 10%, 30%, 60% and 90% of CNT), studying various dilutions of synthetic urine in phosphate buffer pH 8. Dropsens sensors were used with BPA concentration ranging from 1×10^{-8}M to 8×10^{-6}M.

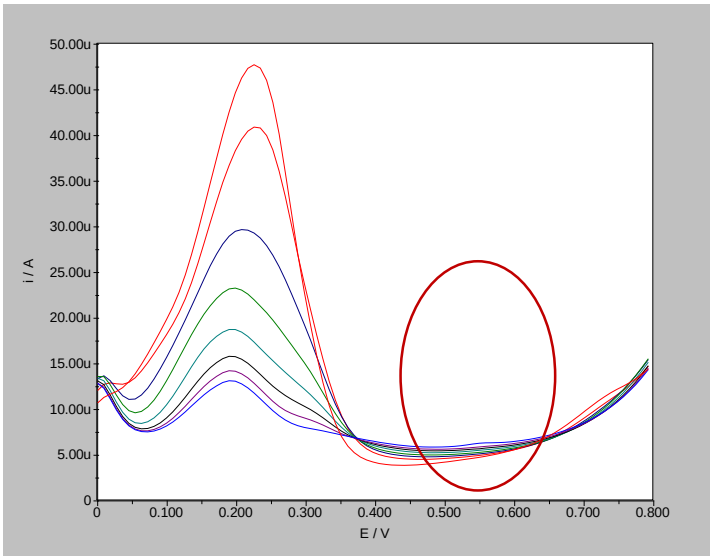

Graph 4.23 – DP (from 0 to 0.8V) curves for concentrations 0 to 2×10^{-7}M of BPA using DropSens sensors in Phosphate Buffer ph8 and Synthetic Urine (1:4 dilution) with 60% CNT (Red – 0 M; Red - 1×10^{-8}M; Dark Blue 2×10^{-8}M; Green – 4×10^{-8}M; Cyan - 6×10^{-8}M; Black - 8×10^{-8}M; Magenta - 1×10^{-7}M; Blue - 2×10^{-7}M). BPA region circled in red.

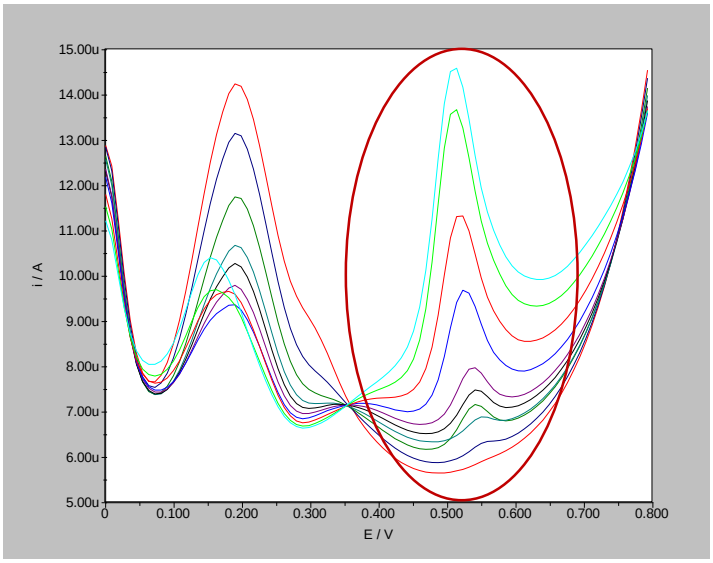

Graph 4.24 - DP (from 0 to 0.8V) curves for concentrations 1×10^{-7}M to 8×10^{-6}M of BPA using DropSens sensors in Phosphate Buffer ph8 and Synthetic Urine (1:4 dilution) with 60% CNT (Red - 1×10^{-7}M; Dark Blue 2×10^{-7}M; Green – 4×10^{-7}M; Cyan - 6×10^{-7}M; Black - 8×10^{-7}M; Magenta - 1×10^{-6}M; Blue - 2×10^{-6}M; Red – 4×10^{-6}M; Light Green – 6×10^{-6}M; Light Cyan – 8×10^{-6}M). BPA peaks circled in red.

When comparing Graph 4.24 to the one previously obtained for BPA detection in buffer (Appendix Graph A18), BPA peaks shifted to higher potentials (now being from 0.3 to 0.7 Volts), but still perfectly detectable as BPA peaks, and maintaining a good linearity with superior slopes in contrast to those obtained in buffer measurements (Graph 4.16 and 4.22). Peaks

present in lower potentials in graphs 4.23 and 4.24 are inherent to synthetic urine due to its composition, nevertheless they seem to not interfere with BPA signal.

Direct detection in synthetic urine was not possible, with the best results being obtained when using dilutions of 1:4 and 1:8. Even though 1:2 proportion of synthetic urine produced a linear response (Graph 4.22), detection with this urine concentration was difficult, though it must be taken into account that only a lower percentage of CNT (5%) was used with this dilution (see Appendix graph A30).

4.6.1 Repetitions for 30% and 60% CNT

Identified 30 and 60% of CNT sensors modifications as the ones which obtained the best results in the previous experiments, considering linearity and slope value, repetitions were made to ensure reproducibility. These were executed using 1:4 synthetic urine dilutions in phosphate buffer pH 8, since this dilution seems to be the one attaining best results.

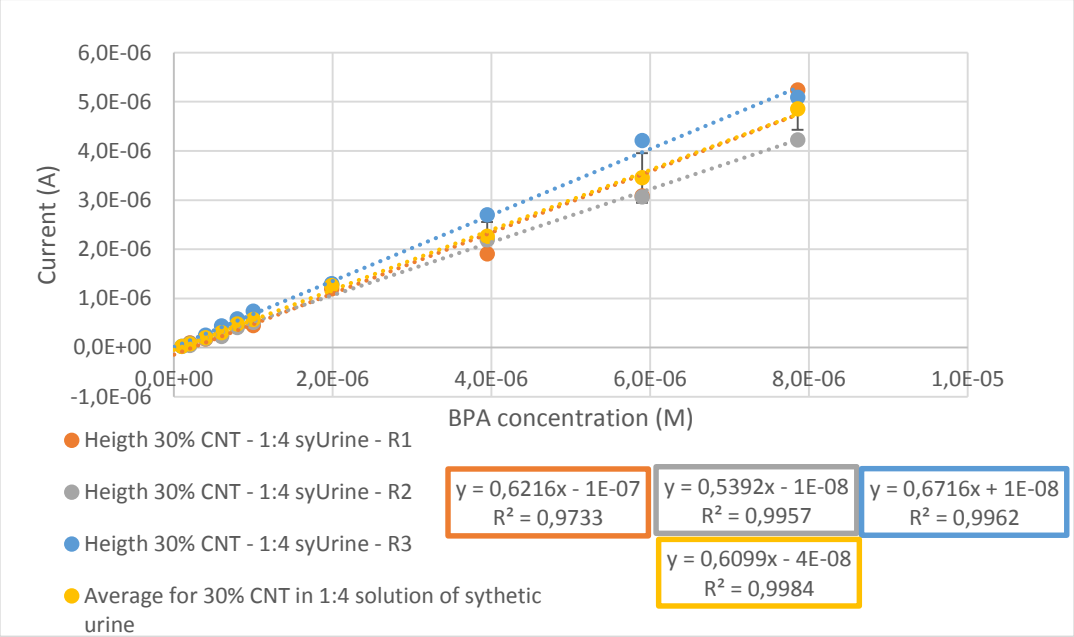

Graph 4.25 - Comparison of 3 repetitions done using sensors modified with 30% CNT and by using a dilution of 1:4 of synthetic urine. Phosphate Buffer pH8 with. Dropsens sensors were used BPA concentration ranging from 1×10^{-8}M to 8×10^{-6}M.

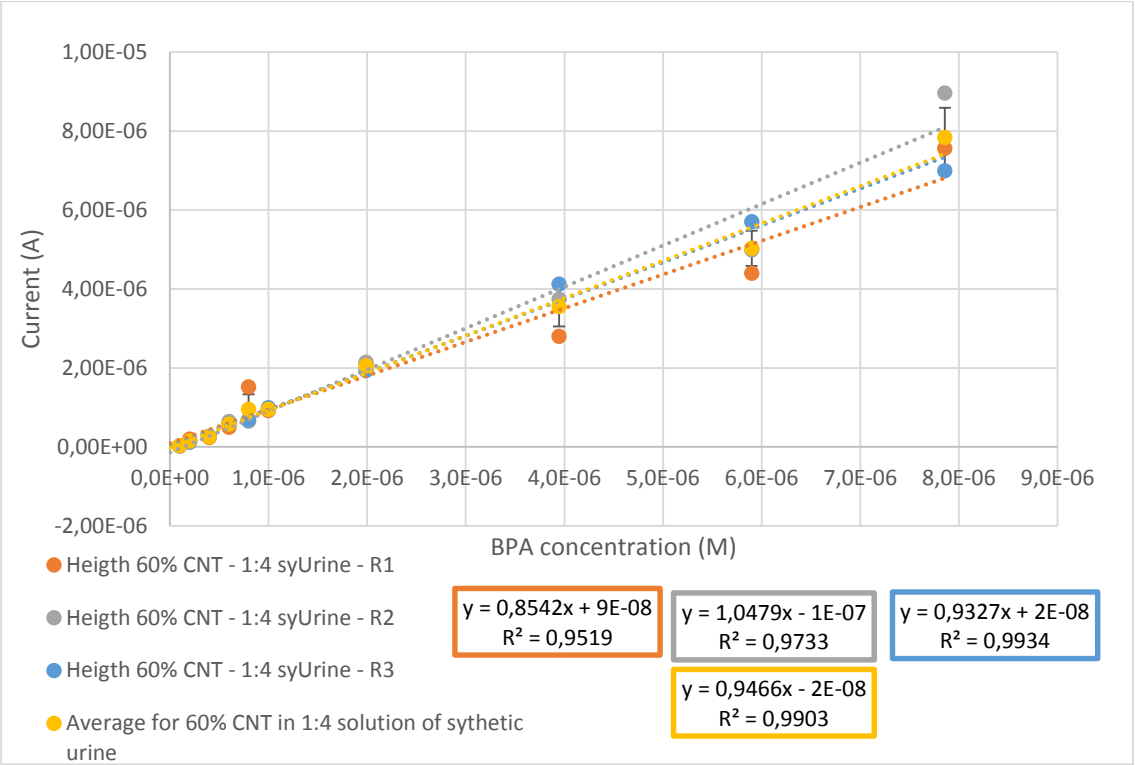

Graph 4.26 - Comparison of 3 repetitions done using sensors modified with 60% CNT and by using a dilution of 1:4 of synthetic urine. Phosphate Buffer pH8 with. Dropsens sensors were used BPA concentration ranging from 1×10^{-8}M to 8×10^{-6}M.

By calculating LOD for the synthetic urine assays (represented in table 4.6), using the previous method already described for buffer assays, it is possible to conclude that sensitivity towards BPA in this medium is lower when compared to the one obtained in buffer, hence the higher LOD. By direct slope observation, it was expected a higher sensitivity than the one obtained in buffer assays, nevertheless the standard deviation in this medium was higher and the coefficient of determination worse, probably due to its more complex nature, thus rising the limit of detection. Although expected higher RSD for this medium when compared to buffer assays, both of the percentages of CNT used in synthetic urine analysis obtained similar results to 90% CNT in buffer assays, which had the best RSD. These values are good considered the complex nature of the medium.

Table 4.6 - Comparison of Limits of Detection (LOD), calculated by DETARCHI software (α=β=0.05), for assays performed in sythetic urine, using CNT percentages of 30 and 60%.

Percentage of CNT	Average Calibration Curve *(y= ax + b)*	Coefficient of determination (R^2)	Standard Deviation (SD)	Residual Standard Deviation (RSD)	Limit of Detection (LOD)
30% CNT in Synthetic Urine	$0.5993x + 4.26 \times 10^{-8}$	0.9984	7.15×10^{-8}	10.94%	2.52×10^{-7} M
60% CNT in Synthetic Urine	$0.9292x + 6.93 \times 10^{-9}$	0.9902	2.71×10^{-7}	10.31%	6.17×10^{-6} M

4.7 Human urine samples

Despite the ability to detect BPA with success in synthetic urine samples, it's important to evaluate the analytical reliability of the proposed sensor for real human sample analysis. Hence, tests were made aiming to detect BPA in a much more complex medium, such as human urine samples. These samples belonged to male donors, in order to screen the possible influence of estradiol, present in female samples, in BPA detection.

Using human urine samples, several experiments were conducted to detect BPA in this sample with increased complexity. As so, concentration of CNT, electrochemical method, urine donor and dilution, as well as changing from cell to single drop experimentation were variables studied. When analyzing Graph 4.29, it is clear to see that, contrary to previous representations of that nature, only some of the CNT percentages were able to detect BPA in human urine samples, being the sensors with fewer nanotubes not capable of doing so.

Results were first attained using a 1:10 urine dilution and 30% CNT modifying electrode surface. BPA peaks shifted to higher potentials, when compared to buffer experiments (now being from 0.3 to 0.5 Volts) (graphs 4.27 and 4.28). Following experiments proved that 60% and 90% CNT also obtained good results in this medium, as can be seen by the analysis of Graph 4.29 and Appendix graphs A31 to A34, with the best results being attained for 30% and 60% CNT, which will be repeated to ensure reproducibility.

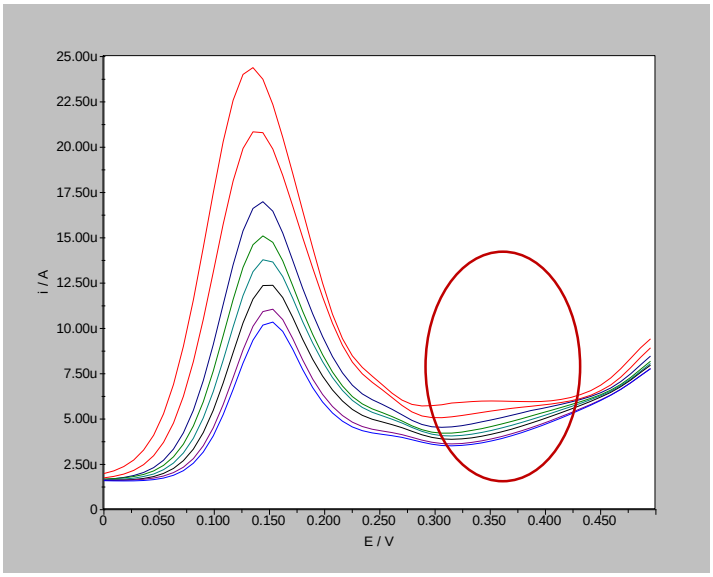

Graph 4.27 - DP curves (from 0 to 0.5V) for concentrations 0 to 2×10^{-7}M of BPA using DropSens sensors in Phosphate Buffer ph8 and Urine sample - GS120390 (1:10 dilution) with 30% CNT (Red - 0 M; Red - 1×10^{-8}M; Dark Blue 2×10^{-8}M; Green - 4×10^{-8}M; Cyan - 6×10^{-8}M; Black - 8×10^{-8}M; Magenta - 1×10^{-7}M; Blue - 2×10^{-7}M). BPA region circled in red.

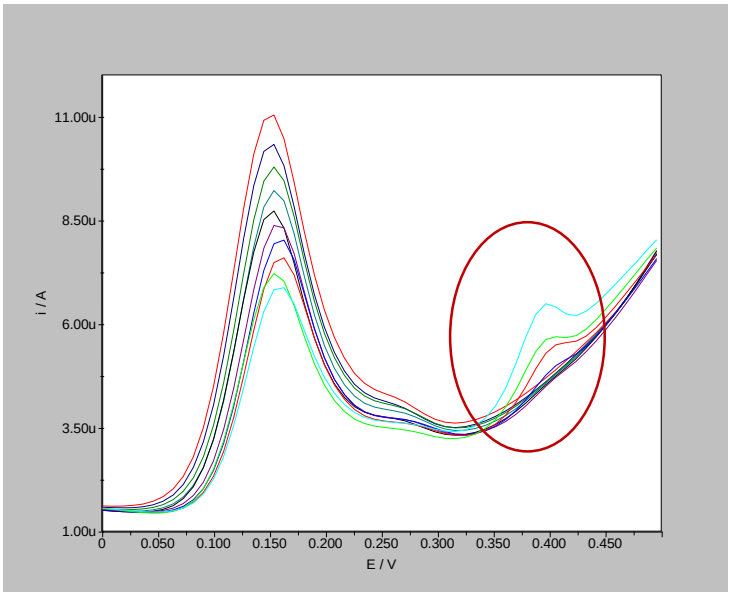

Graph 4.28 - DP curves (from 0 to 0.5V) for concentrations 1×10^{-7}M to 8×10^{-6}M of BPA using DropSens sensors in Phosphate Buffer ph8 and Urine sample - GS120390 (1:10 dilution) with 30% CNT (Red - 1×10^{-7}M; Dark Blue 2×10^{-7}M; Green - 4×10^{-7}M; Cyan - 6×10^{-7}M; Black - 8×10^{-7}M; Magenta - 1×10^{-6}M; Blue - 2×10^{-6}M; Red - 4×10^{-6}M; Light Green - 6×10^{-6}M; Light Cyan - 8×10^{-6}M).

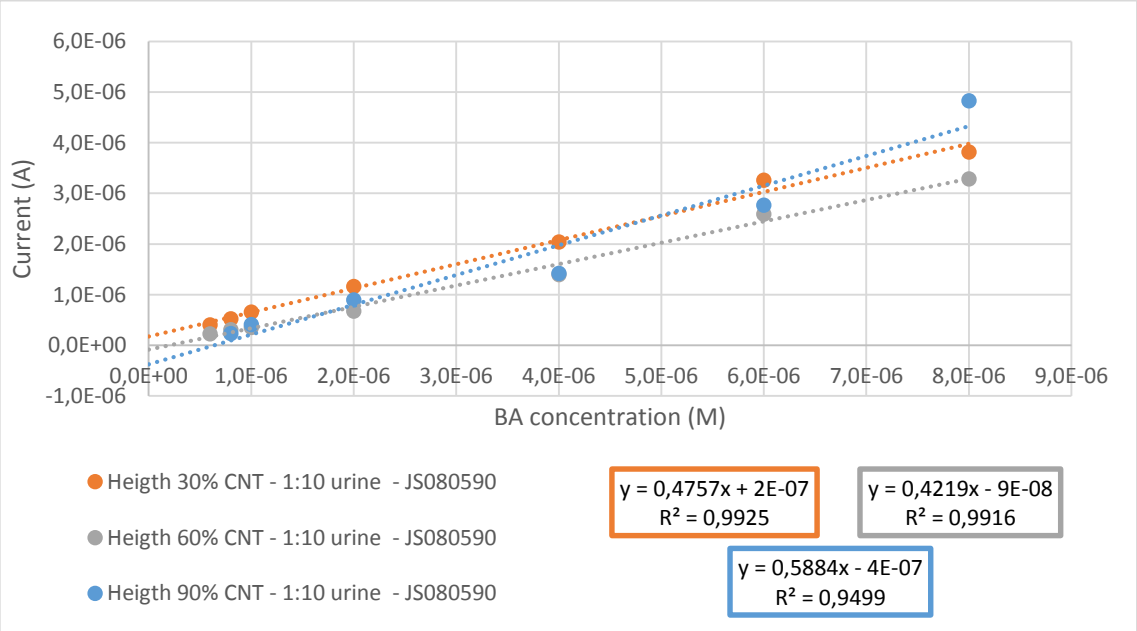

Graph 4.29 - Comparison of curves for height of BPA peaks obtained in Urine Sample - JS080590 with a dilution of 1:10 in phosphate buffer pH8. Dropsens sensors were used, with a BPA concentration range of 1×10^{-8}M to 8×10^{-6}M.

Another question that resided during these assays, due to the potential region were BPA signal appeared, was related to methanol interference, since it was used in BPA solution preparation.

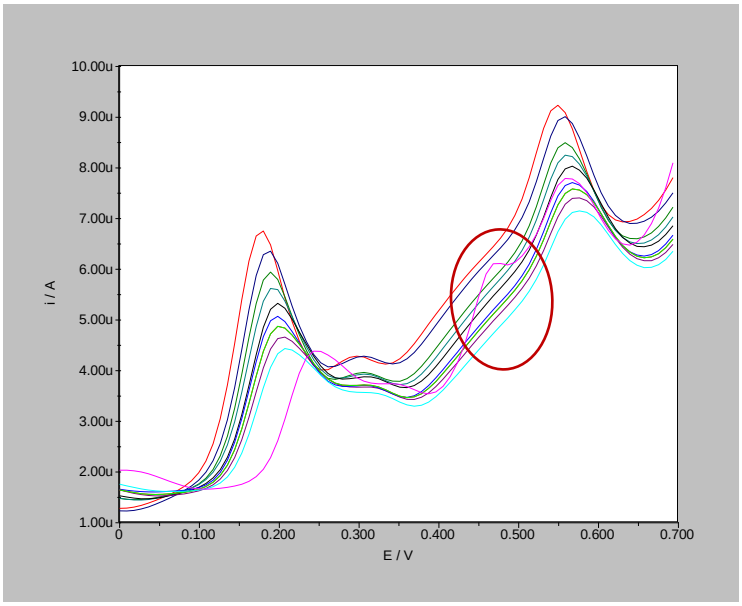

Graph 4.30 – DP curves (from 0 to 0.7) for concentrations 1×10^{-7}M to 8×10^{-6}M of Metanol using DropSens sensors in Phosphate Buffer ph8 and Urine sample – JS080590 (1:10 dilution) with 30% CNT (Red - 1×10^{-7}M; Dark Blue 2×10^{-7}M; Green – 4×10^{-7}M; Cyan - 6×10^{-7}M; Black - 8×10^{-7}M; Magenta - 1×10^{-6}M; Blue - 2×10^{-6}M; Red – 4×10^{-6}M; Light Green – 6×10^{-6}M; Light Cyan – 8×10^{-6}M Light magenta – addition of 400 µL of BPA solution (1×10^{-4}M)). Circled in red is the BPA peak.

As can be noticed, methanol has no influence in BPA detection, since no peak was observed in the 0.3 – 0.5 V potential interval at different methanol concentrations (Graph 4.30), with the methanol peak appearing at other potentials. Only with the addition of BPA to the reaction cell, a peak appear in the 0.3 – 0.5 V potential region. . Therefore, it is possible to support that the peak detected, even though not being present in its original position, is BPA.

4.7.1 Repetitions for 30% and 60 % CNT

Since the sensors with the best results were the ones with 30% and 60% of CNT + Cu-MOF deposited on the surface of the working electrode, these assays were repeated in order to ensure that there is reproducibility and to calculate LOD.

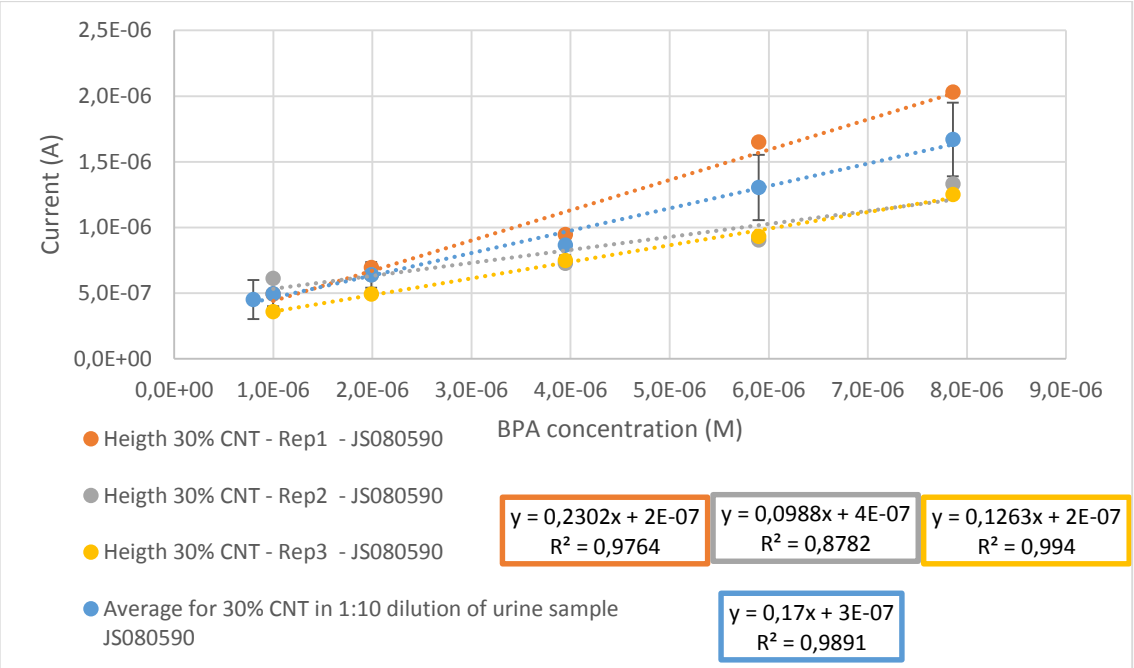

Graph 4.31 - Comparison of three repetitions done using sensors modified with 30% CNT and by using a dilution of 1:10 of urine sample JS080590. Phosphate Buffer pH8. DropSens sensors were used with BPA ranging from 1×10^{-8}M to 8×10^{-6}M.

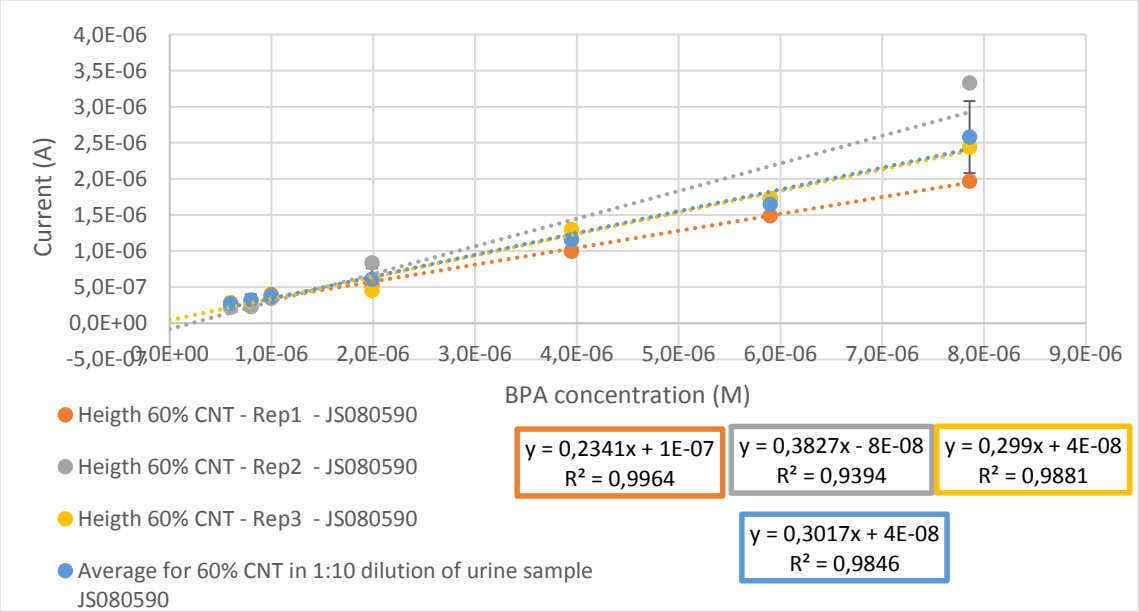

Graph 4.32 - Comparison of three repetitions done using sensors modified with 30% CNT and by using a dilution of 1:10 of urine sample JS080590. Phosphate Buffer pH8. DropSens sensors were used with BPA ranging from 1×10^{-8}M to 8×10^{-6}M.

Though not holding as good slope as the results attained from synthetic urine, slope value is still high when compared to measurements performed only in buffer, not to be forgotten that human urine is much more complex than its synthetic version.

The following table resumes the limits of detection and residual standard deviation accomplished in this work for human urine samples.

Table 4.7 - Comparison of Limits of Detection (LOD) for assays performed in real human urine samples (JS080590), using CNT percentages of 30 and 60%.

Percentage of CNT	Average Calibration Curve *(y= ax + b)*	Coefficient of determination (R^2)	Standard Deviation (SD)	Residual Standard Deviation (RSD)	Limit of Detection *(LOD)*
30% CNT in Human Urine (JS080590)	$0.1601x + 3.39 \times 10^{-7}$	0.9723	8.14×10^{-8}	45.66%	1.09×10^{-6} M
60% CNT in Human Urine (JS080590)	$0.2901x + 8.23 \times 10^{-8}$	0.9832	1.17×10^{-7}	24.37%	8.91×10^{-7} M

In general, LOD were higher when using real human samples as a medium, which was expected due to the complexity of the urine, leading to a worse coefficient of determination and a worse RDS in comparison to both buffer and synthetic urine. In this case, 60% CNT attained better results, with a LOD of 8.91×10^{-7} M and a RDS of 24.37%.

Comparing the sensor with best results for the three mediums (60% CNT in buffer – 1.20×10^{-7} M) with the ones in the literature, the limit of detection is comparable to magnetic MIPs with CTAB surfactant [22], and lower than 2-aminophenol monomer/AuNPs ([39], which also is a MIP, modifiers that have some inherited specificity. Also, the developed sensor has better results than exfoliated graphene [16] and boron doped diamond [53], which are purely chemical sensors, and better LOD than amorphous hydroxy-iron composites with ß-cyclodextrin [51] and polyacrilamid hydrogel-cytochrome P450 2C9 [6], both having biological sensing elements. Even so, it should be taken in consideration that the modifications on the electrode surface are solely chemical and were able to achieve as good results (in all medium) as the ones obtained when biological elements are integrated in the sensor. This is of particular relevance when detecting BPA in human urine samples, an extremely complex medium. These results couldn´t be compared with other sensors, due to lack of data in this medium.

Comparing the performance of the developed sensor with the more traditionally applied methods of detection, an evolution in terms of sensitivity in needed, even when comparing

results in more complex mediums like urine. While having this disadvantage, the fact that the sensor has a better portability and low cost associated plays and important factor to further carry on improving this technology.

6. Conclusions and Future Work

Succeeding a laborious path of optimization, in which parameters such as sensor type, buffer pH and nature, as well as pretreatment voltage and time, electrochemical method and type electrode surface modifier, a successful combination of Cu-MOF (1mg/mL) and CNT (2.33mg/mL), was obtained for the electrochemical detection of BPA.

By combining the two electrode surface modifiers in a 60% proportion of CNT/Cu-MOF on the surface of a commercial screen-printed electrode, a detection limit of 1.20×10^{-7} M was attained in phosphate buffer pH11, which is comparable and even lower to some results already described in previous works.

Besides analyzing BPA in buffer, interesting results were acquired when measuring BPA concentration in both synthetic and human urine diluted samples. In these cases, the lowest limit of detection was 2.52×10^{-7} M, using 30% CNT/Cu-MOF, for synthetic urine and 8.91×10^{-7} M for human urine samples, when using a combination of 60% CNT/Cu-MOF. To our knowledge, this is the first time that electrochemical sensors were used to analyze BPA in urine.

The observed low limits of detection in such complex matrices prove the potentiality of the developed sensor application in on-site monitoring. Furthermore due the fact that the surface modifiers enhancing BPA signal are chemical, they are more stable in a wide range of conditions.

Even with such promising results, further studies on other combinations of surface modifiers will be necessary, in order to attempt lowering the limit of detection and RSD values to levels comparable to the more sensitive electrochemical methods and traditional detection methods, already described in the literature. Application of the sensor for the detection of other emerging pollutants with structure similar to BPA is also of great interest, due to inherit low cost and stability of the developed sensor.

7. Bibliography

[1] Statistica, Production of plastics worldwide from 1950 to 2014, (2016). http://www.statista.com/statistics/282732/global-production-of-plastics-since-1950/ (accessed May 2, 2016).

[2] K.V. Ragavan, N.K. Rastogi, M.S. Thakur, Sensors and biosensors for analysis of bisphenol-A, TrAC Trends Anal. Chem. 52 (2013) 248–260. doi:10.1016/j.trac.2013.09.006.

[3] M. Portaccio, S. Di Martino, P. Maiuri, D. Durante, P. De Luca, M. Lepore, U. Bencivenga, S. Rossi, a. De Maio, D.G. Mita, Biosensors for phenolic compounds: The catechol as a substrate model, J. Mol. Catal. B Enzym. 41 (2006) 97–102. doi:10.1016/j.molcatb.2006.05.002.

[4] X. Tu, L. Yan, X. Luo, S. Luo, Q. Xie, Electroanalysis of Bisphenol A at a Multiwalled Carbon Nanotubes-gold Nanoparticles Modified Glassy Carbon Electrode, Electroanalysis. (2009) NA–NA. doi:10.1002/elan.200900195.

[5] K.S. Kim, J. Jang, W.-S. Choe, P.J. Yoo, Electrochemical detection of Bisphenol A with high sensitivity and selectivity using recombinant protein-immobilized graphene electrodes, Biosens. Bioelectron. 71 (2015) 214–221. doi:10.1016/j.bios.2015.04.042.

[6] P. Sun, Y. Wu, An amperometric biosensor based on human cytochrome P450 2C9 in polyacrylamide hydrogel films for bisphenol A determination, Sensors Actuators B Chem. 178 (2013) 113–118. doi:10.1016/j.snb.2012.12.055.

[7] J.R. Rochester, Bisphenol A and human health: a review of the literature., Reprod. Toxicol. 42 (2013) 132–55. doi:10.1016/j.reprotox.2013.08.008.

[8] I. Rykowska, W. Wasiak, Properties, threats, and methods of analysis of bisphenol A and its derivatives, Acta Chromatogr. (2006) 7–27. http://www.scopus.com/inward/record.url?eid=2-s2.0-33846058490&partnerID=tZOtx3y1.

[9] R. Wonderling, T. Powell, S. Baldwin, T. Morales, S. Snyder, K. Keiser, S. Hunter, E. Best, M.J. McDermott, M. Milhausen, Cloning, expression, purification, and biological activity of five feline type I interferons, Vet. Immunol. Immunopathol. 89 (2002) 13–27. doi:10.1016/S0165-2427(02)00188-5.

[10] M.A. Rahman, M.J. a Shiddiky, J.S. Park, Y.B. Shim, An impedimetric immunosensor for the label-free detection of bisphenol A, Biosens. Bioelectron. 22 (2007) 2464–2470. doi:10.1016/j.bios.2006.09.010.

[11] Merchant Research and Consulting, World BPA Production Grew by Over 372,000 Tonnes in 2012, Bisphenol A 2013 World Mark. Outlook Forecast up to 2017. (2013). https://mcgroup.co.uk/news/20131108/bpa-production-grew-372000-tonnes.html (accessed May 2, 2016).

[12] J. Yang, S.-E. Kim, M. Cho, I.-K. Yoo, W.-S. Choe, Y. Lee, Highly sensitive and selective determination of bisphenol-A using peptide-modified gold electrode, Biosens. Bioelectron. 61 (2014) 38–44. doi:10.1016/j.bios.2014.04.009.

[13] R.S.J. Alkasir, M. Ganesana, Y.-H. Won, L. Stanciu, S. Andreescu, Enzyme functionalized nanoparticles for electrochemical biosensors: A comparative study with applications for the detection of bisphenol A, Biosens. Bioelectron. 26 (2010) 43–49. doi:10.1016/j.bios.2010.05.001.

[14] D. Kharrazian, The Potential Roles of Bisphenol A (BPA) Pathogenesis in Autoimmunity., Autoimmune Dis. 2014 (2014) 743616. doi:10.1155/2014/743616.

[15] X. Wang, X. Lu, L. Wu, J. Chen, 3D metal-organic framework as highly efficient biosensing platform for ultrasensitive and rapid detection of bisphenol A, Biosens. Bioelectron. 65 (2015) 295–301. doi:10.1016/j.bios.2014.10.010.

[16] T. Ndlovu, O. a. Arotiba, S. Sampath, R.W. Krause, B.B. Mamba, An Exfoliated Graphite-Based Bisphenol A Electrochemical Sensor, Sensors. 12 (2012) 11601–11611. doi:10.3390/s120911601.

[17] M. Portaccio, D. Di Tuoro, F. Arduini, D. Moscone, M. Cammarota, D.G. Mita, M. Lepore, Laccase biosensor based on screen-printed electrode modified with thionine–carbon black nanocomposite, for Bisphenol A detection, Electrochim. Acta. 109 (2013) 340–347. doi:10.1016/j.electacta.2013.07.129.

[18] World Health Organization, T. Damstra, S. Barlow, a. Bergman, R. Kavlock, G. Van der Kraak, Chapter 1: Executive Summary, Int. Progr. Chem. Safety. Glob. Assess. Endocrine-Disrupting Chem. (2002) 1–4. doi:10.1089/15305620252933437.

[19] European Comission, Endocrine Disruptors - Definitions, (2016). http://ec.europa.eu/environment/chemicals/endocrine/definitions/endodis_en.htm (accessed March 2, 2016).

[20] A.N. Bezbaruah, H. Kalita, Sensors and biosensors for endocrine disrupting chemicals : State-of-the-art and future trends., 2010.

[21] European Food Safety Authority, No Consumer Health Risk from Bisphenol A, EFSA News. (2015) 4–7. http://www.efsa.europa.eu/en/press/news/150121 (accessed March 3, 2016).

[22] L. Zhu, Y. Cao, G. Cao, Electrochemical sensor based on magnetic molecularly imprinted nanoparticles at surfactant modified magnetic electrode for determination of bisphenol A, Biosens. Bioelectron. 54 (2014) 258–261. doi:10.1016/j.bios.2013.10.072.

[23] M. Portaccio, D. Di Tuoro, F. Arduini, M. Lepore, D.G. Mita, N. Diano, L. Mita, D. Moscone, A thionine-modified carbon paste amperometric biosensor for catechol and bisphenol A determination., Biosens. Bioelectron. 25 (2010) 2003–8. doi:10.1016/j.bios.2010.01.025.

[24] A.C. Pérez, M.J. Arcos-Martínez, O.D. Renedo, Desarrollo y aplicación de sensores y biosensores electroquímicos para la determinación de contaminantes medioambientales y agroalimentarios, Burgos, 2014.

[25] X. Wang, X. Lu, L. Wu, J. Chen, 3D metal-organic framework as highly efficient biosensing platform for ultrasensitive and rapid detection of bisphenol A, Biosens. Bioelectron. 65 (2015) 295–301. doi:10.1016/j.bios.2014.10.010.

[26] M. Li, Y.-T. Li, D.-W. Li, Y.-T. Long, Recent developments and applications of screen-printed electrodes in environmental assays--a review., Anal. Chim. Acta. 734 (2012) 31–44. doi:10.1016/j.aca.2012.05.018.

[27] L. Asturias, M.J. Arcos-Martínez, M.A. Alonso Lomillo, Deveolpment of Electrochemical Devices for the Determination of Drugs of Abuse, 2014.

[28] M. Prudenziati, B. Morten, Thick-film sensors: an overview, Sensors and Actuators. 10 (1986) 65–82. doi:10.1016/0250-6874(86)80035-X.

[29] Metrohm Autolab.B.V, Basic overview of the working principle of a potentiostat/galvanostat (PGSTAT) – Electrochemical cell setup, (2011) 1–3.

[30] A.J. Bard, L.R. Faulkner, Electrochemical Methods: Fundamentals and aplplications, Jonh Wiley and Sons, New York, 1980.

[31] D. Grieshaber, R. MacKenzie, J. Vörös, E. Reimhult, Electrochemical Biosensors - Sensor

Principles and Architectures, Sensors. 8 (2008) 1400–1458. doi:10.3390/s8031400.

[32] H. Yin, Y. Zhou, S. Ai, Q. Chen, X. Zhu, X. Liu, L. Zhu, Sensitivity and selectivity determination of BPA in real water samples using PAMAM dendrimer and CoTe quantum dots modified glassy carbon electrode., J. Hazard. Mater. 174 (2010) 236–43. doi:10.1016/j.jhazmat.2009.09.041.

[33] H. Yin, L. Cui, Q. Chen, W. Shi, S. Ai, L. Zhu, L. Lu, Amperometric determination of bisphenol A in milk using PAMAM–Fe3O4 modified glassy carbon electrode, Food Chem. 125 (2011) 1097–1103. doi:10.1016/j.foodchem.2010.09.098.

[34] Q. Liu, Q. Zhou, G. Jiang, Nanomaterials for analysis and monitoring of emerging chemical pollutants, TrAC - Trends Anal. Chem. 58 (2014) 10–22. doi:10.1016/j.trac.2014.02.014.

[35] J. Lei, R. Qian, P. Ling, L. Cui, H. Ju, Design and sensing applications of metal-organic framework composites, TrAC - Trends Anal. Chem. 58 (2014) 71–78. doi:10.1016/j.trac.2014.02.012.

[36] J.Y. Lee, D.H. Olson, L. Pan, T.J. Emge, J. Li, Microporous metal-organic frameworks with high gas sorption and separation capacity, Adv. Funct. Mater. 17 (2007) 1255–1262. doi:10.1002/adfm.200600944.

[37] B. Lu, M. Liu, H. Shi, X. Huang, G. Zhao, A Novel Photoelectrochemical Sensor for Bisphenol A with High Sensitivity and Selectivity Based on Surface Molecularly Imprinted Polypyrrole Modified TiO2 Nanotubes, Electroanalysis. 25 (2013) 771–779. doi:10.1002/elan.201200585.

[38] P. Deng, Z. Xu, J. Li, Y. Kuang, Acetylene black paste electrode modified with a molecularly imprinted chitosan film for the detection of bisphenol A, Microchim. Acta. 180 (2013) 861–869. doi:10.1007/s00604-013-1001-z.

[39] J. Huang, X. Zhang, S. Liu, Q. Lin, X. He, X. Xing, W. Lian, Electrochemical sensor for bisphenol A detection based on molecularly imprinted polymers and gold nanoparticles, J. Appl. Electrochem. 41 (2011) 1323–1328. doi:10.1007/s10800-011-0350-8.

[40] Y. Li, Y. Gao, Y. Cao, H. Li, Electrochemical sensor for bisphenol A determination based on MWCNT/melamine complex modified GCE, Sensors Actuators B Chem. 171-172 (2012) 726–733. doi:10.1016/j.snb.2012.05.063.

[41] Y. Gao, Y. Cao, D. Yang, X. Luo, Y. Tang, H. Li, Sensitivity and selectivity determination

of bisphenol A using SWCNT-CD conjugate modified glassy carbon electrode., J. Hazard. Mater. 199-200 (2012) 111–8. doi:10.1016/j.jhazmat.2011.10.066.

[42] D.G. Mita, A. Attanasio, F. Arduini, N. Diano, V. Grano, U. Bencivenga, S. Rossi, A. Amine, D. Moscone, Enzymatic determination of BPA by means of tyrosinase immobilized on different carbon carriers., Biosens. Bioelectron. 23 (2007) 60–5. doi:10.1016/j.bios.2007.03.010.

[43] J.A. Rather, K. De Wael, Fullerene-C60 sensor for ultra-high sensitive detection of bisphenol-A and its treatment by green technology, Sensors Actuators B Chem. 176 (2013) 110–117. doi:10.1016/j.snb.2012.08.081.

[44] B. Ntsendwana, B.B. Mamba, S. Sampath, O.A. Arotiba, Electrochemical detection of bisphenol a using graphene-modified glassy carbon electrode, Int. J. Electrochem. Sci. 7 (2012) 3501–3512. http://www.scopus.com/inward/record.url?eid=2-s2.0-84862679402&partnerID=tZOtx3y1.

[45] H. Fan, Y. Li, D. Wu, H. Ma, K. Mao, D. Fan, B. Du, H. Li, Q. Wei, Electrochemical bisphenol A sensor based on N-doped graphene sheets., Anal. Chim. Acta. 711 (2012) 24–8. doi:10.1016/j.aca.2011.10.051.

[46] Z. Zheng, Y. Du, Z. Wang, Q. Feng, C. Wang, Pt/graphene-CNTs nanocomposite based electrochemical sensors for the determination of endocrine disruptor bisphenol A in thermal printing papers., Analyst. 138 (2013) 693–701. doi:10.1039/c2an36569c.

[47] X. Niu, W. Yang, G. Wang, J. Ren, H. Guo, J. Gao, A novel electrochemical sensor of bisphenol A based on stacked graphene nanofibers/gold nanoparticles composite modified glassy carbon electrode, Electrochim. Acta. 98 (2013) 167–175. doi:10.1016/j.electacta.2013.03.064.

[48] Y. Zhang, L. Wang, D. Lu, X. Shi, C. Wang, X. Duan, Sensitive determination of bisphenol A base on arginine functionalized nanocomposite graphene film, Electrochim. Acta. 80 (2012) 77–83. doi:10.1016/j.electacta.2012.06.117.

[49] H. Yin, Y. Zhou, S. Ai, Preparation and characteristic of cobalt phthalocyanine modified carbon paste electrode for bisphenol A detection, J. Electroanal. Chem. 626 (2009) 80–88. doi:10.1016/j.jelechem.2008.11.004.

[50] H. Yin, L. Cui, S. Ai, H. Fan, L. Zhu, Electrochemical determination of bisphenol A at Mg–Al–CO3 layered double hydroxide modified glassy carbon electrode, Electrochim. Acta. 55 (2010) 603–610. doi:10.1016/j.electacta.2009.09.020.

[51] M. Masikini, T.T. Waryo, P.G.L. Baker, L. V. Ngqongwa, A.R. Williams, E.I. Iwuoha, Hydroxy-Iron/ß-cyclodextrin-Film Amperometric Sensor for the Endocrine Disruptor Substance Bisphenol-A in an Aqueous Medium with Reduced Fouling Effects, Anal. Lett. 44 (2011) 2047–2060. doi:10.1080/00032719.2010.539741.

[52] D.J. Browne, L. Zhou, J.H.T. Luong, J.D. Glennon, CE with a boron-doped diamond electrode for trace detection of endocrine disruptors in water samples, Electrophoresis. 34 (2013) 2025–2032. doi:10.1002/elps.201200480.

[53] G.F. Pereira, L.S. Andrade, R.C. Rocha-Filho, N. Bocchi, S.R. Biaggio, Electrochemical determination of bisphenol A using a boron-doped diamond electrode, Electrochim. Acta. 82 (2012) 3–8. doi:10.1016/j.electacta.2012.03.157.

[54] C. Yu, L. Gou, X. Zhou, N. Bao, H. Gu, Chitosan–Fe3O4 nanocomposite based electrochemical sensors for the determination of bisphenol A, Electrochim. Acta. 56 (2011) 9056–9063. doi:10.1016/j.electacta.2011.05.135.

[55] J. Huang, X. Zhang, Q. Lin, X. He, X. Xing, H. Huai, W. Lian, H. Zhu, Electrochemical sensor based on imprinted sol–gel and nanomaterials for sensitive determination of bisphenol A, Food Control. 22 (2011) 786–791. doi:10.1016/j.foodcont.2010.11.017.

[56] H. Yin, Y. Zhou, S. Ai, R. Han, T. Tang, L. Zhu, Electrochemical behavior of bisphenol a at glassy carbon electrode modified with gold nanoparticles, silk fibroin, and PAMAM dendrimers, Microchim. Acta. 170 (2010) 99–105. doi:10.1007/s00604-010-0396-z.

[57] H. Yin, Y. Zhou, J. Xu, S. Ai, L. Cui, L. Zhu, Amperometric biosensor based on tyrosinase immobilized onto multiwalled carbon nanotubes-cobalt phthalocyanine-silk fibroin film and its application to determine bisphenol A., Anal. Chim. Acta. 659 (2010) 144–50. doi:10.1016/j.aca.2009.11.051.

[58] Y. Zhang, Y. Cheng, Y. Zhou, B. Li, W. Gu, X. Shi, Y. Xian, Electrochemical sensor for bisphenol A based on magnetic nanoparticles decorated reduced graphene oxide., Talanta. 107 (2013) 211–8. doi:10.1016/j.talanta.2013.01.012.

[59] C. Mandenius, a Brundin, REVIEW : BIOCATALYSTS AND BIOREACTOR DESIGN Optimization, Bioprocess Methodology, Using Design-of-experiments, Biotechnol Progr. 24 (2008) 1191–1203. doi:10.1021/bp.67.

[60] D. Montgomery, Design and Analysis of Experiments, 2001.

[61] CDC, Laboratory Procedure Manual for Bisphenol A and other enviromental Phenols and

Parabens in Urine, 2009.

[62] C.G. Zoski, Handbook of Electrochemistry, Elsevier Science, 2006. https://books.google.pt/books?id=XWU_gNZ3yxwC.

8. Appendix

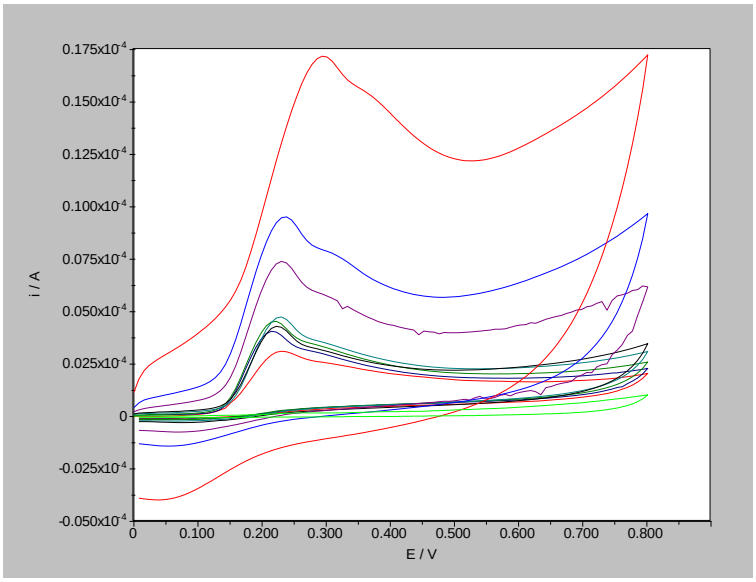

Graph A 1 - CV curves for BPA concentration of 5×10^{-5}M using virgin sensors for each time studied (Red – 0s; Dark Blue – 15s; Green – 30s; Cyan – 60s; Black – 90s; Magenta – 180s; Blue –360s; Red – 720s; Light Green – Buffer)

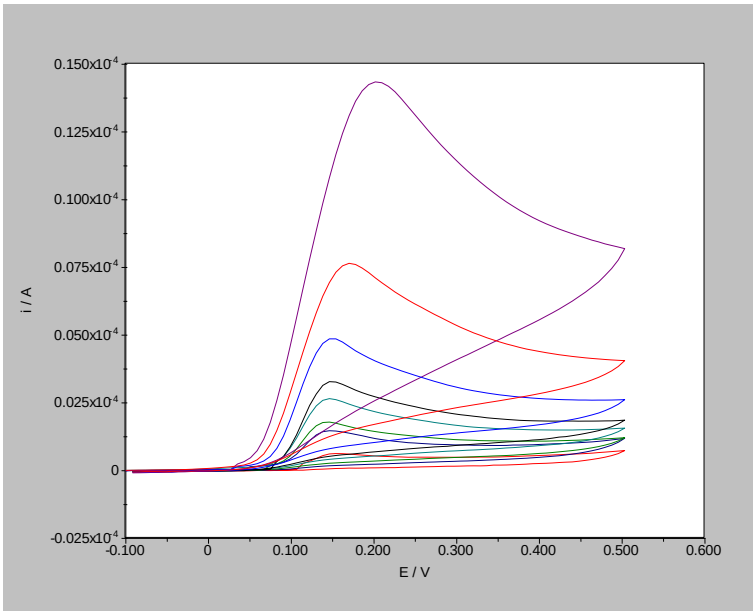

Graph A 2 - CV curves for concentrations 1×10^{-5}M to 4×10^{-4}M of BPA using virgin sensors in Na_3PO_4 pH12 (Red - 1×10^{-5}M; Dark Blue 2×10^{-5}M; Green - 4×10^{-5}M; Cyan - 6×10^{-5}M; Black - 8×10^{-5}M; Blue - 1×10^{-4}M; Red - 2×10^{-4}M; Magenta - 4×10^{-4}M).

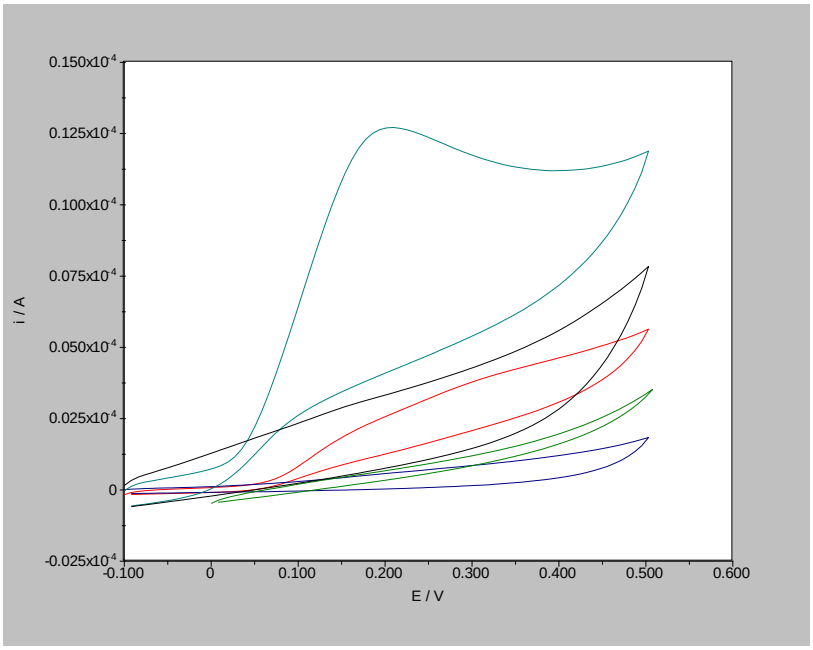

Graph A 3 - CV curves to test electrode surface regeneration using a concentration of 5×10^{-4}M of BPA in Na_3PO_4 ph12 (Red - 1st scan to foul; Green - 2nd scan to foul; Blue - verifying fouling existed; Cyan - Measuring after cleaning in 5×10^{-4}M of BPA; Black - Measuring after cleaning, in buffer).

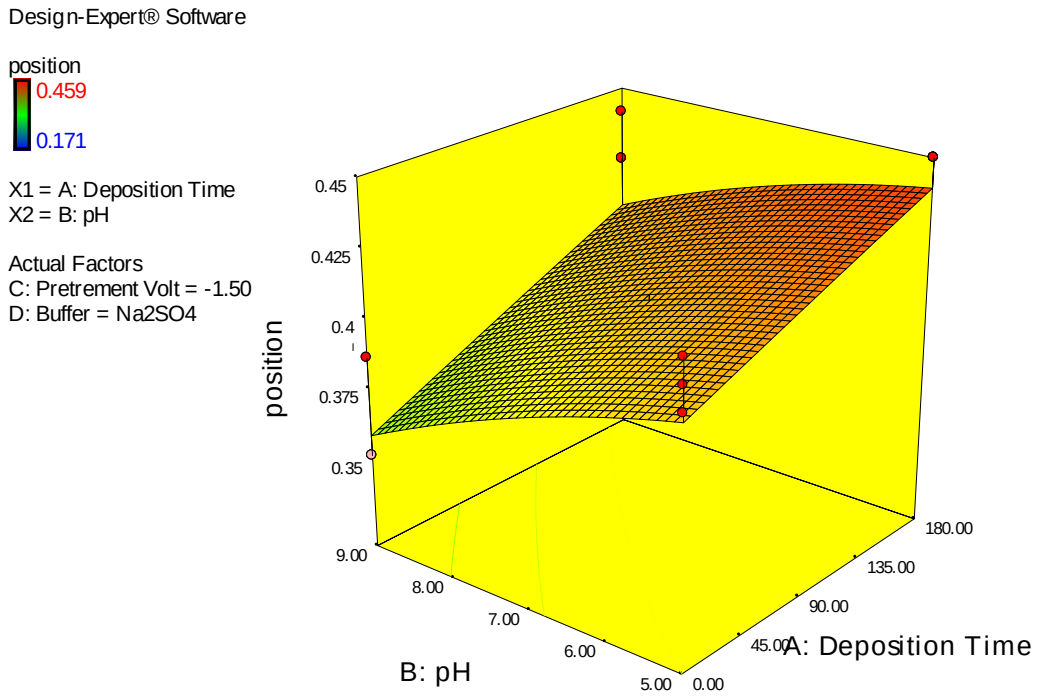

Graph A 4 - Design Expert 3D graph for the response Position (Potential), with pretreatment voltage on the low level (-1.5 V) and using Na_2SO_4.

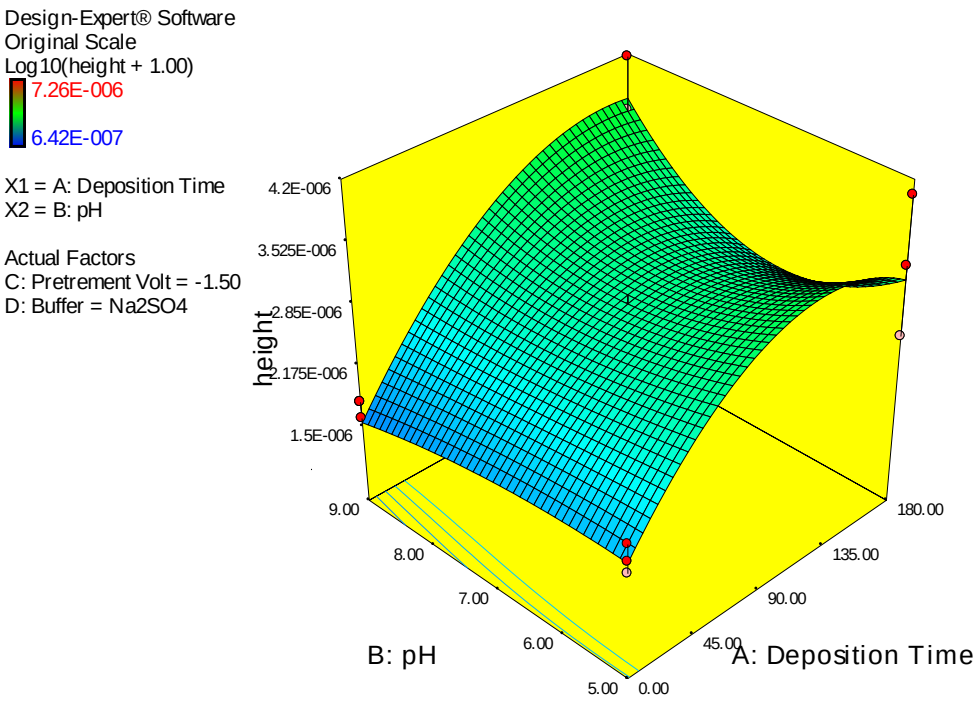

Graph A 5 - Design Expert 3D graph for the response height of peaks, with pretreatment voltage on the low level (-1.5V) and using Na_2SO_4.

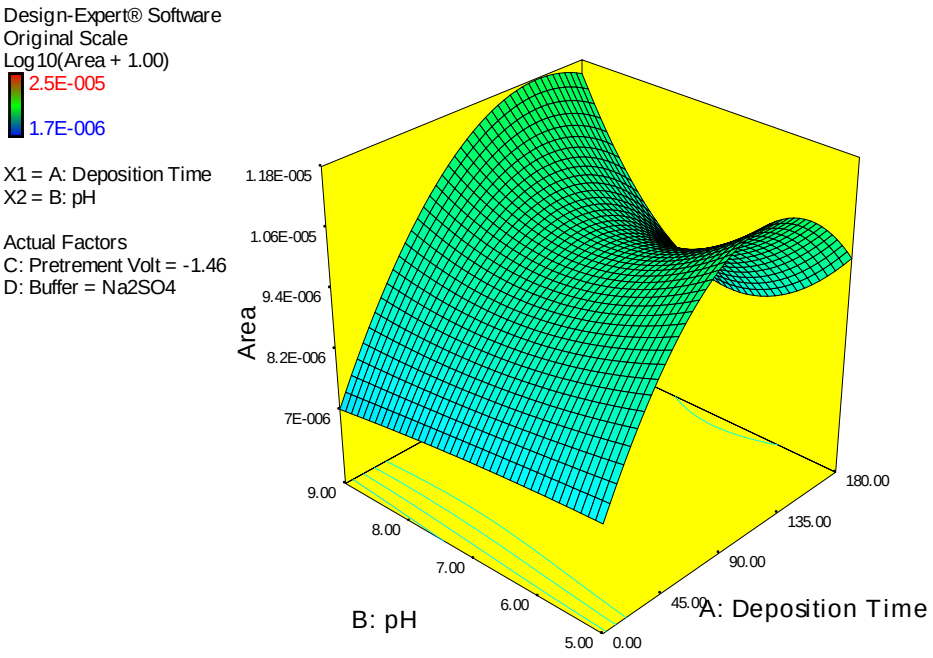

Graph A 6 - Design Expert 3D graph for the response area of the peak, with pretreatment voltage on the low level (-1.5V) and using Na_2SO_4.

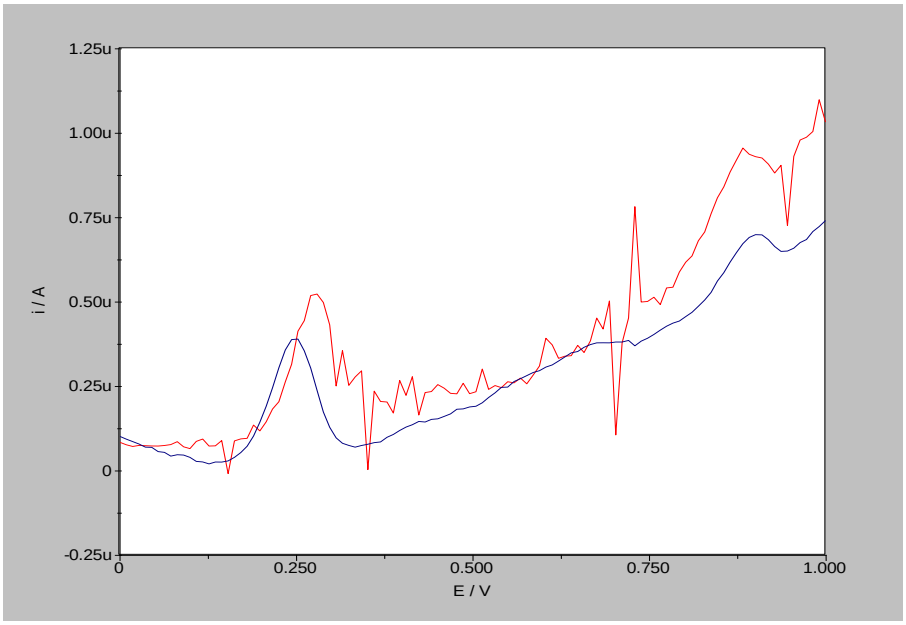

Graph A 7 – Interfering peaks using normal (red) or diluted buffer (blue). Phosphate buffer pH7, using DP electrochemical technique in blank solution.

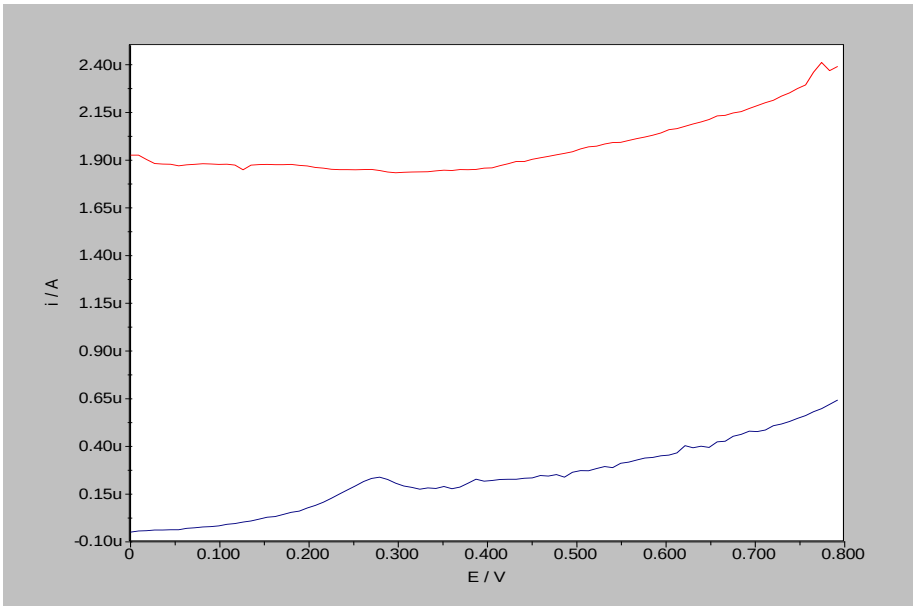

Graph A 8 – Interfering peaks with (red) or without pretreatment (blue) applied to the buffer. Phosphate buffer pH 8.2, using differential pulse technique in blank solution.

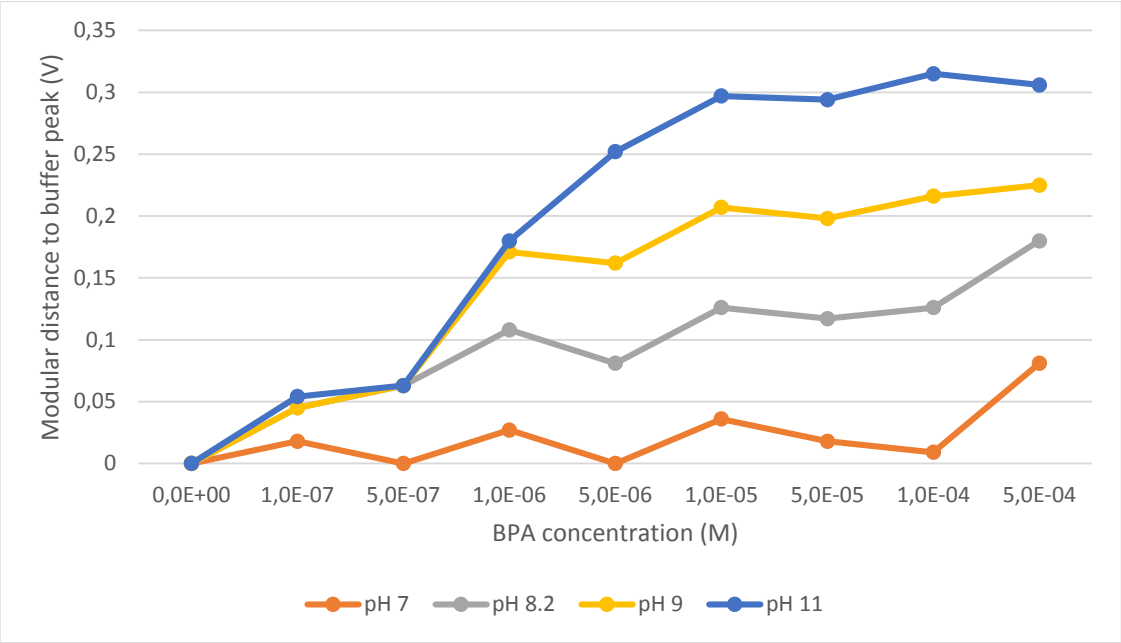

Graph A 9 - Modular potential distance of BPA peaks to buffer peak, in different pH. DP technique with BPA ranging from 1×10^{-7}M to 5×10^{-4}M, using virgin sensors for each concentration. The bigger the difference from the potential of the peak in the blank solution to the potentials of peaks for other BPA concentration, the better is the pH.

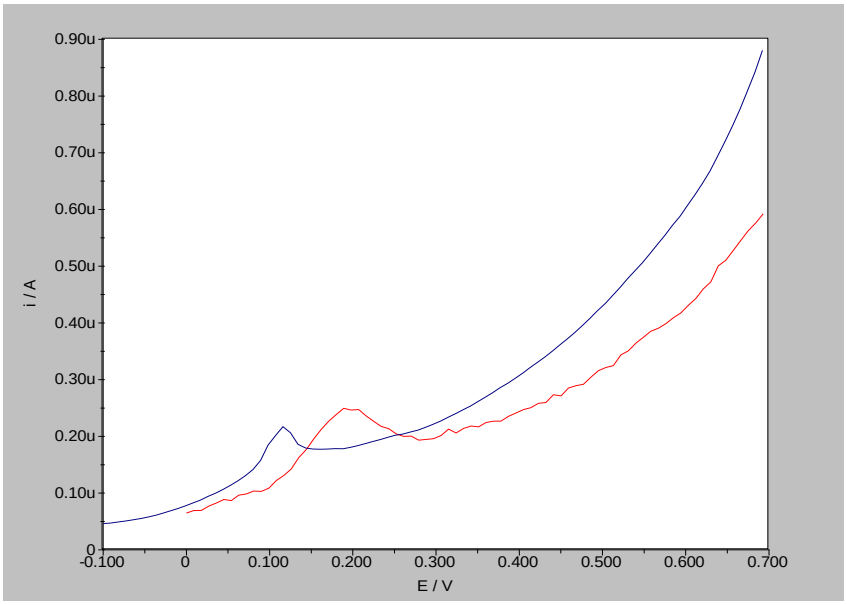

Graph A 10 - Interfering peaks on homemade (red) or DropSens (blue) applied to the buffer. Phosphate buffer pH 11, using differential pulse technique in blank solution.

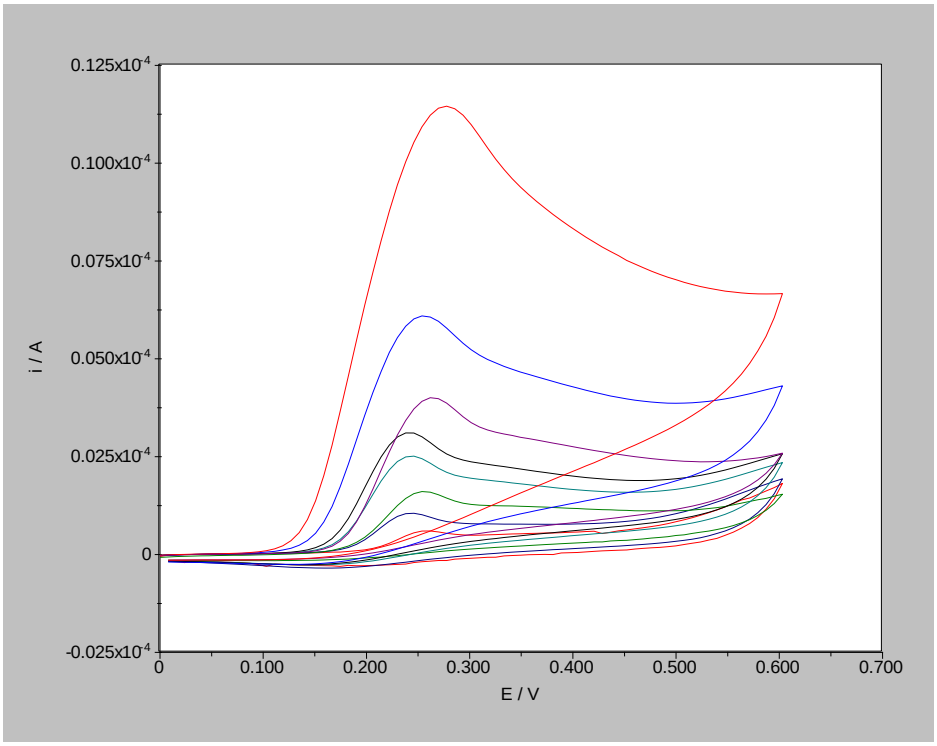

Graph A 11 - CV curves for concentrations 1×10^{-5}M to 4×10^{-4}M of BPA using gold nanoparticles on the electrode surface. Virgin sensors were used for each concnetration in phosphate buffer pH 8.(Red - 1×10^{-5}M ; Dark Blue - 2×10^{-5}M; Green - 4×10^{-5}M; Cyan - 6×10^{-5}M; Black - 8×10^{-5}M; Magenta - 1×10^{-4}M; Blue - 1×10^{-4}M; Red - 41×10^{-4}M).

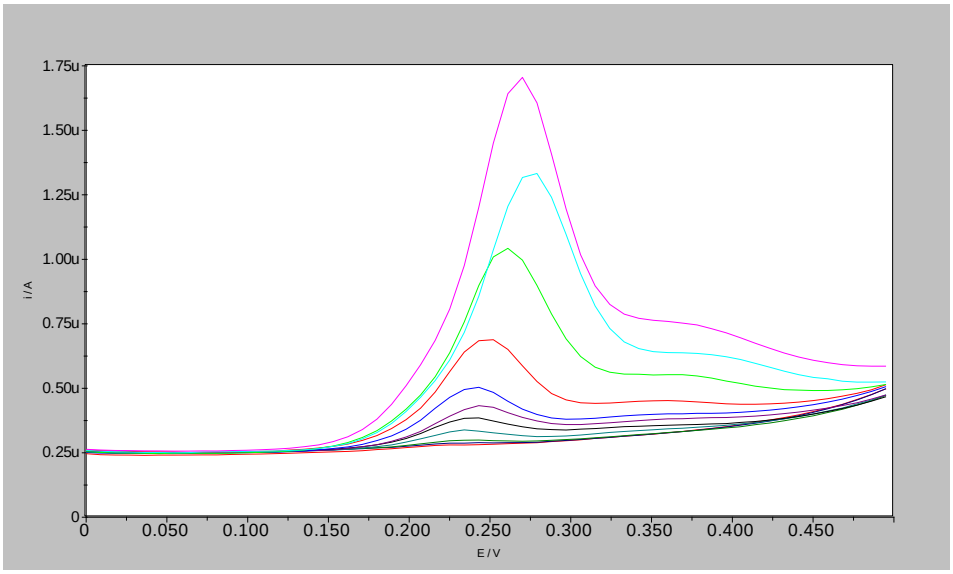

Graph A 12 - BPA peaks using DropSens sensors modified with a commercial solution of nanotubes. 60s of stirring time before measurement. Phosphate buffer pH11. Experiments done at BPA concentrations of 1×10^{-8} to 8×10^{-7}M using DP detection technique.

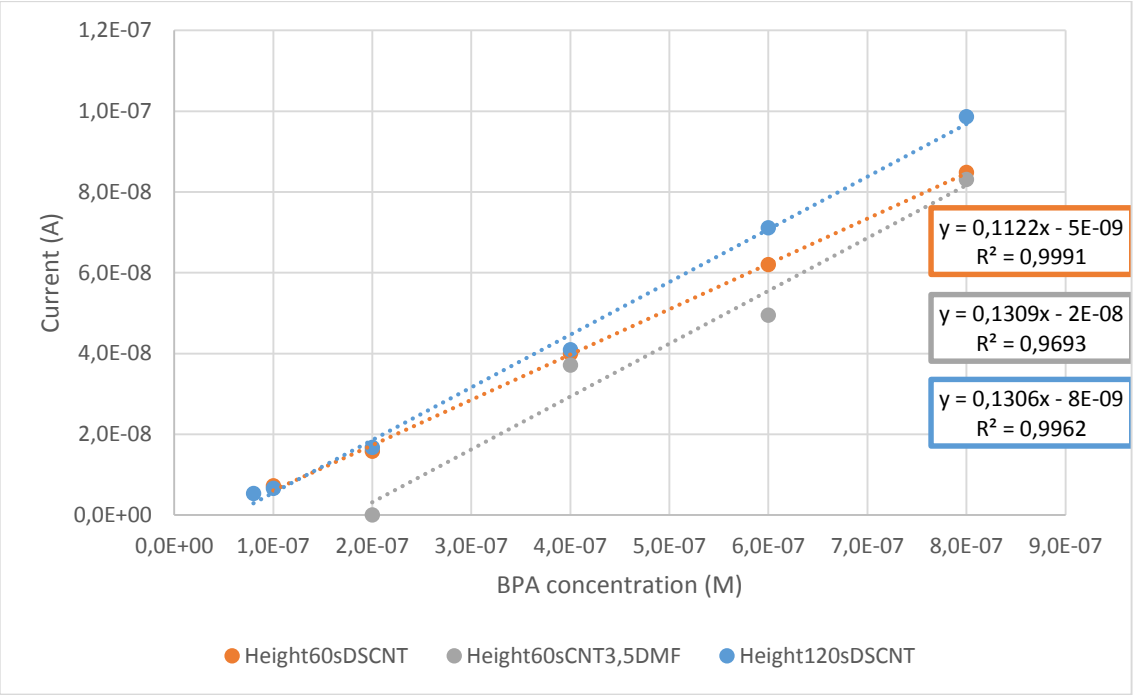

Graph A 13 - Height for BPA peaks using DropSens sensors modified with a commercial (DSCNT) or non-commercial solution (CNT3.5DMF) of nanotubes, deferring in stirring time before measuring. Phosphate buffer pH11. Experiments done at BPA concentrations of 1×10^{-8} to 8×10^{-7}M. DP technique was used.

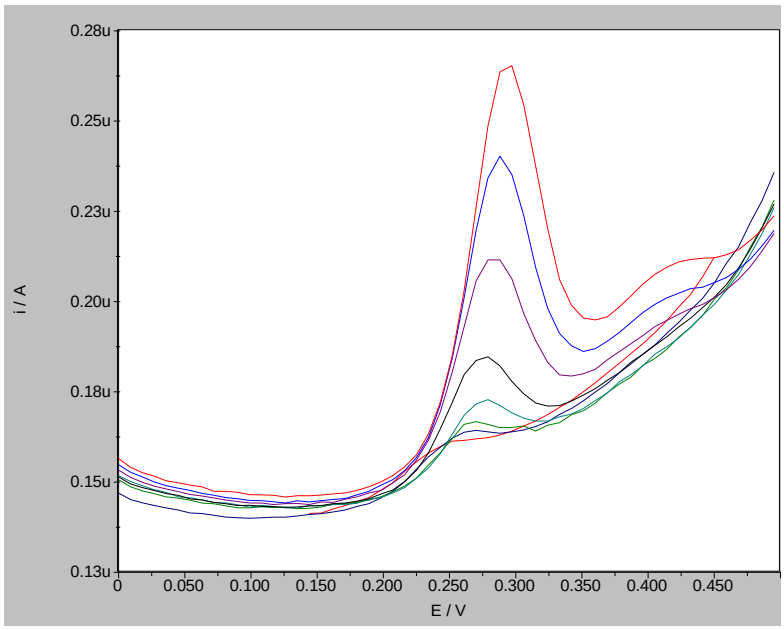

Graph A 14 - DP curves for concentrations 4×10^{-8}M to 8×10^{-7}M of BPA using DropSens sensors in Phosphate Buffer ph11 with Cu-MOF (Red - 4×10^{-8}M; Dark Blue 6×10^{-8}M; Green - 8×10^{-8}M; Cyan - 1×10^{-7}M; Black - 2×10^{-7}M; Magenta - 4×10^{-7}M; Blue - 6×10^{-7}M; Red - 8×10^{-7}M)

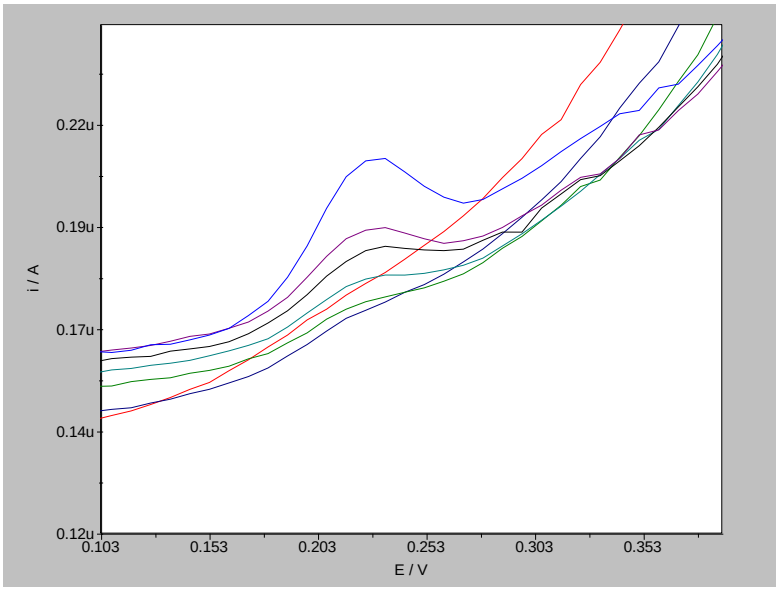

Graph A 15 - DP curves for concentrations 1×10^{-8}M to 2×10^{-7}M of BPA using DropSens sensors in Phosphate Buffer ph11 with 5% CNT (Red - 1×10^{-8}M; Dark Blue 2×10^{-8}M; Green – 4×10^{-8}M; Cyan - 6×10^{-8}M; Black - 8×10^{-8}M; Magenta - 1×10^{-7}M; Blue - 2×10^{-7}M).

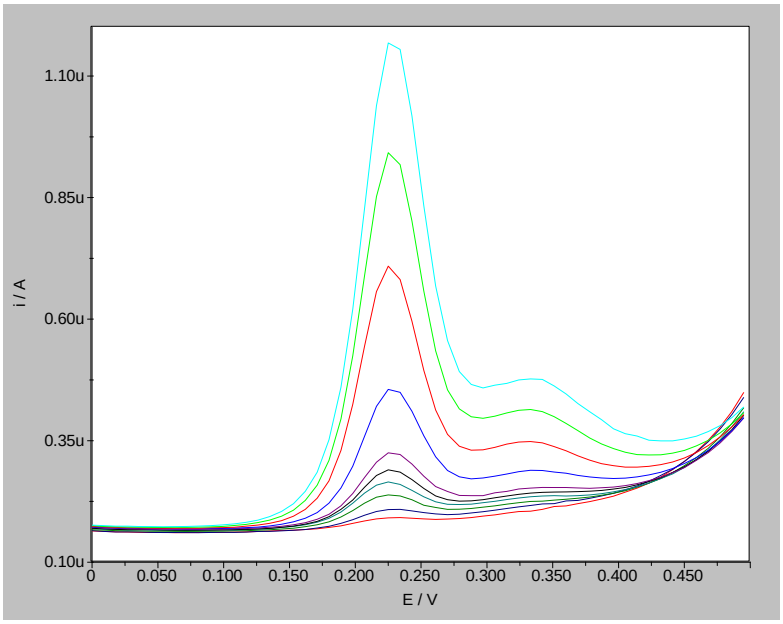

Graph A 16 - DP curves for concentrations 1×10^{-7}M to 8×10^{-6}M of BPA using DropSens sensors in Phosphate Buffer ph11 with 5% CNT (Red - 1×10^{-7}M; Dark Blue 2×10^{-7}M; Green – 4×10^{-7}M; Cyan - 6×10^{-7}M; Black - 8×10^{-7}M; Magenta - 1×10^{-6}M; Blue - 2×10^{-6}M; Red – 4×10^{-6}M; Light Green – 6×10^{-6}M; Light Cyan – 8×10^{-6}M).

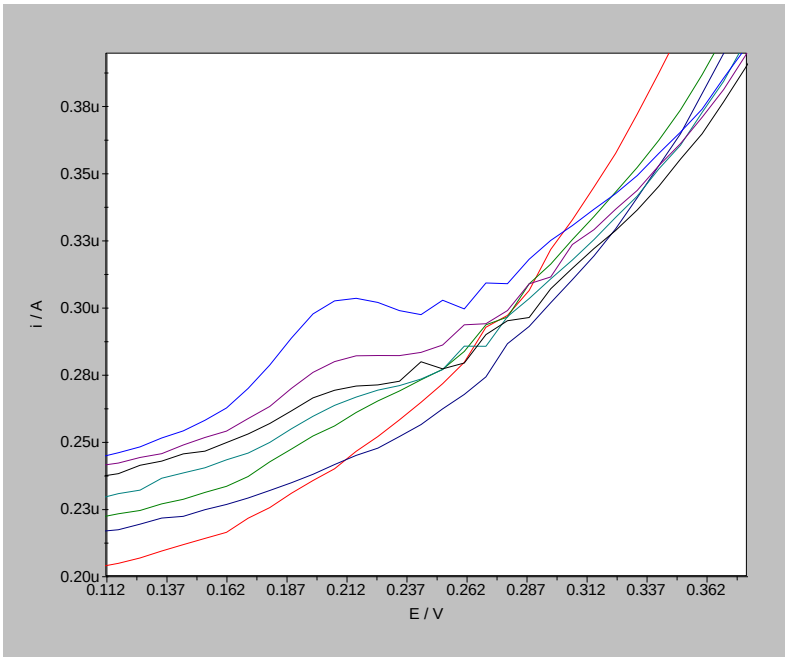

Graph A 17 - DP curves for concentrations 1×10^{-8}M to 2×10^{-7}M of BPA using DropSens sensors in Phosphate Buffer ph11 with 30% CNT (Red - 1×10-8M; Dark Blue 2×10-8M; Green - 4×10^{-8}M; Cyan - 6×10^{-8}M; Black - 8×10^{-8}M; Magenta - 1×10^{-7}M; Blue - 2×10^{-7}M)

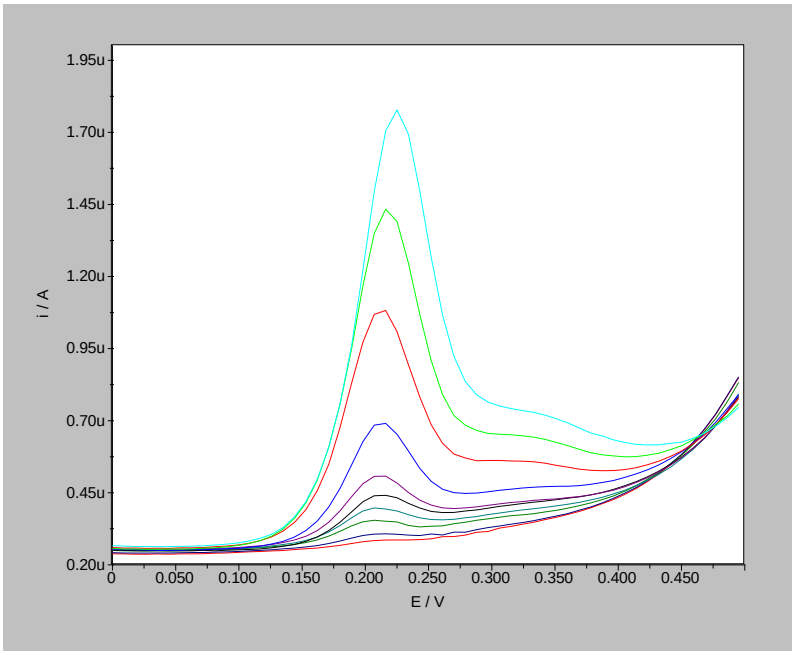

Graph A 18 - DP curves for concentrations 1×10^{-7}M to 8×10^{-6}M of BPA using DropSens sensors in Phosphate Buffer ph11 with 30% CNT (Red - 1×10^{-7}M; Dark Blue 2×10^{-7}M; Green - 4×10^{-7}M; Cyan - 6×10^{-7}M; Black - 8×10^{-7}M; Magenta - 1×10^{-6}M; Blue - 2×10^{-6}M; Red - 4×10^{-6}M; Light Green - 6×10^{-6}M; Light Cyan - 8×10^{-6}M)

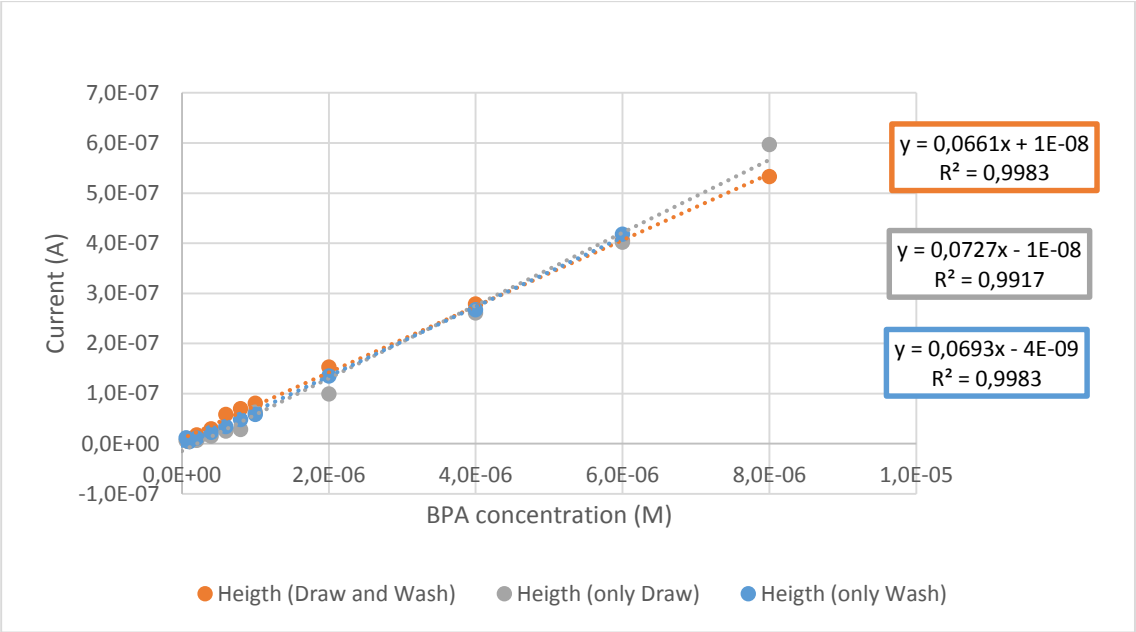

Graph A 19 - Comparison between different cleaning processes in single drop experiments. Drop Volume - 100 µL. Phosphate Buffer pH11. No modification to DropSens Sensors.

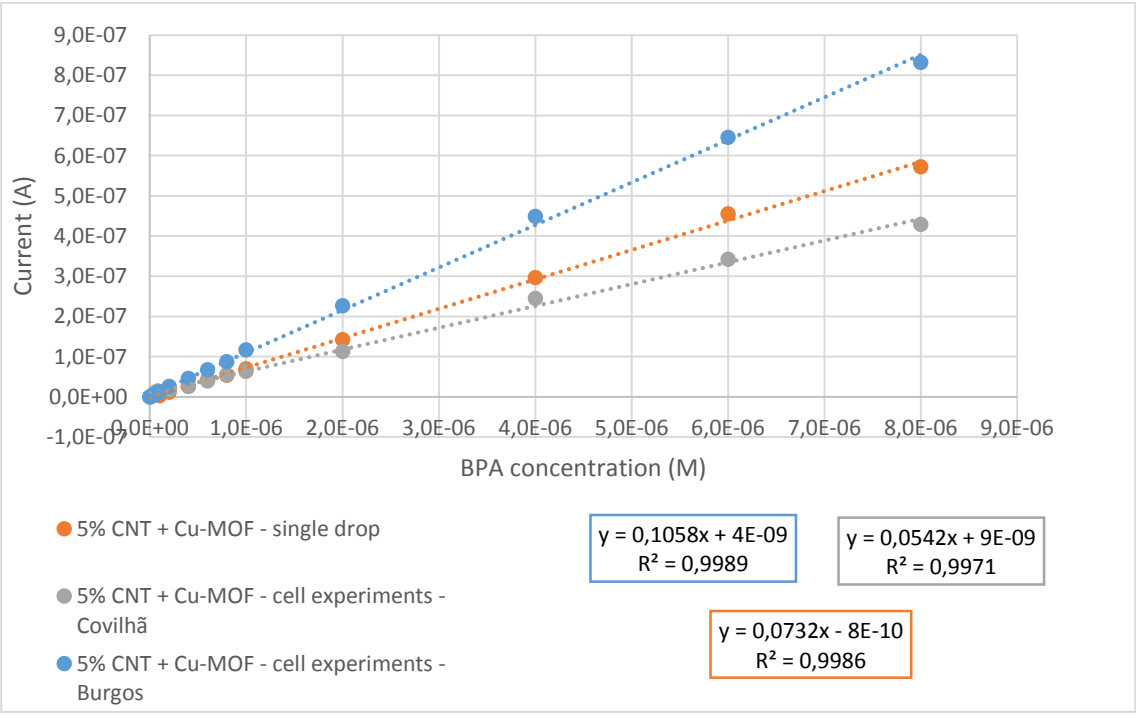

Graph A 20 - Comparison of height of BPA peaks for 5% CNT + Cu-MOF. Different experiments include Single Drop and Cell experiments (performed both in Burgos, Spain and Covilhã, Portugal). Phosphate Buffer pH 11 and BPA concentration ranging from 1×10^{-8}M to 8×10^{-6}M. Dropsens sensors and DP method.

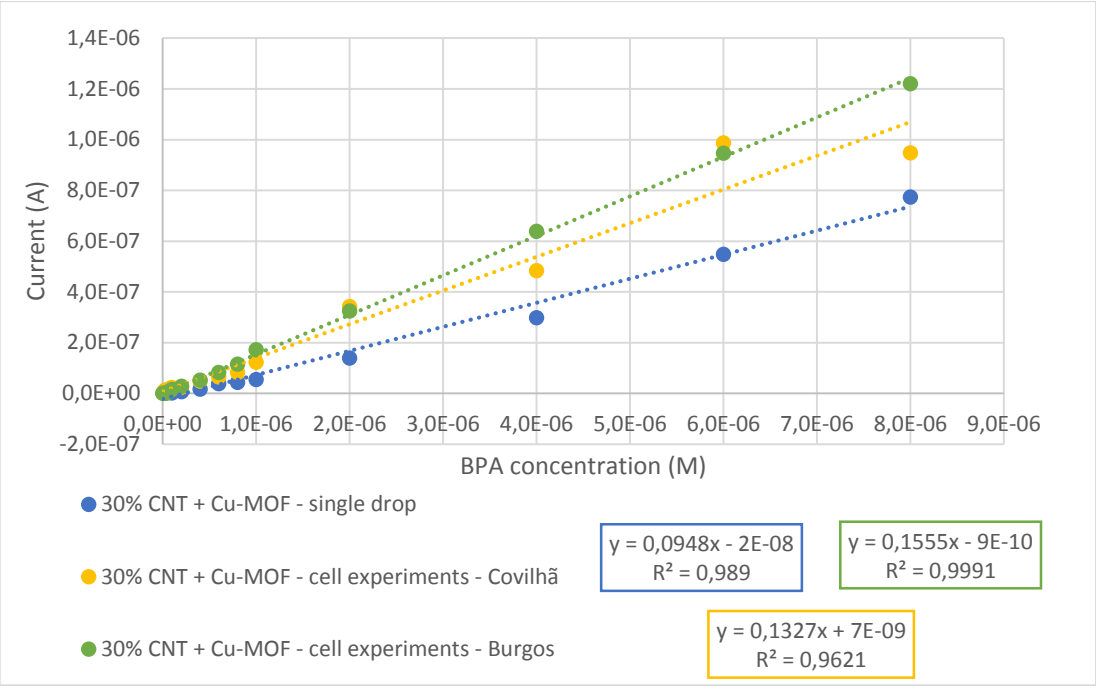

Graph A 21 - Comparison of height of BPA peaks for 30% CNT + Cu-MOF. Different experiments include Single Drop and Cell experiments (performed both in Burgos, Spain and Covilhã, Portugal). Phosphate Buffer pH 11 and BPA concentration ranging from 1×10^{-8}M to 8×10^{-6}M. Dropsens sensors and DP method.

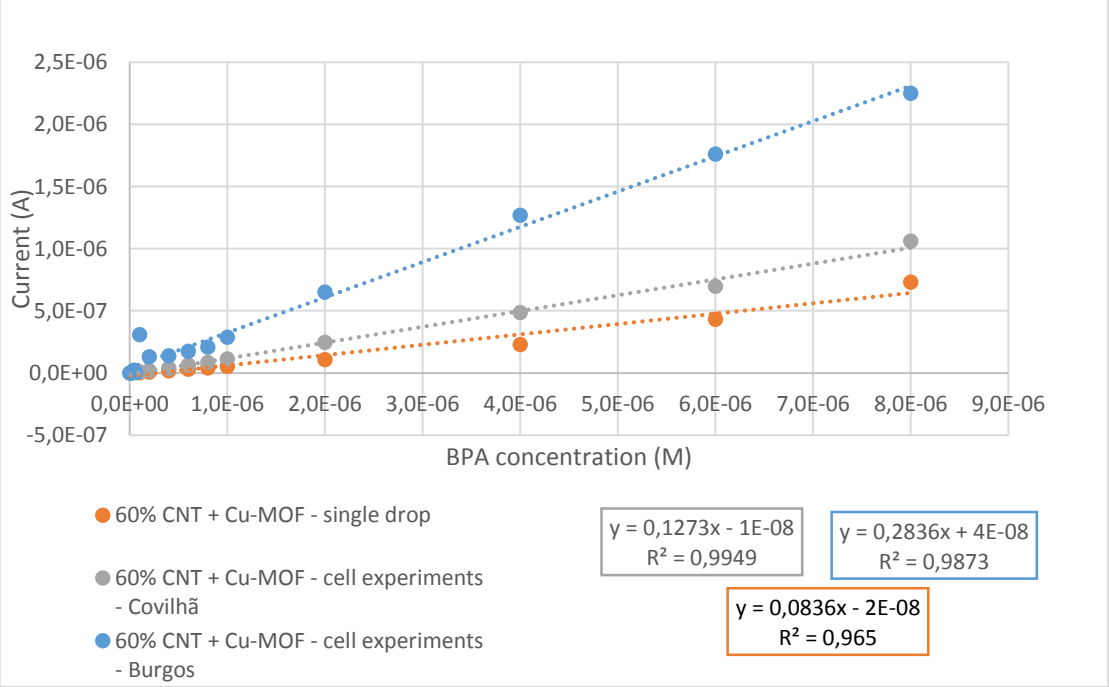

Graph A 22 - Comparison of height of BPA peaks for 60% CNT + Cu-MOF. Different experiments include Single Drop and Cell experiments (performed both in Burgos, Spain and Covilhã, Portugal). Phosphate Buffer pH 11 and BPA concentration ranging from 1×10^{-8}M to 8×10^{-6}M. Dropsens sensors and DP method.

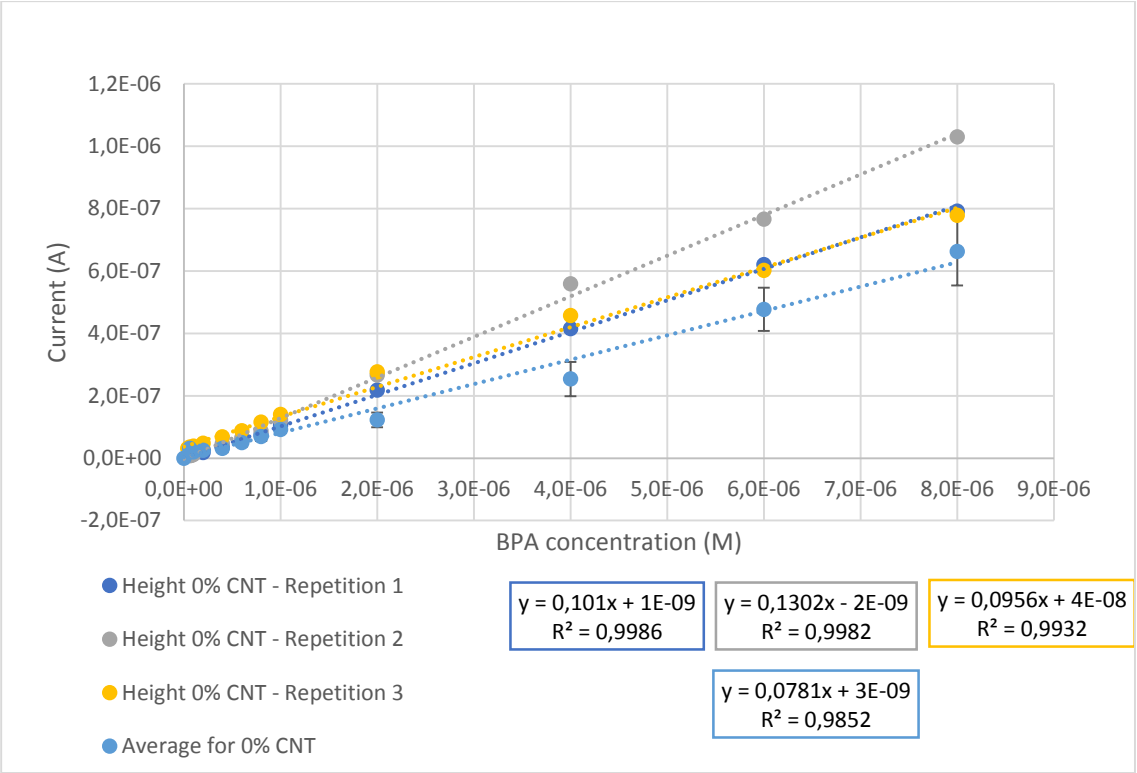

Graph A 23 - Comparison of 3 repetitions for 0% CNT + Cu-MOF and the average curve. Phosphate Buffer pH 11 and BPA concentration ranging from 1×10^{-8}M to 8×10^{-6}M. Dropsens sensors were used.

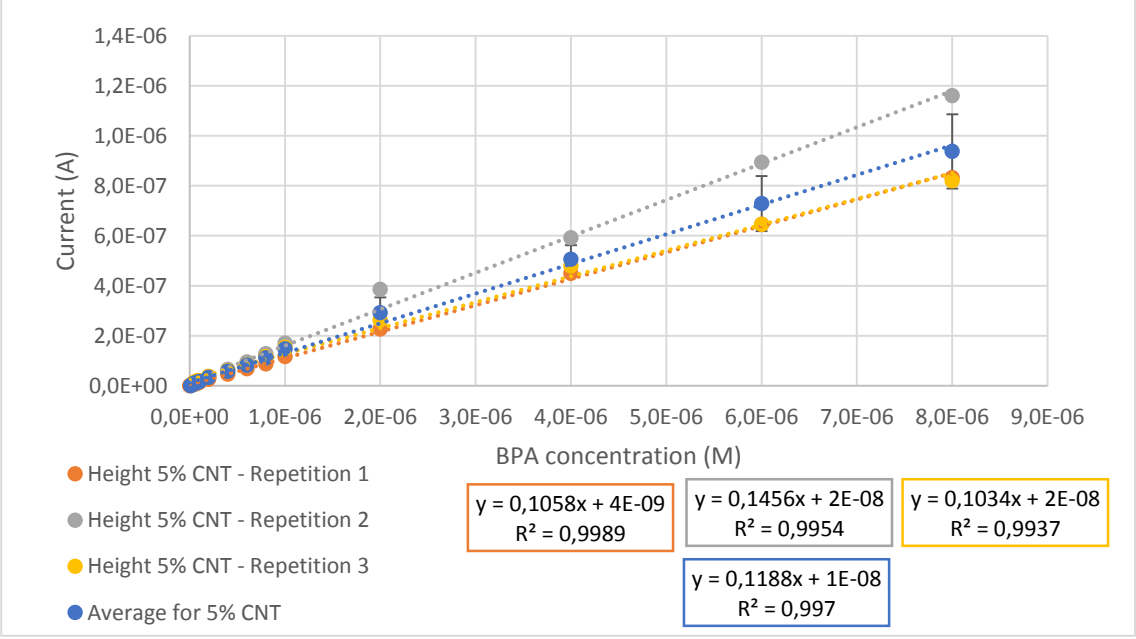

Graph A 24 - Comparison of 3 repetitions for 5% CNT + Cu-MOF and the average curve. Phosphate Buffer pH 11 and BPA concentration ranging from 1×10^{-8}M to 8×10^{-6}M. Dropsens sensors were used.

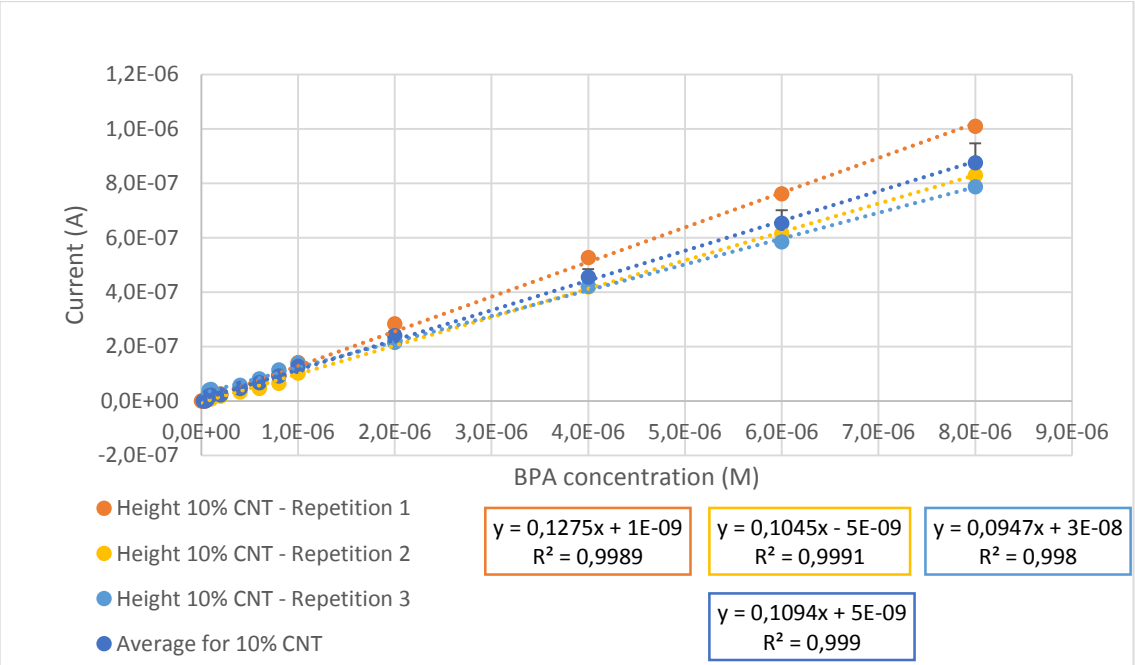

Graph A 25 - Comparison of 3 repetitions for 10% CNT + Cu-MOF and the average curve. Phosphate Buffer pH 11 and BPA concentration ranging from 1×10^{-8}M to 8×10^{-6}M. Dropsens sensors were used.

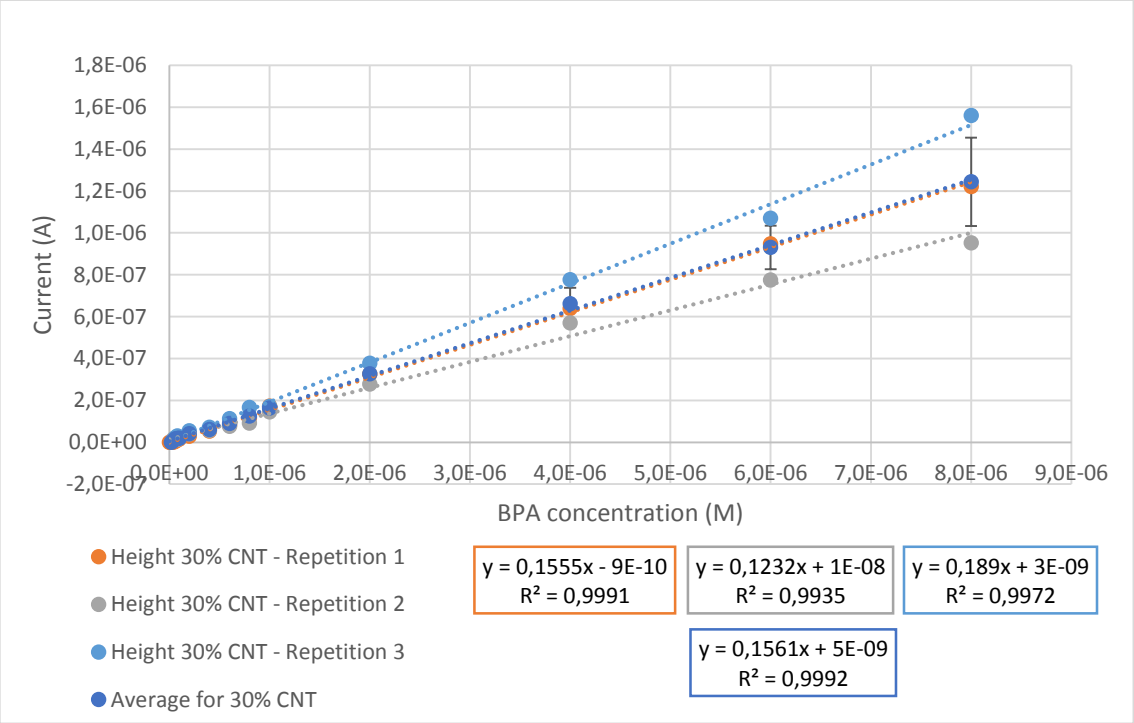

Graph A 26 - Comparison of 3 repetitions for 30% CNT + Cu-MOF and the average curve. Phosphate Buffer pH 11 and BPA concentration ranging from 1×10^{-8}M to 8×10^{-6}M. Dropsens sensors were used.

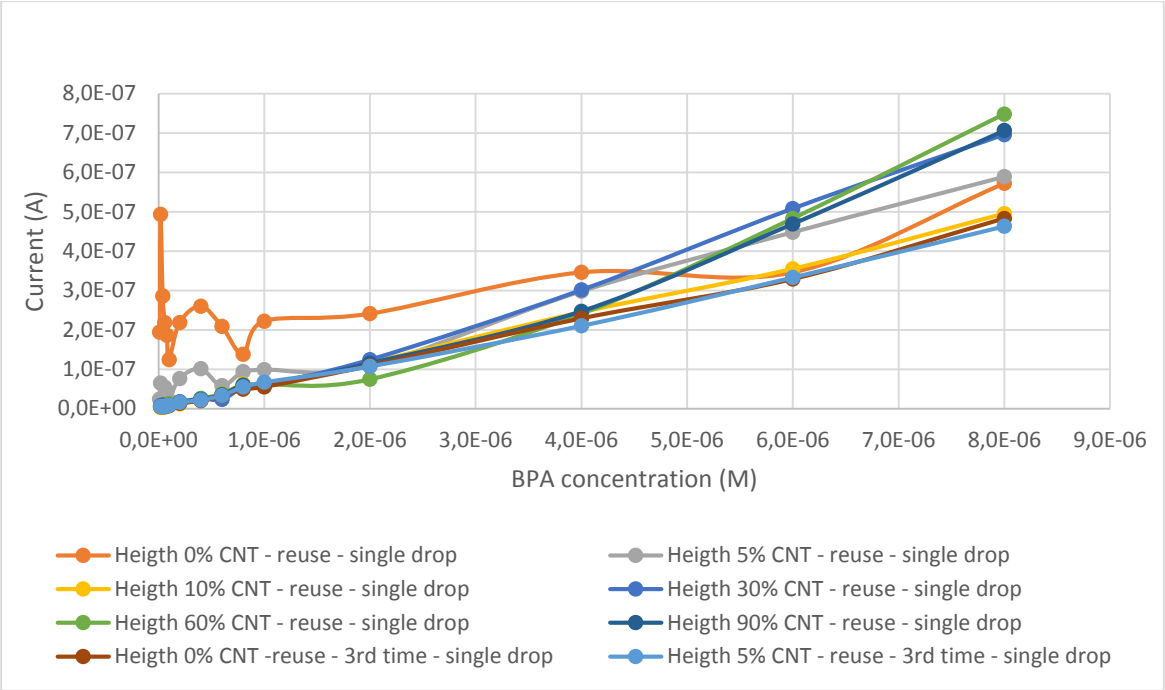

Graph A 27 - Comparison of curves for different CNT and Cu-MOF percentages, when reusing sensors in single drop experiments. Phosphate Buffer pH11 and BPA concentration ranging from 1×10^{-8}M to 8×10^{-6}M. Dropsens sensors were used.

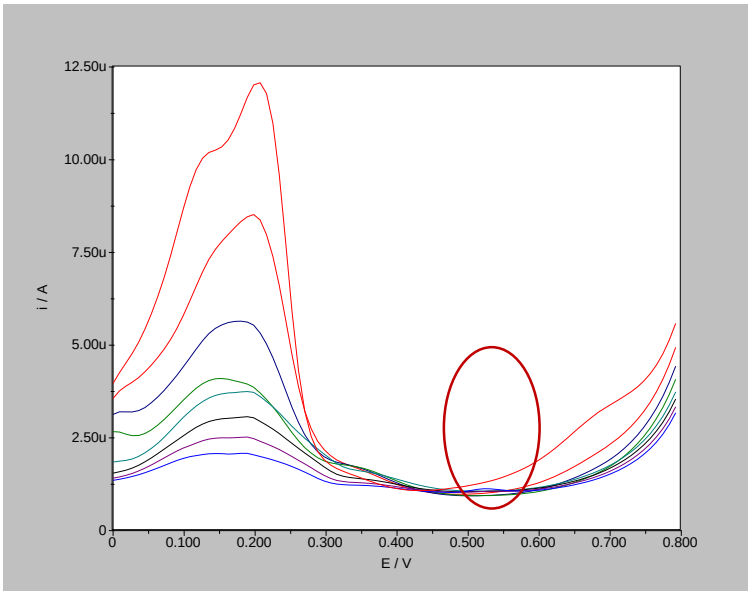

Graph A 28 - DP curves for concentrations 0 to 2×10^{-7}M of BPA using DropSens sensors in Phosphate Buffer ph8 and Synthetic Urine (1:8 dilution) with 30% CNT (Red - 0 M; Red - 1×10^{-8}M; Dark Blue 2×10^{-8}M; Green - 4×10^{-8}M; Cyan - 6×10^{-8}M; Black - 8×10^{-8}M; Magenta - 1×10^{-7}M; Blue - 2×10^{-7}M). BPA region circled in red.

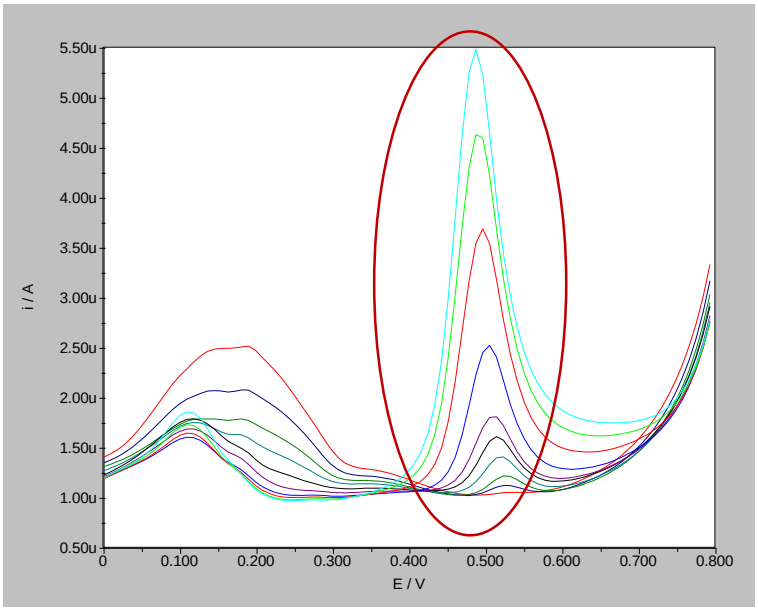

Graph A 29 - DP curves for concentrations 1×10^{-7}M to 8×10^{-6}M of BPA using DropSens sensors in Phosphate Buffer ph8 and Synthetic Urine (1:8 dilution) with 30% CNT (Red - 1×10^{-7}M; Dark Blue 2×10^{-7}M; Green - 4×10^{-7}M; Cyan - 6×10^{-7}M; Black - 8×10^{-7}M; Magenta - 1×10^{-6}M; Blue - 2×10^{-6}M; Red - 4×10^{-6}M; Light Green - 6×10^{-6}M; Light Cyan - 8×10^{-6}M). BPA peaks circled in red.

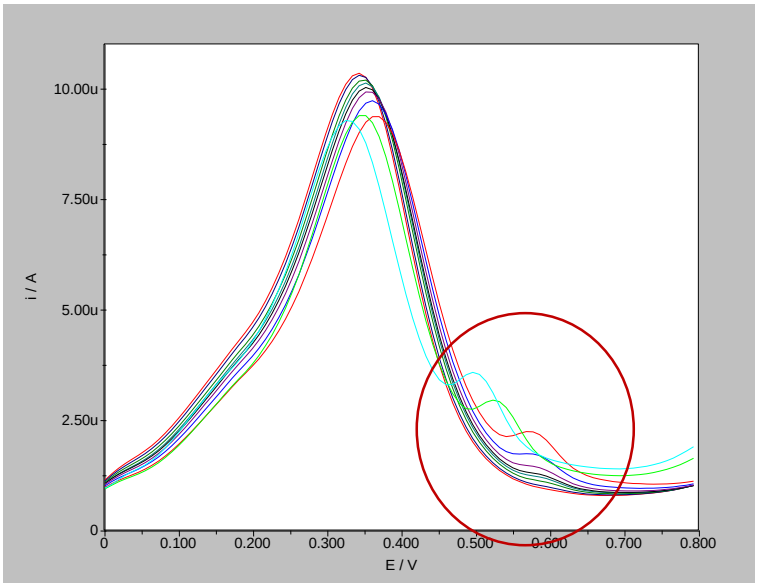

Graph A 30 - DP curves for concentrations 1×10^{-7}M to 8×10^{-6}M of BPA using DropSens sensors in Phosphate Buffer ph8 and Synthetic Urine (1:2 dilution) with 5% CNT (Red - 1×10^{-7}M; Dark Blue 2×10^{-7}M; Green - 4×10^{-7}M; Cyan - 6×10^{-7}M; Black - 8×10^{-7}M; Magenta - 1×10^{-6}M; Blue - 2×10^{-6}M; Red - 4×10^{-6}M; Light Green - 6×10^{-6}M; Light Cyan - 8×10^{-6}M). BPA peaks circled in red.

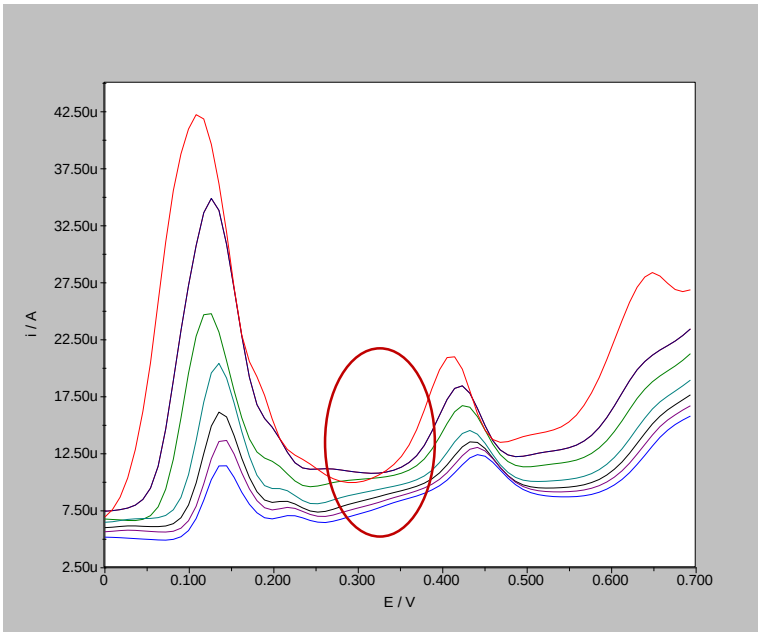

Graph A 31 - DP curves for concentrations 0 to 2×10^{-7}M of BPA using DropSens sensors in Phosphate Buffer ph8 and Urine Sample JS080590 (1:10 dilution) with 30% CNT (Red - 0 M; Red - 1×10^{-8}M; Dark Blue 2×10^{-8}M; Green - 4×10^{-8}M; Cyan - 6×10^{-8}M; Black - 8×10^{-8}M; Magenta - 1×10^{-7}M; Blue - 2×10^{-7}M). BPA region circled in red.

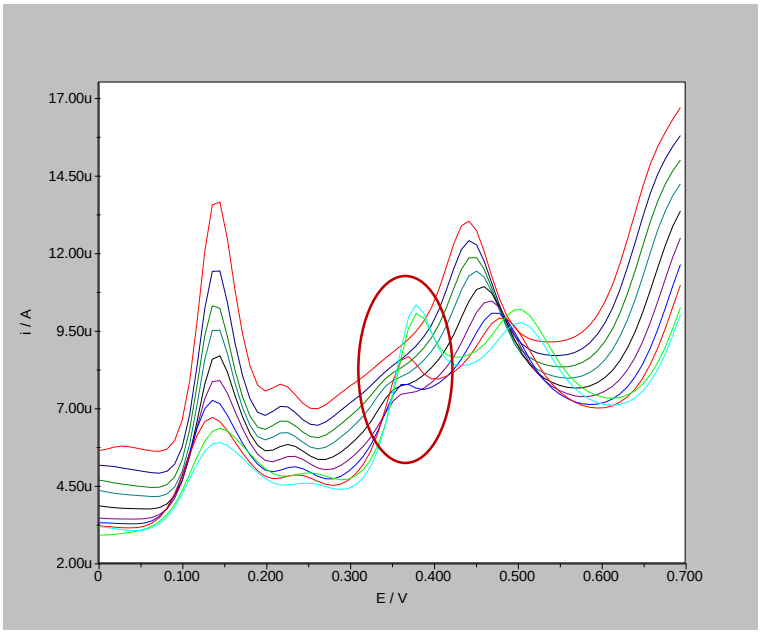

Graph A 32 - DP curves for concentrations 1×10^{-7}M to 8×10^{-6}M of BPA using DropSens sensors in Phosphate Buffer ph8 and Urine Sample - JS080590 (1:10 dilution) with 30% CNT (Red - 1×10^{-7}M; Dark Blue 2×10^{-7}M; Green - 4×10^{-7}M; Cyan - 6×10^{-7}M; Black - 8×10^{-7}M; Magenta - 1×10^{-6}M; Blue - 2×10^{-6}M; Red - 4×10^{-6}M; Light Green - 6×10^{-6}M; Light Cyan - 8×10^{-6}M). Circled in red are the BPA peaks.

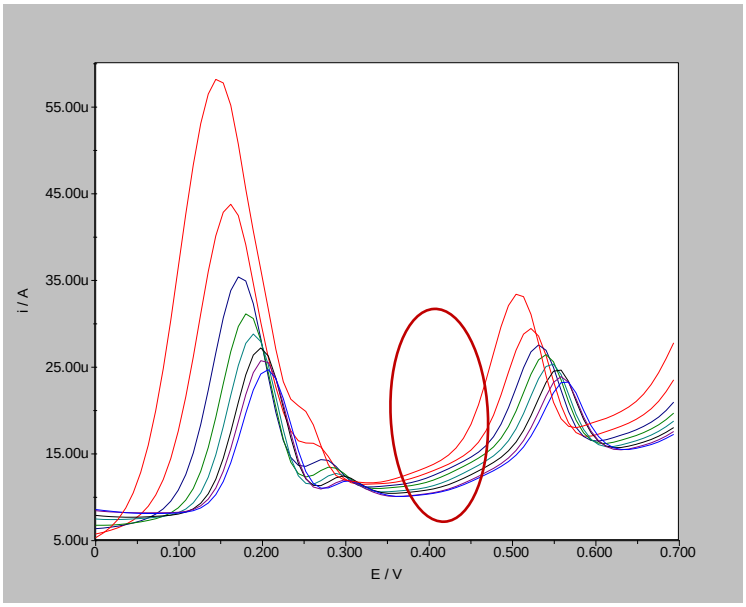

Graph A 33 - DP curves for concentrations 0 to 2×10^{-7}M of BPA using DropSens sensors in Phosphate Buffer ph8 and Urine Sample JS080590 (1:10 dilution) with 60% CNT (Red – 0 M; Red - 1×10^{-8}M; Dark Blue 2×10^{-8}M; Green – 4×10^{-8}M; Cyan - 6×10^{-8}M; Black - 8×10^{-8}M; Magenta - 1×10^{-7}M; Blue - 2×10^{-7}M). BPA region circled in red.

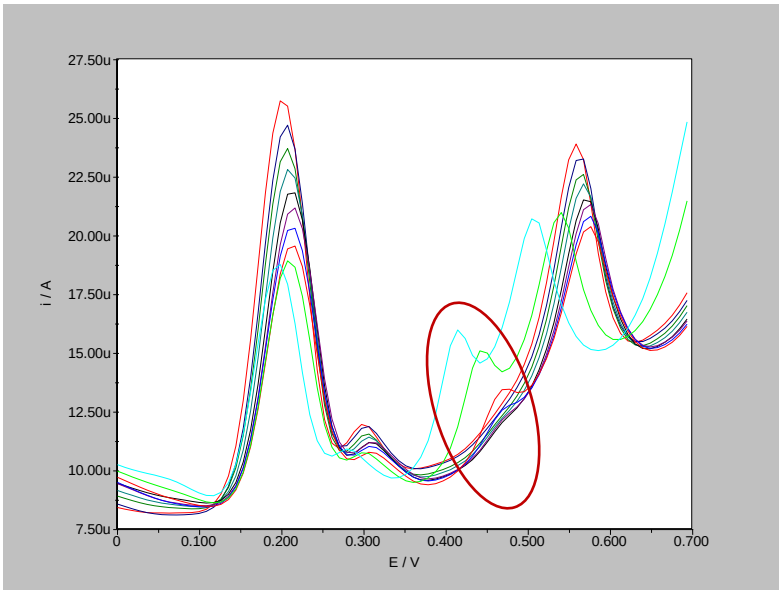

Graph A 34 - DP curves for concentrations 1×10^{-7}M to 8×10^{-6}M of BPA using DropSens sensors in Phosphate Buffer ph8 and Urine Sample – JS080590 (1:10 dilution) with 60% CNT (Red - 1×10^{-7}M; Dark Blue 2×10^{-7}M; Green – 4×10^{-7}M; Cyan - 6×10^{-7}M; Black - 8×10^{-7}M; Magenta - 1×10^{-6}M; Blue - 2×10^{-6}M; Red – 4×10^{-6}M; Light Green – 6×10^{-6}M; Light Cyan – 8×10^{-6}M). Circled in red are the BPA peaks.

LABORATÓRIO DE ANÁLISES CLINICAS DA COVILHÃ, SA

Profª Doutora M. PETRONILA JORGE FRADE ROCHA PEREIRA
Especialista em Análises Clínicas

Rua Pedro Alvares Cabral, nº2-1
6200-162 Covilhã
Telef: 275 334 972 / 275 323 968
Fax: 275 327 972
Posto de Colheita: 275 313 383

3591723
AFK1500 / 65478

Exmo Sr.
GS120390

Análises requisitadas por:
Un. Colheita: **POLO SAUDE**
PARTICULAR
Nº Ben:
P

Data Colheita: 08-05-2014
Data Saida: 14-05-2014 11:30:04

14-05-2014 11:29:56

Análises	Resultados / Unidades	Valores de Referência	R. Anteriores

Bioquímica Urina

Urina, análise bioquimica semiquantitativa

Cor	**Amarelo**	
Aspecto	**Limpido**	
pH	**6.0**	5.0 - 8.0
Densidade	**1.013**	1.012 - 1.025
Proteínas	**Negativo**	
Glucose	**Negativo**	
Corpos Cetónicos	**Negativo**	
Urobilinogénio	**Negativo**	
Bilirrubina	**Negativo**	
Hemoglobina	**Negativo**	
Nitritos	**Negativo**	

Este Laboratório pratica Controlo de Qualidade Interno e Externo

Validação Biopatológica efectuada pela Directora Técnica-Cientifica
Petronila Rocha Pereira, CP Nº 06649

Image A 1 – Laboratorial analysis performed for human urine sample encoded GS120390.

LABORATÓRIO DE ANÁLISES CLINICAS DA COVILHÃ, SA

Profª Doutora M. PETRONILA JORGE FRADE ROCHA PEREIRA
Especialista em Análises Clinicas

Rua Pedro Alvares Cabral, nº2-1
6200-162 Covilhã
Telef: 275 334 972 / 275 323 968
Fax: 275 327 972
Posto de Colheita: 275 313 383

3591720
AFK1497 / 65475

Exmo Sr.

JS080590

Análises requisitadas por:

Un. Colheita: **POLO SAUDE** **PARTICULAR**

Nº Ben:
P

Data Colheita: 08-05-2014
Data Saida: 14-05-2014 11:29:58

14-05-2014 11:29:50

Bioquímica Urina

Análises	Resultados / Unidades	Valores de Referência	R. Anteriores
Urina, análise bioquimica semiquantitativa			
Cor	**Amarelo**		
Aspecto	**Limpido**		
pH	**6.0**	5.0 - 8.0	
Densidade	**1.024**	1.012 - 1.025	
Proteínas	**Negativo**		
Glucose	**Negativo**		
Corpos Cetónicos	**Negativo**		
Urobilinogénio	**Negativo**		
Bilirrubina	**Negativo**		
Hemoglobina	**Negativo**		
Nitritos	**Negativo**		

Este Laboratório pratica Controlo de Qualidade Interno e Externo

Validação Biopatológica efectuada pela Directora Técnica-Científica
Petronila Rocha Pereira, CP Nº 06649

Image A 2 - Laboratorial analysis performed for human urine sample encoded JS080590.